

General Disclaimer

One or more of the Following Statements may affect this Document

- This document has been reproduced from the best copy furnished by the organizational source. It is being released in the interest of making available as much information as possible.
- This document may contain data, which exceeds the sheet parameters. It was furnished in this condition by the organizational source and is the best copy available.
- This document may contain tone-on-tone or color graphs, charts and/or pictures, which have been reproduced in black and white.
- This document is paginated as submitted by the original source.
- Portions of this document are not fully legible due to the historical nature of some of the material. However, it is the best reproduction available from the original submission.



DEPARTMENT OF MATHEMATICAL SCIENCES
SCHOOL OF SCIENCES AND HEALTH PROFESSIONALS
OLD DOMINION UNIVERSITY
NORFOLK, VIRGINIA

(NASA-CR-169366) MODELING OF THIN FILM GaAs
GROWTH Progress Report, 16 Jun. - 16 Sep.
1982 (Old Dominion Univ., Norfolk, Va.)
91 p HC A05/MF A01 CSCL 20L

N83-10963

G3/76 Unclas
35541

MODELING OF THIN-FILM GaAs GROWTH

By

John H. Heinbockel, Principal Investigator

Progress Report

For the period June 16, 1982 to September 16, 1982

Prepared for the
National Aeronautics and Space Administration
Langley Research Center
Hampton, Virginia

Under

Research Grant NAG1-148
Ronald A. Outlaw, Technical Monitor
Space Systems Division



September 1982

DEPARTMENT OF MATHEMATICAL SCIENCES
SCHOOL OF SCIENCES AND HEALTH PROFESSIONS
OLD DOMINION UNIVERSITY
NORFOLK, VIRGINIA

MODELING OF THIN-FILM GaAs GROWTH

By

John H. Heinbockel, Principal Investigator

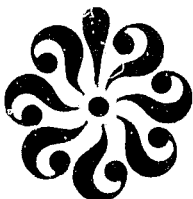
Progress Report

For the period June 16, 1982 to September 16, 1982

Prepared for the
National Aeronautics and Space Administration
Langley Research Center
Hampton, Virginia 23665

Under
Research Grant NAG1-148
Ronald A. Outlaw, Technical Monitor
Space Systems Division

Submitted by the
Old Dominion University Research Foundation
P.O. Box 6369
Norfolk, Virginia 23508-0369



September 1982

TABLE OF CONTENTS

	<u>Page</u>
SUMMARY.....	1
INTRODUCTION.....	1
LIST OF SYMBOLS.....	2
MODELING OF CRYSTAL GROWTH.....	4
The SOS Monte Carlo Model.....	4
Potential Scaling of Adatoms.....	5
Energy Distribution and Time.....	12
Random Walk and Incorporation.....	14
Generalizations.....	15
Description of the Computer Program.....	16
COMPUTER RESULTS AND DISCUSSION.....	18
THREE-DIMENSIONAL CONCEPTS AND EXTENSIONS OF MODEL.....	24
CONCLUSIONS.....	30
ACKNOWLEDGMENTS.....	31
REFERENCES.....	32
APPENDIX: COMPUTER PROGRAM.....	34

LIST OF TABLES

Table

1	Potential energy changes associated with central site (i,j) and neighbor sites due to deposition of an adatom (for a 100 orientation).....	6
2	Potential changes for addition of an adatom to an arbitrary site.....	11
3	Computer experiments.....	19

LIST OF FIGURES

<u>Figure</u>	<u>Page</u>
1	SOS model for crystal growth..... 64
2	Profile of surface potentials (a) uniform homogenous surface (b) vacancies, dislocations, kinks, jogs and impurities disturb the surface potential..... 65
3	Potentials for a uniform flat surface (solid line) and potential after an adatom has been added to site (i,j) (dashed line)..... 66
4	Potential variation at an arbitrary site (i,j)..... 67
5	FCC model and potential changes associated with different crystal orientations..... 68
6	Probability density for the Boltzmann ordered statistic $E_{(n)}$ with $n = 10^7, 10^8, 10^9$ and $T = 500$ K..... 69
7	Flowchart for the Monte Carlo SOS computer simulation of thin film growth..... 70
8	A 20×20 square array with periodic extension..... 71
9	Diffusion coefficient vs. inverse temperature..... 72
10	Clustering of dispersed adatoms on a uniform surface: $T = 600$ K, (a) $t = 0$, (b) $t = 0.1$ s, (c) $t = 0.3$ s, (d) $t = 0.5$ s, (e) $t = 0.7$ s, (f) $t = 1.0$ s..... 73
11	Trap potential variation for first and second layer..... 74
12	Growth around a trap: $T = 550$ K, (a) $t = 0.5$ s, (b) $t = 0.8$ s, (c) $t = 1.1$ s, (d) $t = 1.4$ s (e) $t = 1.7$ s, (f) $t = 2.0$ s, $R_d = 0.2778$ nm/sec..... 75
13	Surface roughness factor for $T = 500$ K and several deposition rates..... 76
14	Thin film growth for $R_d = 0.2778$ nm/sec for two different temperatures, $T = 300$ K, (a) $t = 0.5$ s, (b) $t = 3.0$ s, (c) $t = 6.0$ s, $T = 400$ K, (d) $t = 0.5$ s, (e) $t = 3.0$ s (f) $t = 6.0$ s..... 77
15	Thin film growth for $R_d = 0.2778$ nm/sec, $T = 500$ K, (a) $t = 0.5$ s, (b) $t = 0.8$ s, (c) $t = 1.1$ s, (d) $t = 1.4$ s, (e) $t = 1.7$ s, (f) $t = 2.0$ s..... 78

LIST OF FIGURES .. CONCLUDED

<u>Figure</u>		<u>Page</u>
16	Thin film growth for $R_d = 0.5556$ nm/sec, $T = 600$ K, (a) $t = 0.5$ s, (b) $t = 0.8$ s, (c) $t = 1.1$ s, (d) $t =$ 1.4 s, (e) $t = 1.7$ s, (f) $t = 2.0$ s.....	79
17	Thin film growth for $R_d = 1.389$ nm/sec, $T = 600$ K, (a) $t = 0.25$ s, (b) $t = 0.4$ s, (c) $t = 0.55$ s, (d) $t =$ 0.7 s, (e) $t = 0.85$ s (f) $t = 1.0$ s.....	80
18	Surface roughness factor for $R_d = 0.2778$ nm/sec and various temperatures.....	81
19	Nucleation density N_s as a function of time with constant cluster curves for 25, 50, 100 and 200 atoms. The decrease in n_s corresponds to growth coalescence.....	82
20	Annealing results (a) initial configurations: $T = 600$ K, (b) $t = 3.0$ s, (c) $t = 6.0$ s, $T = 700$ K, (d) $t = 3.0$ s, (e) $t = 6.0$	83
21	Basis vectors for P,I,F lattice structures.....	84
22	Crystal planes (a) their orientation and coverage with dis- tance (b) and (c), and (d) \vec{A}, \vec{B} , \vec{C}, \vec{A} and \vec{B}, \vec{C} primitive cells.....	85
23	Graphic output from computer program. Snapshots are read from top to bottom and right to left. Each snapshot represents 0.1 sec., $R_d = 0.556$ nm/sec., $\Delta t = 10^{-4}$ sec. (1,000 samples of each surface adatom during each snap- shot interval), $T = 600$ K, (100) surface, $U_o = -3.87$ eV, $\Delta H_{ads} = 1.7$ eV, $Q_d = 0.7$ eV, $U_m = -1.0$ eV, $n = 10^8$ (Boltzmann ordered statistic parameter).....	86

MODELING OF THIN-FILM GaAs GROWTH

By

John H. Heinbockel*

SUMMARY

A potential scaling Monte Carlo model of crystal growth is developed. The model is a modification of the solid-on-solid method for studying crystal growth in that potentials at surface sites are continuously updated on a time scale reflecting the surface events of migration, incorporation and evaporation. The model allows for B on A type of crystal growth and lattice disregistry by the assignment of potential values at various surface sites. The surface adatoms are periodically assigned a random energy from a Boltzmann distribution and this energy determines whether the adatoms evaporate, migrate or remain stationary during the sampling interval. For each addition or migration of an adatom, the surface potentials are adjusted to reflect the adsorption, migration or desorption potential changes.

INTRODUCTION

Numerous methods have been applied to obtaining thin-film, single crystals of GaAs, including free-standing wafers, peel films removed from a single crystal substrate, and films grown on lightweight substrates. The most promising method is a version of the latter technique called "graphoepitaxy." It is generally known that overlayers of crystalline materials deposited upon smooth microcrystalline substrates tend to be more or less randomly polycrystalline. The absence of long-range order in the microcrystalline substrate is reflected in the absence of long-range order in the overlayer. The basic concept of graphoepitaxy is that, by introducing an artificial surface relief structure having a long-range order on a microcrystalline substrate, long-range order can be induced in an overlayer. In other words, a crystalline film can be grown on a microcrystalline substrate.

*Professor, Department of Mathematical Sciences, Old Dominion University, Norfolk, Virginia 23508.

The degree of crystalline order achieved during a growth process will be controlled by the adsorption, nucleation and lateral growth behavior in the first few deposited layers. The parameters which will affect the crystal growth are: The deposition rate, the surface temperature, surface diffusion, surface defect density and lattice registry of the system. We present a Monte Carlo solid-on-solid (SOS) computer simulation which utilizes a potential scaling technique (ref. 1) over a 20×20 array of sites. Although numerous Monte Carlo models for crystal growth exist (refs. 2-12), the approach developed herein is a more physical model in that the events which occur at each site are constrained by the surrounding potential field and the thermal energy fluctuations associated with a given substrate temperature. Also, the method of ordered statistics is utilized to construct a time scale of events compatible with computer times in order that the simultaneous changing and updating of site potentials can be done in a reasonable amount of computer time and still allow the model to simulate thin film growth in a physically realistic manner.

LIST OF SYMBOLS

a_0	lattice constant (nm)
M	size of square array
$H(i,j)$	height at position (i,j)
ϕ_0	potential energy change (eV)
ϕ_1, ϕ_2, ϕ_3	first, second, third nearest neighbor potential changes (eV)
ω_i	(i = 1, ..., 8) potential energy changes (eV)
Δt_s	scanning time interval (sec)
$E(R)$	random energy
$U_0(i,j), U_{os}(i,j)$	potential at site (i,j) for adsorbate and substrate (eV)
$U(i,j)$	total potential at site (i,j) (eV)
U_e, U_{es}	evaporation level of adsorbate and substrate (eV)
U_m, U_{ms}	migration level of adsorbate and substrate (eV)

ϕ^* , R^* , n_0 , m_0	Mie potential parameters
K	Boltzmann constant (8.62×10^{-5}) eV/°K
T	absolute temperature (°K)
α_2 , α_3	scale factors for crystal orientation
ξ	crystal orientation factors
R	uniform random number ($0 < R < 1$)
R_d	deposition rate (nm/sec)
R_e	evaporation rate
Δt	time interval associated with surface "snapshot"
$\lambda = 1/KT$	parameter of Boltzmann distribution
E	random energy (eV)
E(n)	ordered statistic
n	sample size
i,j	site numbers
f(E)	Boltzmann distribution
F(E)	cumulative distribution
g(E)	distribution of ordered statistic E(n)
G(E)	cumulative distribution
(100) (111) (110)	crystal orientations
ΔH_{sub}	heat of sublimation
ΔH_{ads}	heat of adsorption for single adatom
Q_d	diffusion activation energy (eV)
τ	lifetime (sec)
τ_d	mean time between hops
Δt_0	output snapshot or stop action time interval (sec)
U_i	incorporation energy

$U_{ks}^{(1)}, U_{ks}^{(2)}$	kink site potentials
m_o, n_o, ϕ^*, R^*	Mie potential parameters
D_-, D_+	diffusion coefficients into and from bulk
$S_i = S$	sticking coefficient
τ_o	period of vibration of surface atom (sec)
λ	parameter for surface diffusion

MODELING OF CRYSTAL GROWTH

The SOS Monte Carlo Model

In this model we consider a simple cubic (SC), body centered cubic (BCC) and face centered cubic (FCC) crystal lattice. It is required that each occupied site be directly above another occupied site and so the name solid-on-solid (SOS) model. This model is characterized by an array of interacting columns of varying integer heights with respect to some orientation such as the (100) (111) or (110) crystal planes. The terrace-ledge-kink (Kossel) Model (refs. 13-14) is illustrated in figure 1. The model employs a 20×20 square array upon which columns are constructed. Adatoms are deposited upon the surface in a random fashion where they are free to migrate, remain localized, diffuse into the bulk (incorporation) or diffuse from the bulk to the surface, or evaporate. These changes alter the stacking heights of each column as well as producing new potentials at and in the neighborhood of the surface sites involved in the process of surface adatom interaction.

Each surface site is located at the top of the stack of adatoms from an arbitrary row i and column j of a 20×20 array. The physical constraints which determine the temporal behavior of every adatom located at the surface of each column from an arbitrary site (i,j) is based upon the interaction potential that the surface adatom has with its nearest neighbors and the rest of the solid. Spatial disregistry, that normally occurs due to size differences between adsorbate and adsorbent atoms, is accounted for by changes in the interaction potential. In figure 2(a), the interaction

potential across a perfectly homogeneous surface is depicted as uniformly changing from site to site. Figure 2(b) illustrates a typical interaction potential across a heterogeneous surface. We developed a set of "rules" whereby the columns of the SOS model interact by assigning values to the potential energy changes associated with the processes of adsorption, migration and desorption.

Potential Scaling of Adatoms

The rules, by which the columns of the SOS model interacted, were governed by the following ideas relating to the potential energy and potential energy changes associated with the adsorption, migration, or desorption of adatoms from an arbitrary row i and column j of an 20×20 array. Energies associated with an arbitrary site (i,j) were defined as follows: $U_0 = U_0(i,j)$ --the potential energy at a site because of surface bonding and crystal structure; ϕ_0 --the potential energy change at site (i,j) because of the deposition of an adatom (assumed the same for all sites); $-W_i$ ($i = 1, \dots, 8$)--the potential energy changes at neighboring sites when an adatom is deposited at site (i,j) ; $E(i,j)$ --the random surface energy associated with site (i,j) and time interval Δt_s ; $U(i,j) = U_0(i,j) + E(i,j)$ --the total energy associated with site (i,j) during the time interval Δt_s ; U_e --the evaporation potential; and U_m --the migration potential. All of the above energies are measured in electron volts.

We developed a Monte Carlo computer simulation of crystal growth by developing rules that determined the SOS kinetics of condensation, evaporation or surface migration of adatoms. These rules led to a consistent and physically reasonable description of the fundamentals associated with crystal growth. We first considered the adsorption of a thermally accommodated adatom onto the surface at some general site where the potential at this site was changed and, simultaneously, potential energy changes at all of the neighboring sites occurred. In Table 1, the potential energy changes are depicted by the mnemonic mask. The center of this mask is placed over the site (i,j) to illustrate the changes to be made in the potential at the central site as well as the potential changes in the surrounding neighboring sites.

The potential changes in the case of desorption of an adatom from the central site are again depicted with the mask of Table 1, with the opposite signs on the potential changes. The case of surface migration was treated as a desorption from a site (i,j), followed by an adsorption at a nearest or second nearest neighbor location, together with the correct potential mask changes associated with each process. The neighboring migration site was determined by a weighted random walk to one of the unoccupied neighbor sites.

Table 1. Potential energy changes associated with central site (i,j) and neighbor sites due to deposition of an adatom (for a 100 orientation).

$-w7 = -w7(i-1,j-1)$	$-w8 = -w8(i-1,j)$	$-w1 = -w1(i-1,j+1)$
$-w6 = -w6(i,j-1)$	$\phi_0 = \phi_0(i,j)$	$-w2 = -w2(i,j+1)$
$-w5 = -w5(i+1,j-1)$	$-w4 = -w4(i+1,j)$	$-w3 = -w3(i+1,j+1)$

The Monte Carlo simulation of crystal growth involved a random deposition of thermally accommodated surface adatoms during a time interval Δt . These deposited adatoms changed the potential energies at the random surface sites under consideration. The values assigned to the central potential change ϕ_0 and neighboring potential changes $-w_i$, $i = 1, \dots, 8$ dictated the new potential energy values when an adatom was deposited or removed from a site. In this way each surface site had an energy barrier to translation or evaporation, represented by a potential well.

Figure 3 illustrates the potential changes that occur along a lineal section of a homogeneous surface upon the adsorption of a single adatom at site (i,j). Note that the potential increases by an incremental amount ϕ_0 , and the adjacent sites decrease in potential by an incremental amount ϕ_1 . This represents the actual physical condition that the adsorbed adatom requires less energy to desorb or to migrate as compared to the original surface adatom which was surrounded by all its nearest neighbors. Note also that the deeper potentials at the neighboring sites reflect the increased energy necessary to desorb an atom from these sites due to the increased

coordination or ligancy created by the adatoms. Figure 4 illustrates the potential variation at an arbitrary site (i,j) as nearest neighbors are progressively added onto a (100) surface orientation.

The term epitaxy means "an arrangement on," and is used to denote the growth of one substance upon the crystal surface of a foreign substance. The term autoepitaxy refers to the oriented growth of a substance onto itself, and heteroepitaxy is the growth over another material. Autoepitaxy requires that the initial potential U_0 (before adsorption) be recovered when the adatom has all its neighboring adatoms surrounding the central site.

In assuming values to the potential changes ϕ_0 and ω_i , $i=1, \dots, 8$, we must take into account the type of crystal structure and orientation we are trying to simulate with our SOS model. Consider figure 5 which illustrates the GaAs fcc structure. For growth on the (100) face we can set up a correspondence between a central site, the nearest neighbor sites, second nearest neighbor sites, and the adatom potential changes for the mask in Table 1 (i.e., $\omega_1 = \phi_2$, $\omega_2 = \phi_1$, etc.). Similarly, we can set up the correspondence illustrated in figures 5(b and c) for the (111) and (110) orientations and we can construct an appropriate mnemonic mask.

In figure 5 we must choose $\phi_0, \phi_1, \phi_2, \phi_3$ in such a way that, when the first level of adatoms covers the surface, then the potential distribution must return to its original value. We will require that adjustments be made in the potential energy changes during the transition from heteroepitaxy to autoepitaxy. Here we let a negative sign denote an attractive potential. By simply adding adatoms to a surface it is readily verified that the potential changes must adhere to the rules given in Table 2 if after one layer the potential energy returns to its initial value.

For heteroepitaxy we require that an adjustment be made in the central site potential change to reflect the potential energy differences of the materials involved. The potential energy changes $\phi_0, \phi_1, \phi_2, \phi_3$ can be different for the substrate and growing material. For the substrate material we could use the depth of the surface potentials and migration levels to stimulate a variety of surface morphologies. In this model we envision a flat substrate as a periodic lattice structure where each lattice site is a potential well. The substrate can vary from flat to rough and the

potentials adjusted to reflect various surface preparations. For an ideal ly flat substrate we assume that the depths of the potential wells are uniform, given by U_{os} . After one layer of growing material covers the surface, the potentials at each site are assumed to convert to the auto-epitaxy potentials U_o . In order to make this transition we assume that

$\phi_o = \sum_{i=1}^8 \omega_i + (U_o - U_{os})\Gamma_{ij}$ where Γ_{ij} is zero if the height h_{ij} at position (i,j) is greater than or equal to one, and Γ_{ij} is one in the case where $h_{ij} = 0$. Thus, if an adatom is deposited at a first layer site (i,j) , we adjust the potentials at this site by the relation $U_o - U_{os}$, in addition to the mask potential changes at the surface sites as this produces the desired change that hetroepitaxy produces in the value of the potential.

The energy behavior at each surface site is monitored over a sampling interval Δt_s , every sampling interval. The simulation of thermal energy fluctuations is done by random number generation. For each site (i,j) we generate a random energy $E(R)$ and add it to the interaction potential $U_o(i,j)$ to obtain a total energy of

$$U(i,j) = U_o(i,j) + E(R). \quad (1)$$

This energy is then compared to energy barriers for desorption, surface migration and incorporation. If the total energy exceeds one of these barriers, we allow the adatom to proceed accordingly. If the total energy is less than the lowest barrier, then the adatom remains localized. In summary, our Monte Carlo procedure entails the generation of a random energy for each site and calculating a total energy U , if this value U is such that:

- (a) $U < U_m$, the adatom remains localized;
- (b) $U_m < U < U_i$, surface migration is allowed to occur;
- (c) $U_i < U < U_e$, surface migration or incorporation into the bulk is allowed to occur;
- (d) $U_e < U$, evaporation occurs.

During each time interval Δt_s , a random energy $E(R)$ was assigned to each of the surface adatoms. We let

$$U(i,j) = U_0(i,j) + E(R) \quad (2)$$

denote the total energy possessed by a surface adatom at a site (i,j) during this time interval. This total energy is the sum of the potential energy U_0 due to the lattice structure and a random energy E from a modified Boltzmann distribution to be discussed in the next section which characterizes the random surface energy. When U was less than some material-dependent migration level U_m , the adatom remained stationary at the surface site. If $U_m < U < U_e$, surface migration by random walk was allowed to occur. If U was greater than the evaporation potential U_e , the adatom was removed from the site and for $U_i < U < U_e$ incorporation or migration was assumed to occur.

The rate of impingement of adatoms upon the surface was independent of the surface configuration. The rates associated with the evaporation and migration of adatoms depended upon the potential barriers U_e and U_m and also upon the values assigned to the potential changes ϕ_0 and $-w_i$, ($i = 1, \dots, 8$). These later potential changes had to take into account the type of crystal structure and orientation of the growth we were trying to simulate with the SOS model. In figure 5(a), for growth on the (100) face, we set up a correspondence between the central site, the nearest neighbor potentials ϕ_1 , second nearest neighbor potentials ϕ_2 , and the adatom potential changes for the mask in Table 1 (e.g., $w_1 = \phi_2$, $w_2 = \phi_1$). In a similar manner we were able to set up the correspondences illustrated in figure 5(b) and (c) for the (111) and (110) orientations. In Table 2, we selected the relation between the neighbor potentials $\phi_0, \phi_1, \phi_2, \phi_3$ in such a way that when the first level of adatoms covered the surface, the potential distribution returned to its original value. This produced the constraint conditions on the neighboring potentials which are illustrated in Table 2. We assumed that $\phi_0 = \Delta H_{ads}$ and were left with decisions on how to assign the ϕ_1, ϕ_2, ϕ_3 values. For the (100) orientation we let $\phi_3 = 0$ and were left with having to assign values to ϕ_1, ϕ_2 . One possible choice was to assign ϕ_1 a value based upon nearest neighbor bond strength and then calculate the ϕ_2 value based upon the constraint.

Alternatively, we let ϕ_1 denote the change in the nearest neighbor potentials due to the addition of an adatom to the surface and let ϕ_2, ϕ_3 denote the second and third nearest neighbor potential changes. We assumed that $\phi_2 = \alpha_2 \phi_1$ and $\phi_3 = \alpha_3 \phi_1$ where α_2, α_3 are scale factors which are less than one. This allowed us to define the crystal orientation factor ξ as

$$\xi = \begin{cases} 2 + 2\alpha_2 & , \quad (100) \\ 3 + 3\alpha_2 & , \quad (111) \\ 1 + \alpha_2 + 2\alpha_3 & , \quad (110) \end{cases} \quad (3)$$

which takes into account the different crystal orientations. We also defined the kink site potentials before $U_{ks}^{(1)}$ and after $U_{ks}^{(2)}$ and the capture of an adatom as $U_{ks}^{(1)} = U_o - \xi\phi_1$, $U_{ks}^{(2)} = U_o + \xi\phi_1$. (Note that $\phi_o = 2\xi\phi_1$.) Note that the values assigned to the mask potential changes are not necessarily the same for the different orientations: for example, the ϕ_1, ϕ_2, ϕ_3 values for each case in Table 2 could have different values.

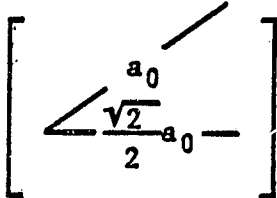
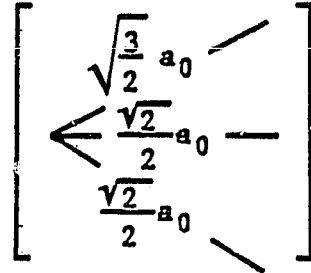
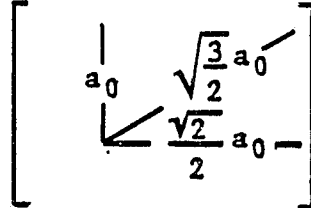
We can assign arbitrary values to the neighbor potential changes ϕ_1, ϕ_2, ϕ_3 as long as these values satisfy the constraint that $\phi_o = 2\xi\phi_1$. If we arbitrarily assign values to α_2, α_3 then we can solve for ϕ_1 and consequently ϕ_2 , and ϕ_3 . Instead of arbitrarily assigning values to α_2 and α_3 , we examine a (m_o, n_o) Mie potential curve with $m_o < n_o$ (ref. 15)

$$\phi = \phi^* \left[\left(\frac{R^*}{R} \right)^{n_o} - \frac{n_o}{m_o} \left(\frac{R^*}{R} \right)^{m_o} \right] \quad (4)$$

Here R^* is the distance at which ϕ obtains its minimum value of $\phi^* \left(1 - \frac{n_o}{m_o} \right)$. If we examine the potential values at various distances $R = a_o, \frac{\sqrt{2}}{2} a_o, \frac{\sqrt{3}}{2} a_o, \frac{\sqrt{3}}{2} a_o$, with $R^* = a_o$, then the ratio of the Mie potential values at these distances can be used to approximate the values of $\alpha_2 = \phi_2/\phi_1$ and $\alpha_3 = \phi_3/\phi_1$ for different crystal orientations and different m_o, n_o values.

CRISTALLOGRAFIA
OF FOUR QUANTUM

Table 2. Potential changes for addition of an adatom to an arbitrary site.

<u>Crystal Face</u>	<u>Relation Between Neighbor Potentials</u>	<u>Potential Changes for Addition to Arbitrary Site</u>	<u>Distances to Neighboring Sites</u>
		$\begin{bmatrix} -\omega_7 & -\omega_8 & -\omega_1 \\ -\omega_6 & \phi_0 & -\omega_2 \\ -\omega_5 & -\omega_4 & -\omega_3 \end{bmatrix}$	
(100)	$\phi_0 = 4\phi_1 + 4\phi_2$	$\begin{bmatrix} -\phi_2 & -\phi_1 & -\phi_2 \\ -\phi_1 & -\phi_0 & -\phi_1 \\ -\phi_2 & -\phi_1 & -\phi_2 \end{bmatrix}$	
(111)	$\phi_0 = 6\phi_1 + 6\phi_2$	$\begin{bmatrix} -\phi_2 & -\phi_2 & -\phi_1 & -\phi_2 \\ -\phi_1 & -\phi_1 & \phi_0 & -\phi_1 \\ -\phi_2 & -\phi_2 & -\phi_1 & -\phi_2 \end{bmatrix}$	$-\phi_2 \left[\begin{array}{c} \sqrt{\frac{3}{2}} a_0 \\ \frac{\sqrt{2}}{2} a_0 \\ \frac{\sqrt{2}}{2} a_0 \end{array} \right]$ 
(110)	$\phi_0 = 2\phi_1 + 2\phi_2 + 4\phi_3$	$\begin{bmatrix} -\phi_3 & -\phi_2 & -\phi_3 \\ -\phi_1 & \phi_0 & -\phi_1 \\ -\phi_3 & -\phi_2 & -\phi_3 \end{bmatrix}$	

Energy Distribution and Time

During each sample interval Δt_s , an atom in an arbitrary site (i,j) has the total energy

$$U(i,j) = U_0(i,j) + E(R)$$

where $E(R)$ is determined by random number R from the Boltzmann distribution

$$f(E) = \lambda \exp [-\lambda E], \quad E > 0 \quad (5)$$

where $\lambda = 1/KT$ is the parameter of this exponential distribution. The mean energy of this distribution is

$$\langle E \rangle = \int_0^{\infty} E f(E) dE = KT = \frac{1}{\lambda} \quad (6)$$

and the cumulative energy distribution is given by

$$F(E) = \int_0^E f(E)dE = 1 - \exp [-\lambda E]. \quad (7)$$

A random variate E can be generated from this distribution by using the inverse function associated with the cumulative distribution. For R a uniform random number between 0 and 1 and with $R = F(E)$, the inverse function gives the random energy

$$E = E(R) = -KT \ln (1 - R) \quad (8)$$

so that (1) becomes

$$U(i,j) = U_0(i,j) - KT \ln (1 - R) \quad (9)$$

The residence or stay-time of an adatom on a surface is given by the Frenkel equation (ref. 16)

$$\tau = \tau_0 \exp [-\lambda \Delta H_{ads}] \quad (10)$$

where ΔH_{ads} is the heat of adsorption and τ_0 is the period of vibration for the surface adatoms ($\tau_0 \sim 10^{-12}$ sec). Ideally then, the most physically real sampling time corresponding to changes in vibrational energy and, therefore, changes in $U(i,j)$ is to choose $\Delta t_s = \tau_0$. Computer costs and time, of course, prohibit the extensive amount of computations that would be necessary to sample 400 sites 10^{12} times each second. In order to circumvent this difficulty, the method of ordered statistics is applied. Essentially, most of the time-dependent energy variation at a particular site results in insufficient thermal energy for adatom movement and adatoms remain localized over most of the sampling interval. Since this large time of atomic localization is not important to the actual thin film growth, only the fraction of the sampling interval that movement does occur need be considered. Thus we desire that fraction of the time that the site energy is in excess of the minimum activation barrier for adatom activity.

Let E_1, E_2, \dots, E_n denote n random samples from the exponential distribution (3) and let $E_{(1)}, E_{(2)}, \dots, E_{(n)}$ denote the ordered arrangement (from low to high) of the n random samples with $E_{(i-1)} < E_{(i)}$ for all $i=2,3,\dots,n$. The probability distribution of the largest ordered statistic $E_{(n)} = \max \{E_1, E_2, \dots, E_n\}$ is given by (ref. 17)

$$g(E) = n[F(E)]^{n-1} f(E), \quad 0 < E < \infty \quad (11)$$

where $f(E)$ and $F(E)$ are given by equations (3) and (5). The cumulative frequency distribution is given by

$$G(E) = \int_0^E g(E)dE = (1 - e^{-\lambda E})^n \quad (12)$$

To generate a random variable $E_{(n)}$ from this distribution, a uniform random number R , with $0 < R < 1$, is generated such that $G(E_{(n)}) = R$, then the inverse function gives the random energy

$$E_{(n)} = -KT \ln (1 - R^{1/n}) \quad (13)$$

which can be compared with equation (6). Note that for large values of n , we can approximate the random energy $E_{(n)}$ by

$$E_{(n)} = -KT \ln \left(-\frac{1}{n} \ln R \right). \quad (14)$$

If for example, $T = 500$ K and the activation energy for diffusion is $Q_d = 0.7$ eV, then the mean time between hops is $\tau_d = 10^{-12} \exp [\lambda Q_d] = 10^{-5}$ sec or, in a sampling interval of $\Delta t_s = 10^{-5}$ sec, a single hop occurs. Any smaller sampling interval is not necessary because no movement occurs. Any larger sampling interval would result in multiple events for a single adatom and the less physical the model becomes. Figure 6 illustrates the probability distribution of the ordered statistic $E_{(n)}$ with $n = 10^7, 10^8, 10^9$ at $T = 500$ K.

The minimum activation energy for diffusion (ref. 18) determines the sampling interval and therefore the number of random samples, n . We make the following assumptions concerning the activation barriers for adatom activity (see figure 3): $U_o = \Delta H_{sub}$, $U_e = 0$, $\phi_o = \Delta H_{sub} - \Delta H_{ads}$, $U_m = -\Delta H_{ads} + Q_d$, $\tau_d = \tau_o \exp (\lambda Q_d)$, then the mean number of hops in Δt_s sec is given by $\Delta t_s / \tau$ and $n = \Delta t_s / \tau_o$. Let Δt_o denote the output "snapshot" time interval where we perform a stop action and view the surface. The number of surface scans during this time interval is given by $\Delta t_o / \Delta t_s$. For example, if $\Delta t_o = 0.1$ and $\Delta t_s = 10^{-4}$ we would scan each of the 400 surface sites 10^3 times and generate $4(10^5)$ random energies $E_{(n)}$ from the modified Boltzmann ordered statistic probability distribution.

Random Walk and Incorporation

For a fixed uniform deposition rate R_d , adatoms are deposited at random positions on the surface based upon the value assigned to Δt_s . For small Δt_s , we must wait for some multiple of this time before adding a single adatom. Each time an adatom is deposited, or removed from a site, the potentials surrounding the site are updated. In the case of surface migration, an adatom has sufficient energy to migrate and we treat migration as an evaporation followed by a deposition at a neighboring site. The availability of more than one site for migration is another decision which is made according to the ligancy or coordination number associated with the

available sites. From an interaction potential perspective, this is physically reasonable since the site that has a deeper well (more attractive) will have an energy barrier to migration that is smaller, thus having a higher probability for migration to that site. The experimental evidence to support this assumed behavior is sizeable (ref. 19). Each unoccupied nearest neighbor and second neighbor site is given a weight which is the ligancy if an adatom had random walked to that site. These weights are then normalized and a weighted random walk to one of these sites is determined by a random number. If all nearest neighbor and second nearest neighbor sites are occupied, the adatom is assumed to jump up onto the next level at an unoccupied nearest neighbor site with equal probability.

In the case $U_i < U < U_e$, an adatom is considered to be either incorporated or to surface migrate by weighting the two possibilities according to their relative probabilities. In the case of incorporation an adatom is removed from the surface in the same way an adatom desorbs. It is assumed that the bulk vacancy concentration is sufficient to receive the adatoms and therefore the adatom just disappears from the surface site. The excess energy after an event is assumed to be reabsorbed into the thermal energy of the solid.

Generalizations

Various modifications and extensions of the ideas presented in the previous sections will make the model more general. Some of the modifications will be presented in this section as these reflect modifications of the SOS model. Three-dimensional model concepts which differ from the SOS model concepts will be presented in a later section.

As adatoms are deposited upon the surface we will label them as "A-type" or "B-type" where the A-types represent substrate adatoms and the B-types represent the growing material. As the vertical growth increases the fraction of A's mixed with the B's is allowed to decrease. In this way we can simulate adatom diffusion through the growing film to the surface by randomly depositing substrate adatoms on the surface, at a rate controlled by the diffusions equations for the adsorbate/adsorbent system. Also,

instead of one potential change mask we will introduce four such masks to reflect the potential changes associated with the composition process of: A on A, A on B, B on A, or B on B type of interactions. This additional complexity increases the bookkeeping to keep track of where the A and B type adatoms are located.

By judiciously choosing the A on A, A on B, B on A, and B on B potential changes we can use the SOS model to simulate A-B type crystal growth. By assigning an initial substrate of an A-B checkerboard pattern we can make the A on A interaction subject to a high probability of migration of A adatoms to a nearest neighbor B-site. Similar considerations hold for B on B interactions. The nature of interatomic potentials (ref. 20) can also be varied from site to site.

Description of the Computer Program

A flowchart of the computer program is given in figure 7 and the FORTRAN computer program is presented in Appendix A. The program is liberally spiced with comment statements to help the reader. An attempt was made to make the program modular in character in the event extensive revision was needed. The following is a brief description of the subroutines:

Program Crystal

Here parameters are read in and other variables are initialized and, before the program actually runs, a printout of all initial values and parameters is made.

Subroutine SETUP

Assumes a (m_o, n_o) Mie potential and calculates $\phi_1, \alpha_2, \alpha_3$ given the initial value for ϕ_o .

Subroutine FACE

Calculates the potential changes associated with a (100), (111), or (110) crystal orientation and distances to nearest neighbor site.

Subroutine INITIAL

Initializes and prints out the substrate geometry and assigned values of the potentials at each site.

Subroutine DIFF

A weighted random walk surface diffusion is simulated by an evaporation followed by a deposition at the nearest neighbor site.

Subroutine PBOND

Calculates the weights associated with the random walk processes on one of the crystal orientations.

Subroutine ADATOM

Updates the potential sites at i,j and the surrounding neighbor sites when an adatom is added to site (i,j) .

Subroutine SUBATOM

Updates all neighboring potentials when an adatom is removed from a site (i,j) .

Subroutines EDGE, EDD, XYX, CORRECT

The geometry of the 20×20 square array assumes periodic boundary conditions as illustrated in figure 8. This 20×20 array is embedded into a 24×24 square array and addition or removal of adatoms along an edge, or migration across an edge, requires that the outer border of the 24×24 array be updated to reflect the periodic conditions. These periodic conditions are maintained by the subroutines EDGE, EDD, XYX, and CORRECT.

Subroutine STOFIN

Starts and finishes a computer run. This subroutine analyzes the deposition rate and scan time and deposits adatoms on the surface, if required. Surface scanning of each site is performed and computer output is printed.

Subroutine URNS

Calculates random sites and type of adatom (A or B) to be deposited on the surface.

Subroutine UPDATE

Scans the top layer of the surface and counts the size and frequency of clusters. Also calculated are coverage for the two highest layers, roughness factor, and number of A and B type adatoms on the surface.

Subroutine MIXUP

Takes the vector (1,2,3,...,N) and randomizes the position of the integers to form a vector (u₁,u₂,u₃,...,u_N) which is some rearrangement of the initial vector.

Subroutine GROW

Optional computer graphics of output data.

COMPUTER RESULTS AND DISCUSSIONS

Various computer experiments were performed with the model. These experiments are listed in Table 3. The computer experiments were performed for a (100) fcc surface to assess the physical behavior of the model.

Because there exists no real data on semiconductor crystals for the interaction and potential energy changes associated with adatom movement, we chose the following set of nominal parameters:

$$\Delta H_{ads} = 1.7 \text{ eV}$$

$$\Delta H_{sub} = 3.87 \text{ eV}$$

$$D_{-z} (\text{Ge/Ge}) = 7.8 \exp(-2.98 \lambda) \text{ cm}^2 \text{ s}^{-1}$$

$$D_{-z} (\text{Si/Fe}) = 0.44 \exp(-2.09 \lambda) \text{ cm}^2 \text{ s}^{-1}$$

$$D_{+z} (\text{Fe/Ge}) = 0.13 \exp(1.08 \lambda) \text{ cm}^2 \text{ s}^{-1}$$

$$Q_d = 0.7 \text{ eV}$$

$$S = S_i = 1$$

which represents the best available data for a Germanium type system.

In experiment 1, we examined the surface migration of a single adatom which performed a random walk to the nearest neighbor sites whenever the random energy associated with a single scan dictated such behavior. The number of migrations as a function of time is linear and varies exponentially with temperature. Figure 9 shows a plot of diffusion coefficient vs.

Table 3. Computer experiments.

Experiment	Deposition Rate ($\text{cm}^{-2}\text{s}^{-1} \times 10^{15}$)	Temperature (K)	Run Time
1. Surface diffusion of a single adatom	0	400, 500, 600	2
2(a) Nine adatoms in a row	0	400, 500, 600	2
(b) Nine adatoms randomly distributed	0	400, 500, 600	2
3. Thin film growth with defect site	0.5	400, 500, 600	2
4. Thin film growth with variable deposition rate	0.25, 0.5, 1, [$2.5 (10^{-3})$]	500 400	2 40
5. Thin film growth with variable substrate temperature	0.5, 1.0	300, 400, 500 600, 700	2
6. Annealing of thin film growth	0	600, 700	6

inverse temperature as calculated from the computer model. The linear behavior of the diffusion constant follows from the equation

$$D = \frac{\ell a_0^2}{\tau_0} \exp(-\lambda Q_d) \quad (15)$$

where a_0 is the jump distance and $\ell = 1/4$ for a (100) face. The slope of the Arrhenius plot yields the activation barrier $Q_d = 0.7$ eV which is our input condition. This provides a self consistent check on the physics of the computer model. In figure 9, the number by the circles is the average number of migrations for each temperature given. The results in experiment 1 are for a flat surface. In the case of nonuniform surface the mean diffusion length and migration frequency would be substantially reduced due to the lower probability of escape from kink sites, steps and other defects.

In experiments 2(a,b) we examined the clustering of lineal and randomly dispersed adatoms as a function of temperature. In both cases the adatoms tended to seek out the most stable configuration in that each adatom ultimately tried to maximize its number of nearest neighbors and hence form a 3×3 array. In the first case 2(a) the lineal adatoms were all connected and the probability of adatoms breaking away from the row increased with temperature. The adatoms tended to form stable clusters with the migration of single adatoms along a step being the dominant form of motion. For this experiment a 3×3 array was the most stable cluster. In the second case 2(b) the dispersed adatoms performed random walks and collided to form dimers, trimers, and eventually a nine adatom cluster. Figure 10 is a graphic display of the sequence of events as a function of time. At some of the temperatures the 3×3 array was not completely achieved. However, given sufficient time, these configurations eventually became a 3×3 array.

The question of cluster growth is perceived to occur by either adatom capture or by actual enmasse motion of one of the smaller clusters into a larger cluster. The subsequent collision and reorientation of the adatoms to registry with the second cluster was assumed to occur. In the formulation of this model no consideration was given to the motion of whole

clusters, but as these computer experiments show whole clusters can move by individual adatom motion at the periphery of the cluster resulting in a net motion of its center of mass [see figures 10(b,c)].

In experiment 3, a generalized point defect was modeled by adjusting the potential to be very large at a single point and its four nearest neighbors sites. After one layer covered this site only the central site was allowed to have a larger potential and after a second layer the potential was allowed to return to the normal value of that of its neighbors. Figure 11 shows the prescribed potential changes for the first two layers of growth. After the second layer covered the trap, the potential was allowed to return to its normal value. Figure 12 illustrates the effect of a trap and the resulting growth around the trap for a constant deposition rate and several surface temperatures. Many interesting phenomena occurred in our study of a trap and we will pursue this case in more detail in a later report. For the time being, a brief description of the observed phenomena will have to suffice. At low temperatures the surface adatoms initially adsorbed do not statistically interact with the site and ordinary homogeneous nucleation and growth occurs uniformly over the surface. As adatoms impinge upon the trap site heterogeneous nucleation occurs and growth is much more rapid in this vicinity. Further the vertical growth in the vicinity of the trap is initially larger because the potential at the trap site is still lower after being covered by the first layer which is an island upon which impinging adatoms can migrate and find this lower potential. It is thus likely that the growth in the vicinity of the trap would be dominated by this effect. At higher temperatures the major growth occurs by way of vapor phase transport as opposed to surface defect density (ref. 21) and to the magnitude of the deposition rate. Growths have been achieved at very low temperatures on appropriate substrates if, and only if, the surface was relatively smooth and defect free as determined by Kikuchi lines present in the RHEED patterns. If the defect density is too high, then epitaxy is inhibited by the dominance of growth from the defects. If the deposition rate is too high then even with low defect density the growth around a defect is so rapid that epitaxy is also limited. Therefore, the understanding of the growth rate about different types of defects would be helpful in assessing the probability of epitaxy for a given system, and we will pursue these questions at a later time.

In experiment 4, we varied the deposition rate (1 nm/sec = $1.8 \cdot 10^{15}$ adatoms/cm² sec), and figure 13 illustrates the effect of this variation on the surface roughness. More experimentation in this area is necessary as we will see from the next computer experiment, which also includes variable deposition rates.

In experiment 5, the substrate temperature was varied. Figures 14-17 illustrate the effect of this variation. The uniformity of the surface is progressively improved as the temperature increases and the deposition rate decreases. Figure 13 illustrates the roughness factor as a function of time and demonstrates the changing surface uniformity. The oscillatory nature of the curves is a consequence of the growing multilayers and that surface migration tends to fill in the vacancies, ledges and kink sites. The surface adatoms becomes more mobile at the higher temperatures and tend to fill in these sites. This behavior has been observed by Weeks and Gilmer (ref. 6) for crystal growth from the melt. Figures 14(a-c) illustrate the growth sequence at T = 300 K as compared to figures 14(d-f) which show the growth sequence at T = 400 K. Figure 15 illustrates the growth sequence for $R_d = 0.2778$ nm/sec and T = 500 K. Figure 16 illustrates growth occurring by an advancing ledge that was formed upon the coalescence of two large clusters. Growth by this mechanism has been discussed by Weeks and Gilmer (ref. 6), but in this particular case it is statistical in nature rather than the dominant phenomena.

Coalescing clusters at submonolayer levels have been illustrated in figure 15 to show the possible development of a grain boundary. Although a graphic representation of different growing grain orientations is not easily done with the SO₃ model, the potential field surrounding a particular defect or nucleation site does provide some information on the probable growth orientation and, therefore, may permit a way of deciding if the coalescing grains will be in, registry, near registry (low angle grain boundary) or whether a high angle grain boundary will be formed.

A plot of nucleation density n_s and maximum cluster size N_s as a function of time is given in figure 19 for a deposition rate of 0.2778 nm/sec. Clusters of size n_i ($i > 1$) have a total density of

$$\sum_{i=2}^{\infty} n_i = n_s . \quad (16)$$

Definite maxima are observed for all temperatures tested. As is apparent from the time frames of figures 14-17, the decay in n_g is due to the growth coalescence of clusters. This behavior has also been observed by Donahoe and Robbins (Au/NaCl) (ref. 22), Hamilton and Logel (Ag/C, Pd/C) (ref. 23), and Corbett and Boswell (Ag/MoS₂) (ref. 24). The maximum cluster size is also shown to decrease with increasing temperature as was also observed by Poppa for (Bi/C, Ag/C) (ref. 25). The most probable size of clusters for the maxima at $T = 300$ K and $t = 5.5$ sec. is approximately 2-3 adatoms. The initial slope of these curves is the nucleation rate which is given by

$$T_0 = z \sigma^* \frac{R}{v_0} i^{*+1} \exp \left[\frac{E_i^* + (i^{*+1}) \Delta H_{ads} - Q_d}{KT} \right] \quad (17)$$

where z is the Zeldovitch factor, σ^* is the capture number, E_i^* is the cluster energy, and i^* is the critical cluster size.

In experiment 6, we studied the effects of annealing. In a similar manner to the ordering that occurs in experiment 2, the annealing of a given deposition of growth proceeds by surface diffusion or monologue exchange between clusters (Ostwald ripening). As discussed previously, cluster peripheral motion may also occur to effect an increase in the order of the growth. Figure 20(a) illustrates the initial growth condition used in our study. Then with $R_d = 0$, the substrate temperature is increased. Each island or cluster is driven to maximize its number of nearest neighbors giving rise to more ordered arrangements as shown in figures for the anneal temperatures of $T = 600$ and $t = 700$ K. Note that the number of smaller nuclei has not noticeably decreased. Figure 19 shows the effect of temperature on the average density of the clusters. This same sort of behavior was observed by Donahoe and Robins for the Au/NaCl system. Annealing at deposition temperature did not seem to have a significant effect even for large times. However, when the temperature was increased the low density clusters ultimately broke up by monomer exchange to the larger more stable clusters.

In the (111) face we assumed that $\phi_2 = 0$ for ease of computation and results for the other crystal faces (111) and (110) are not yet available at this time.

ORIGINAL PAGE IS
OF POOR QUALITY

THREE-DIMENSIONAL CONCEPTS AND EXTENSIONS OF MODEL

In order to get away from a SOS model one must get involved with the three-dimensional geometry of crystal growth. With this purpose in mind, consider figure 21 which illustrates a set of orthogonal axes with basis vectors $\vec{e}_1 = \frac{a_0}{2} \hat{i}$, $\vec{e}_2 = \frac{a_0}{2} \hat{j}$, $\vec{e}_3 = \frac{a_0}{2} \hat{k}$ together with a cubic (P), body centered (I) and face centered (F) lattices.

For the simple cubic lattice all crystal lattice sites are given by

$$\vec{r} = 2\ell \vec{e}_1 + 2m\vec{e}_2 + 2n\vec{e}_3$$

where ℓ , m , n are integers. From any lattice point there are six nearest neighbor (NN) positions given by the directions $\pm (\vec{n}_1, \vec{n}_2, \vec{n}_3)$ where $\vec{n}_1 = 2\vec{e}_1$, $\vec{n}_2 = 2\vec{e}_2$, $\vec{n}_3 = 2\vec{e}_3$. There are 12 second nearest neighbors (SNN) given by the directions $\pm (\vec{s}_1, \vec{s}_2, \vec{s}_3, \vec{s}_4, \vec{s}_5, \vec{s}_6)$ where $\vec{s}_1 = \vec{n}_1 + \vec{n}_2$, $\vec{s}_2 = \vec{n}_2 + \vec{n}_3$, $\vec{s}_3 = \vec{n}_1 + \vec{n}_3$, $\vec{s}_4 = \vec{n}_1 - \vec{n}_3$, $\vec{s}_5 = \vec{n}_2 - \vec{n}_3$, $\vec{s}_6 = \vec{n}_1 - \vec{n}_2$. There are 8 third nearest neighbors (TNN) given by $\pm (\vec{t}_1, \vec{t}_2, \vec{t}_3, \vec{t}_4)$ where $\vec{t}_1 = \vec{n}_1 + \vec{n}_2 + \vec{n}_3$, $\vec{t}_2 = \vec{n}_1 - \vec{n}_2 + \vec{n}_3$, $\vec{t}_3 = \vec{n}_1 + \vec{n}_2 - \vec{n}_3$, $\vec{t}_4 = \vec{n}_1 - \vec{n}_2 - \vec{n}_3$.

For the body centered cubic lattice, all sites are given by

$$\vec{r} = 2\ell \vec{e}_1 + 2m\vec{e}_2 + 2n\vec{e}_3, \quad \ell, m, n \text{ integers}$$

together with the set of points

$$\vec{r} = (2I+1)\vec{e}_1 + (2J+1)\vec{e}_2 + (2K+1)\vec{e}_3, \quad I, J, K \text{ integers.}$$

For the neighboring atoms about a given point we have the following directions:

NN directions (8 total) $\pm (\vec{n}_1, \vec{n}_2, \vec{n}_3, \vec{n}_4)$

$$\vec{n}_1 = \vec{e}_1 + \vec{e}_2 + \vec{e}_3, \quad \vec{n}_2 = \vec{e}_1 + \vec{e}_2 - \vec{e}_3, \quad \vec{n}_3 = \vec{e}_1 - \vec{e}_2 + \vec{e}_3$$

$$\vec{n}_4 = \vec{e}_1 - \vec{e}_2 - \vec{e}_3$$

SNN directions (6 total) $\pm (\vec{s}_1, \vec{s}_2, \vec{s}_3)$

ORIGINAL PAGE IS
OF POOR QUALITY

$$\vec{s}_1 = 2\vec{e}_1, \quad \vec{s}_2 = 2\vec{e}_2, \quad \vec{s}_3 = 2\vec{e}_3$$

TNN directions (12 total) $\pm (\vec{t}_1, \vec{t}_2, \vec{t}_3, \vec{t}_4, \vec{t}_5, \vec{t}_6)$

$$\vec{t}_1 = \vec{s}_1 + \vec{s}_2 \quad \vec{t}_4 = \vec{s}_2 - \vec{s}_3$$

$$\vec{t}_2 = \vec{s}_1 + \vec{s}_3 \quad \vec{t}_5 = \vec{s}_1 - \vec{s}_3$$

$$\vec{t}_3 = \vec{s}_2 + \vec{s}_3 \quad \vec{t}_6 = \vec{s}_1 - \vec{s}_2$$

Similarly, we find for the face centered cubic crystal that all lattice sites are given by

$$\vec{r} = 2\ell \vec{e}_1 + 2m\vec{e}_2 + 2n\vec{e}_3, \quad \ell, m, n \text{ integers}$$

together with the set of points

$$\left. \begin{aligned} \vec{r} &= (2I+1)\vec{e}_1 + (2J+1)\vec{e}_2 + 2K\vec{e}_3 \\ \vec{r} &= 2I \vec{e}_1 + (2J+1)\vec{e}_2 + (2K+1)\vec{e}_3 \\ \vec{r} &= (2I+1)\vec{e}_1 + 2J\vec{e}_2 + (2K+1)\vec{e}_3 \end{aligned} \right\} \quad I, J, K \text{ integers}$$

For the neighboring adatoms we have:

NN directions (12 total) $\pm (\vec{n}_1, \vec{n}_2, \vec{n}_3, \vec{n}_4, \vec{n}_5, \vec{n}_6)$

$$\vec{n}_1 = \vec{e}_1 + \vec{e}_2 \quad \vec{n}_4 = \vec{e}_1 - \vec{e}_3$$

$$\vec{n}_2 = \vec{e}_2 + \vec{e}_3 \quad \vec{n}_5 = \vec{e}_2 - \vec{e}_3$$

$$\vec{n}_3 = \vec{e}_1 + \vec{e}_3 \quad \vec{n}_6 = \vec{e}_2 - \vec{e}_1$$

SNN directions (6 total) $\pm (\vec{s}_1, \vec{s}_2, \vec{s}_3)$

$$\vec{s}_1 = 2\vec{e}_1, \quad \vec{s}_2 = 2\vec{e}_2, \quad \vec{s}_3 = 2\vec{e}_3$$

TNN directions (24 total) $\pm (\vec{t}_1, \vec{t}_2, \vec{t}_3, \vec{t}_4, \dots, \vec{t}_{12})$

$$\vec{t}_1 = 2\vec{e}_1 + \vec{e}_2 + \vec{e}_3$$

$$\vec{t}_2 = 2\vec{e}_1 + \vec{e}_2 - \vec{e}_3$$

$$\vec{t}_3 = \vec{e}_1 + 2\vec{e}_2 + \vec{e}_3$$

$$\vec{t}_4 = \vec{e}_1 + 2\vec{e}_2 - \vec{e}_3$$

$$\vec{t}_5 = \vec{e}_1 + \vec{e}_2 + 2\vec{e}_3$$

$$\vec{t}_6 = \vec{e}_1 + \vec{e}_2 - 2\vec{e}_3$$

$$\vec{t}_7 = -2\vec{e}_1 + \vec{e}_2 + \vec{e}_3$$

$$\vec{t}_8 = -2\vec{e}_1 + \vec{e}_2 - \vec{e}_3$$

$$\vec{t}_9 = -\vec{e}_1 + 2\vec{e}_2 + \vec{e}_3$$

$$\vec{t}_{10} = -\vec{e}_1 + 2\vec{e}_2 - \vec{e}_3$$

$$\vec{t}_{11} = -\vec{e}_1 + \vec{e}_2 + 2\vec{e}_3$$

$$\vec{t}_{12} = -\vec{e}_1 + \vec{e}_2 - 2\vec{e}_3$$

For a three-dimensional model of crystal growth we imagine an infinite number of lattice sites of one of the three types discussed. We assign some initial geometry of occupied sites in the first octant and assume symmetry conditions at the boundaries which separate the first octants from the other (in order to simplify the upcoming bookkeeping). Each occupied site has a potential determined by the number of NN, SNN, and TNN sites which are occupied and we write

$$U(i,j,k) = NN_{ijk} \phi_1 + SNN_{ijk} \phi_2 + TNN_{ijk} \phi_3$$

Note that the maximum potential when all bonds are in effect are given by:

$$\text{SC: } U = 6\phi_1 + 12\phi_2 + 8\phi_3$$

$$\text{BCC: } U = 8\phi_1 + 6\phi_2 + 12\phi_3$$

$$\text{FCC: } U = 12\phi_1 + 6\phi_2 + 24\phi_3$$

(18)

Here (ϕ_1) SC does not equal (ϕ_1) BCC which does not equal (ϕ_1) FCC. The symbol ϕ_1 is used to denote the nearest neighbor bond associated with a fixed crystal type. Similar considerations hold for the SNN and TNN bonds ϕ_2, ϕ_3 .

Having defined an initial geometry we can label those occupied crystal sites, where the total bond structure is incomplete, as occupied surface sites (OSS). Those lattice sites which are unoccupied, and which are needed to complete the bonding of OSS, are labeled unoccupied surface sites (USS). Consider only those OSS and USS in the first octant. We can randomly deposit adatoms onto USS and convert these sites to OSS or bulk surface sites and simultaneously update the potentials at all NN, SNN, and TNN sites effected by the deposition as well as recording of the creation of any new USS. We can also scan all OSS and assign a random thermal energy to the potentials at these sites and determine whether the adatoms at these sites remain localized, migrate to NN or SNN sites, incorporate or evaporate. Again, the recording of all potential changes of the sites involved, as well as the updating of OSS and USS locations, must be performed.

In order to analyze the three-dimensional growth, the following is proposed: Consider the plans illustrated in figure 10 which have direction numbers $[h_1, h_2, h_3]$. This plane passes through the point $(Ia, 0, 0)$ and can be expressed

$$h_1x + h_2y + h_3z = Ih_1a \quad (19)$$

where I is an fixed integer and h_1, h_2, h_3 are integers. We next construct the vectors $\vec{A}, \vec{B}, \vec{C}$ which also lie in the plane and are defined as

$$\begin{aligned} \vec{A} &= -h_1\vec{e}_3 + h_3\vec{e}_1 \\ \vec{B} &= -h_1\vec{e}_2 + h_2\vec{e}_1 \\ \vec{C} &= h_2\vec{e}_3 - h_3\vec{e}_2 \end{aligned} \quad (20)$$

Let $\vec{r}_0 = 2I\vec{e}_1$ be a vector to $(Ia, 0, 0)$. Then, to determine all lattice sites in this plane, we determine rational numbers f, g such that for a given crystal structure,

$$\vec{r} = \vec{r}_0 + f\vec{B} + g\vec{A} = x\vec{e}_1 + y\vec{e}_2 + z\vec{e}_3$$

where x, y, z are lattice sites. In the case of a simple cubic crystal we would require that

$$2I\vec{e}_1 + f(h_1\vec{e}_2 - h_2\vec{e}_1) + g(h_1\vec{e}_3 - h_3\vec{e}_1) = 2\ell\vec{e}_1 + 2m\vec{e}_2 + 2n\vec{e}_3$$

where $I, h_1, h_2, h_3, \ell, m, n$ are integers. This equation requires that

$$2I - fh_2 - gh_3 = 2\ell$$

$$fh_1 = 2m$$

$$gh_1 = 2n$$

For these equations to possess integer solutions, ℓ, m, n must satisfy

$$hI = h_1\ell + h_2m + h_3n \quad (21)$$

Consider first the case $I = 0$, then integer solutions (ℓ, m, n) to $h_1\ell + h_2m + h_3n = 0$ are given by the points $A = (h_3, 0, \bar{h}_1)$, $B = (h_2, \bar{h}_1, 0)$ and $C = (0, h_3, \bar{h}_2)$. These points define the primitive vectors $\vec{A}, \vec{B}, \vec{C}$ in (20) and the primitive cells in figure 22. The primitive cell A, \bar{B} has a maximum of (h_1-1) interior solutions. Similarly, the primitive cells \bar{B}, \bar{C} and \bar{A}, \bar{C} have a maximum of h_2-1 and h_3-1 solutions. In the primitive \bar{A}, \bar{B} cell of figure 22, we let n take on the integer values from 1 to (h_1-1) . For a fixed value of n we let m vary from $\bar{1}$ to (\bar{h}_1-1) and find the integer solution for the other variable ℓ . A similar analysis applies to the primitive cells \bar{B}, \bar{C} and \bar{A}, \bar{C} .

Example: Consider the (295) plane of a simple cubic crystal. Here we want integer solutions (ℓ, m, n) to the equation

$$2\ell + 9m + 5n = 0$$

We take the obvious solutions $(0, 0, 0)$, $A = (5, 0, \bar{2})$, $B = (9, \bar{2}, 0)$ and $C = (0, 5, \bar{9})$ and construct primitive cells. For the \bar{A}, \bar{B} cell we let $n = \bar{1}$ and let $m = \bar{1}$ (only one solution) and solve for ℓ . Thus we develop for

$n = \bar{1}$ the equation, $2\ell + 9m - 5 = 0$ with the solution of $(7, \bar{1}, \bar{1})$. Other solutions are $(7 - 9K, \bar{1} - 2K, \bar{1})$. $K = \pm 0, 1, 2, \dots$. Similarly, for the \vec{A}, \vec{C} primitive cell, we let $\ell = 1, 2, 3, 4$ and $m = 1, 2, 3, 4$ and we solve for n . Thus:

for $\ell = 1$, $2 + 9m + 5n = 0$ and for $m = 1, 2, 3, 4$ we find $(1, 2, \bar{4})$ is the solution with $(1, 2 + 5K, -4 - 9K)$ as the general solution;

for $\ell = 2$ $(4 + 9m + 5n = 0) \rightarrow (2, 4, \bar{8}) \rightarrow (2, 4 + 5K, -8 - 9K)$;

for $\ell = 3$, $6 + 9m + 5n = 0 \rightarrow (3, 1, \bar{3}) \rightarrow (3, 1 + 5K, \bar{3} - 9K)$;

for $\ell = 4$, $8 + 9m + 5n = 0 \rightarrow (4, 3, \bar{7}) \rightarrow (4, 3 + 5K, -7 - 9K)$;

For the \vec{B}, \vec{C} primitive cell we let $n = \bar{1}, \bar{2}, \bar{3}, \bar{4}, \bar{5}, \bar{6}, \bar{7}, \bar{8}$ and $\ell = 1, 2, 3, 4, 5, 6, 7, 8$ and solve for integer solutions m . This gives

$$n = -1, 2\ell + 9m - 5 = 0 \rightarrow (7, \bar{1}, \bar{1}) \rightarrow (7, + 9K, \bar{1} - 2K, \bar{1})$$

$$n = -2, 2\ell + 9m - 10 = 0 \rightarrow (5, 0, \bar{2}) \rightarrow (5 + 9K, - 2K, \bar{2})$$

$$n = -3, 2\ell + 9m - 15 = 0 \rightarrow (3, 1, \bar{3}) \rightarrow (3 + 9K, 1 - 2K, \bar{3})$$

$$n = -4, 2\ell + 9m - 20 = 0 \rightarrow (1, 2, \bar{4}) \rightarrow (1 + 9K, 2 - 2K, \bar{4})$$

$$n = -5, 2\ell + 9m - 25 = 0 \rightarrow (8, 1, \bar{5}) \rightarrow (8 + 9K, 1 - 2K, \bar{5})$$

$$n = -6, 2\ell + 9m - 30 = 0 \rightarrow (6, 2, \bar{6}) \rightarrow (6 + 9K, 2 - 2K, \bar{6})$$

$$n = -7, 2\ell + 9m - 35 = 0 \rightarrow (4, 3, \bar{7}) \rightarrow (4 + 9K, 3 - 2K, \bar{7})$$

$$n = -8, 2\ell + 9m - 40 = 0 \rightarrow (2, 4, \bar{8}) \rightarrow (2 + 9K, 4 - 2K, \bar{8})$$

The example illustrates that we can determine and count the coverage of a given region in a given plane. A similar counting procedure can be established for all parallel regions in planes parallel to a given plane as in figures 10(b-c). We can then plot coverage vs. distance as we move outward on parallel planes. Eventually, the coverage becomes zero and we can stop our counting procedure. Those directions for which the coverage vs.

distance curves are like step functions, can be labeled as preferred directions of growth. Also the distance in these directions (number of growth planes measured from some reference) will increase with time at a faster rate than other nonpreferred growth directions. During the simulation of a three-dimensional crystal growth only the lower ordered planes need to be considered as the majority of the growth occurs on these planes.

CONCLUSIONS

An SOS Monte Carlo computer simulation utilizing a potential scaling technique has been developed to model the initial stages of thin film growth. The model makes use of ordered statistics to simulate the surface activity of a 20×20 array with periodic boundary conditions. Adsorption, desorption, surface migration, incorporation and substrate atom diffusion to the surface are considered. The results of several computer experiments show consistency with the expected behavior of thin-film growth. Surface migration data taken at different substrate temperatures returned the activation energy as determined by an Arrhenius plot. Dispersed adatoms were observed to cluster into dimers, trimers, and finally a single cluster in its most stable configuration. A point defect was designed by varying the interaction potential in the x, y, z directions and illustrated that preferred growth occurred at such defects. This suggests a technique for studying such defects.

The experimentation, with varying deposition rate and substrate temperature, modeled the expected behavior of thin film growth by nucleation, cluster growth and then coalescence of clusters. The nucleation rate was proportional to the square of the deposition rate in agreement with the atomic theory of nucleation. Finally, annealing experiments showed the time ordering of clusters with increased temperatures.

By adjusting the potential interaction changes and by varying the initial geometry and type of surface adatoms, various A-B crystal growth models can be investigated. The choice of the A on B, A on A, B on B or B on A interaction should produce interesting types of thin film growth phenomenon, and this area still has to be investigated. Also three-dimensional extensions will require large computer times and storage, but the basic scanning, testing and updating of potentials will be the main concern.

ACKNOWLEDGEMENTS

The author would like to thank R.A. Outlaw, the grant technical monitor and G.H. Walker, for their help and discussions in the foundation of the Monte Carlo model for the simulation of crystal growth. The author would also like to thank Claudia B. Speller and Marc Seguinot of the Old Dominion University Research Foundation for the preparation of this report.

REFERENCES

1. Heinbockel, J.H.; Outlaw, R.A.; and Walker, G.H.: A Potential Scaling Model Simulating the Initial Stages of Thin-Film Growth, NASA TP Sept. 1982.
2. Abraham, F.F.; and White, G.M.: Computer Simulation of Vapor Deposition on Two-Dimensional Lattices. *J. Appl. Phys.*, Vol. 41, No. 4, March 15, 1970, pp. 1841-1849.
3. Gilmer, G.H.: Simulation of Crystal Growth from the Vapor. Proc. 1976 Internat'l. Conf. on Computer Simulation for Materials Applications, April 19-26, 1976, Nat'l. Bureau of Standards (Gaithersburg, Md.), Arsenault, R.J.; Beller, J.R., Jr.; and Simmons, J.A., eds.
4. Gilmer, G.H.: Computer Models of Crystal Growth. *Science*, Vol. 28, 1980, pp. 355-363.
5. Gilmer, G.H.: Transients in the Rate of Crystal Growth. *J. Crystal Growth*, Vol. 49, 1980, pp. 465-474.
6. Weeks, J.D.; and Gilmer, G.H.: Dynamics of Crystal Growth. In: *Advances in Chemical Physics*, Vol. 40, John Wiley & Sons (N.Y.), 1979.
7. Leamy, H.J.; Gilmer, G.H.; and Jackson, K.A.: Statistical Thermodynamics of Clean Surfaces. In: *Surface Physics of Materials I*. Blakely, J.M., ed., Academic Press (N.Y.), 1975.
8. Van der Erden, J.P.; Bennema, P.; and Cherepanova, T.A.: Survey of Monte Carlo Simulations of Crystal Surfaces and Crystal Growth, *Progress in Crystal Growth and Characterization*, Vol. 1, B.R. Pamplin editor, 1978, pp. 219-254.
9. Gilmer, G.H.; and Bennema, P.: Simulation of Crystal Growth with Surface Diffusion. *J. Appl. Phys.*, Vol. 43, No. 4, April 1972, pp. 1347-1360.
10. Singh, J.; and Madhukar, A.: Monte Carlo Simulation of the Growth of $A_{1-x}B_x$ Layers on Lattice Matched Substrates in Molecular Beam Epitaxy, *J. Vac. Sci. Technol.*, Vol. 20, No. 3, March 1982.
11. Johansson, T; and Persson, B.: Computer Simulation of Nucleation and Growth of Atom Clusters in Thin Films, *Physica Scripta*, Vol. 2, 309-312, 1970.
12. Van der Erden, J.P.; Van Leeuwen, C.; Bennema, P.; Van der Kruk, W.L.; and Veltman, B.P.: Crystal Growth: A Comparison of Monte Carlo Simulation Nucleation and Normal Growth Theories, *J. Appl. Physic*, Vol. 48, No. 6, June 1977.
13. Barton, W.K.; Gabrera, N.; and Frank, F.C.: The Growth of Crystals and the Equilibrium Structure of their Surfaces. *Phil. Trans. R. Soc. (London)*, Vol. 243A, 1951, pp. 299-358.

14. Gevers, R.: The Advance of Mono-Molecular Steps on the Surface of a Growing Kossel Crystal as a Random Walk Problem, *Physica*, Vol. 22, pp. 832-842, 1956.
15. Lewis, B.; Anderson, J.C.: Nucleation and Growth of Thin Films, Academic Press (N.Y.), 1978.
16. Chopra, K.L.: Thin Film Phenomena. McGraw Hill Book Company (N.Y.), 1969.
17. Hogg, R.V.; and Craig, A.T.: Introduction to Mathematical Statistics, 3rd edition, MacMillan Co., 1970.
18. Neumann, G.; and Neumann, G.M.: Surface Self-Diffusion of Metals, Diffusion Monograph Series. F.H. Wohlbiel editor, 1972.
19. Van Hove, M.A.: Surface Crystallography and Bonding, Chapter 4 The Nature of the Surface Chemical Bond, North Holland, 1979.
20. Torrens, I.M.: Interatomic Potentials. New York: Academic Press, 1978.
21. Psinz, G.A., Ferrari, J.M.; and Goldenberg, M.: Molecular Beam Epitaxial Growth of Single-Crystal Al Films on GaAs (110) *Appl. Physics Lett.*, 40(2), Jan. 1982.
22. Donohoe, A.J.; and Robbins, J.L.: Mobility and Coalescence of Nuclei in Metal Vapor Deposition on Alkali Halide Substrates. *J. of Crystal Growth*, Vol. 17, 1972, p. 70.
23. Hamilton, J.F.; Loyel, P.C.: Nucleation and Growth of Ag and Pd on Amorphous Carbon by Vapor Deposition. *Thin Solid Films*, Vol. 16, 1973, p. 49.
24. Corbett, J.M.; and Boswell, F.W.: Experimental Investigations of Nucleation of Ag on Molybdenite. *J. of Applied Physics*, Vol. 40, 1969, p. 2663.
25. Poppa, H.: Heterogeneous Nucleation of Bi and Az on Amorphous Substrates (In situ Electron Microscopy Studies) *J. of Applied Physics*, Vol. 38, 1967, p. 3882.

APPENDIX: COMPUTER PROGRAM

The following computer program is representative of that used in the studies of this report. It evolved from earlier models and is currently undergoing changes in order to better simulate and model AB, AA, BA, and BB types of crystal growth. Graphics output is illustrated in figure 23.

ORIGINAL PAGE IS
OF POOR QUALITY

```
PROGRAM CRYSTAL(INPUT,OUTPUT,TAPE5=INPUT,TAPE6=OUTPUT,SSET,  
1TAPE7=SSET)  
COMMON/BLK1/H, EPS(30,30), ITRAC(30,30,20)  
COMMON/BLK2/UO,UM,UE,UOS,UMS,UES,DELT  
COMMON/BLK3/XLAM,TSNAP,M,T, TMIG,IEVAP,ICREAT  
COMMON/BLK4/FAA(9),D(9),FAB(9),FBA(9),DS(9),FBB(9)  
COMMON/BLK5/LAYER(30,30)  
COMMON/BLK6/N1,N2,LETA,M2, LAST  
COMMON/BLK7/PHI1,PHI2,PHI3,PHIO,J,PHS1,PHS2,PHS3,PHSO  
COMMON/BLK8/ISWTCH  
COMMON/BLK9/A,AS,EVIB,EVIBS,RD  
COMMON/BLK10/LL1,LL2,U1,MAXH,TA,TB  
INTEGER H(30,30)  
NAMelist/PARAM/M,J,T,DELT,MO,NO,MOS,NOS,PHIO,PHSO,  
1RD,TSNAP,ISWTCH,A,AS,TSTOP,UO,UM,UE,UOS,UMS,UES,U1  
C NAMelist VARIABLES M=20 IS SIZE OF ARRAY,J=1(100)SURFACE,J=2(111)SUR  
C J=3(110)SURFACE,T=TEMP DEG K,DELT=TIME INTERVAL OF SCAN,NO,MO MIE  
C POTENTIAL OF GROWING MATL,MOS,NOS,MIE POTENTIALS FOR SUBSTRATE  
M=20 $ J=1 $ T=500. $ DELT=1.0E-4 $ MO=4 $ NO=10  
MOS=4 $ NOS=10 $ PHIO=2.17 $ PHSO=2.17 $ TREF=300. $ TSTOP=2.  
RD=200. $ TSNAP=.1 $ UO=-3.87 $ UOS=-3.87 $ UM=-1.  
UMS=-1. $ UE=0. $ UES=0. $ U1=1.7 $ A=5.61 $ AS=3.7  
ISWTCH=0  
C ISWTCH=1 GIVES PICTURES, ISWTCH=0 NO PICTURES IF ISWTCH=0  
C SET R1=0 IN JCL AND IF ISWTCH=1,SET R1=0 IN JCL(AFTER LGO)  
C INTERACTION WITH SUBSTRATE,PHIO=HEAT EVAP-HEAT ADSORPTION, PHSO IS PHIO  
C OF SUBSTRATE SURFACE, RD=RATE OF ADATOM DEPOSIT,ADATOMS/SEC,  
C A,AS,CRYSTAL LATTICE SPACING,TSTOP=STOP TIME,UO=HEAT EVAP,UM=  
C MIGRATION BARRIER,ASSUMED CONSTANT,UE=0 IS EVAP REFERENCE,U1 NOT USED NOW  
C POTENTIAL ENERGIES IN ELECT. VOLTS U EV=23KCAL/MOLE,M=20 FOR GRAPHICS  
CALL PSEUDO  
500 CONTINUE  
DO 12 II=1,30  
DO 13 JJ=1,30  
DO 14 KK=1,20  
ITRAC(II, JJ, KK)=0  
14 CONTINUE  
13 CONTINUE  
12 CONTINUE  
MAXH=1  
DO 8 II=1,30  
DO 9 JJ=1,30  
H(II, JJ)=0  
EPS(II, JJ)=0.  
LAYER(II, JJ)=0  
9 CONTINUE  
8 CONTINUE  
READ(5,PARAM)  
IF(EOF(5)) 600,601
```

ORIGINAL PAGE IS
OF POOR QUALITY

```
600 WRITE(6,603)
603 FORMAT(1X,28HEND OF FILE ENCOUNTERED-HELP )
    CALL CALPLT(0.0,0.0,999)
    STOP 6666
601 CONTINUE
    LL1=
    M2=M*M
    LL2=2+M
    CALL SETUP(MOS,NOS,PHS1,UOS,UMS,TREF,PHSO ,J,ALPHA2,ALPHA3)
    PHS2=ALPHA2*PHS1
    PHS3=ALPHA3*PHS1
    CALL SETUP(MO,NO,PHI1,UD ,UM,TREF,PHIO,J,ALPHA2,ALPHA3)
    PHI2=ALPHA2*PHI1
    PHI3=ALPHA3*PHI1
C M=SIDE OF SQUARE ARRAY M MAX=60
    TMIG=0
    XLAM=RD*DELT
    IEVAP=0
    ICREAT=0
C INITIALIZE SUBSTRATE GEOMETRY AND POTENTIALS
    DO 11 JJ=1,30
    DO 10 II=1,30
10  LAYER(II,JJ)=0
11  CONTINUE
    CALL INITIAL
    EMEAN=T*(8.62E-5)
    QD=UM-UO-PHIO
    WRITE(6,399)
    WRITE(6,400) J,DELT,RD,T,M
    WRITE(6,401) M2 ,XLAM ,EMEAN,TSNAP,TSTOP
    WRITE(6,402) PHI1,PHI2,PHI3,PHIO,ALPHA2
    WRITE(6,403) PHS1,PHS2,PHS3,PHSO,ALPHA3
    WRITE(6,404) UD,UM,UE,A,U1
    WRITE(6,405) UOS,UMS,UES,AS,QD
    WRITE(6,407)MO,NO,MOS,NOS
    WRITE(6,406) FBB,FAA,D,DS
407  FORMAT(T5,3HMO=,I3,T15,3HNO=,I3,T25,4HMOS=,I3,T35,4HNOS=,I3)
399  FORMAT(1X,15HPARAMETERS ARE: )
400  FORMAT(T10,2HJ=,I3,T34,5HDELT=,1PE14.7,T63,3HRD=,0PF7.1,T91,2HT=,
1F8.1,T118,2HM=,I5)
401  FORMAT(T6,6H M2 =,I6 ,T33,6HXLAM =,E14.6,T60,6HEMEAN=,F8.4,T90,
16HTSNAP=,F5.3,T114,6HTSTOP=,F7.1 )
402  FORMAT(T7,5HPHI1=,F10.4,T34,5HPHI2=,F10.4,T61,5HPHI3=,F10.4,T88,
15HPHIO=,F10.4,T113,7HALPHA2=,F10.4)
403  FORMAT(T7,5HPHS1=,F10.4,T34,5HPHS2=,F10.4,T61,5HPHS3=,F10.4,T88,
15HPHSO=,F10.4,T112,7HALPHA3=,F10.4 )
404  FORMAT(T9,3HUD=,F10.4,T36,3HUM=,F10.4,T63,3HUE=,F10.4,T91,2HA=,
1F10.4 ,T115,5HHADS=,F7.3 )
405  FORMAT(T8,4HUOS=,F10.4,T35,4HUMS=,F10.4,T62,4HUES=,F10.4,T90,
```

ORIGINAL PAGE IS
OF POOR QUALITY

```
13HAS=,F10.4 ,T117,3HQD=,F7.3)
406  FORMAT(T10,4HFBB=,9(2X,F8.4),/,T9,4HFAA=,9(2X,F8.4),/,T10,2HD=,
19(2X,F8.4),/,T9,3HDS=,9(2X,F8.4),/// )
WRITE(6,408)FAB,FBA
408  FORMAT(T10,4HFAB=,9(2X,F8.4),/,T10,4HFBA=,9(2X,F8.4))
WRITE(6,308)
308  FORMAT(1H1)
CALL STOFIN(0,TSTOP)
GO TO 500
END
SUBROUTINE GROW(ITHREE)
COMMON/BLK5/LAYER(30,30)
DIMENSION X1(4),X2(4),Y1(4),Y2(4)
SF=20./3.
X1(3)=0.
Y1(3)=0.
X1(4)=SF
Y1(4)=SF
X2(3)=0.
Y2(3)=0.
X2(4)=SF
Y2(4)=SF
IF(ITHREE.EQ.1) CALL CALPLT(0.0,12.0,-3)
FS=3./20.
IF(ITHREE.EQ.1)GO TO 1
CALL CALPLT(0.0,-4.0,-3)
GO TO 4
1  CALL CALPLT(0.0,-3.0,-3)
4  CONTINUE
CALL GRID(0.0,0.0,FS,FS,20,20)
C  GRID COMPLETE SHADE IN LEVELS
DO 10 II=3,22
DO 15 JJ=3,22
IH=MOD(LAYER(II,JJ),4)
IF(IH.EQ.3)GO TO 15
X1(1)=II-3
Y1(1)=JJ-2
X1(2)=II-2
Y1(2)=JJ-2
X2(1)=II-3
Y2(1)=JJ-3
X2(2)=II-2
Y2(2)=JJ-3
C  SHADE AREA BTWN POINTS
INT=1+IH+2*(IH-1)*IH
CALL HAFTONE(X1,Y1,2,X2,Y2,2,INT)
15  CONTINUE
10  CONTINUE
IF(ITHREE.LT.3)RETURN
```

ORIGINAL PAGE IS
OF POOR QUALITY

```
CALL NFRAME
ITHREE=0
RETURN
END
SUBROUTINE SETUP(MO,NO,APHI,AUD,AUM,AT,APH,JA,ALPHA2,ALPHA3)
PHID=APH
J=JA
UD=AUD
UM=AUM
T=AT
R1=1./SQRT(2.)
R2=1./SQRT(3.)
R3=FLOAT(NO)/FLOAT(MO)
A21=(R1**NO)-R3*(R1**MO)
A31=(R2**NO)-R3*(R2**MO)
D1=1.-R3
A2=A21/D1
A3=A31/D1
IF(J.EQ.2)GO TO 111
IF(J.EQ.3)GO TO 110
C 100 FACE
ALPHA2=A2
ALPHA3=0.
PHI1=PHID/(1.+ALPHA2)
PHI1=PHI1/4.
GO TO 12
111 ALPHA2=A3
ALPHA3=0.
PHI1=PHID/(6.+2.*ALPHA2)
GO TO 12
110 ALPHA2=A2
ALPHA3=A3
PHI1=PHID/(2.*(1.+ALPHA2)+4.*ALPHA3)
12 CONTINUE
PHI1=-PHI1
APHI=PHI1
RETURN
END
SUBROUTINE FACE(F,D,A,J,PHI1,PHI2,PHI3,PHIO,EVIB,T)
DIMENSION F(9),D(9)
A2=A/SQRT(2.)
A3=A/SQRT(2./3.)
C PHI1,PHI2,PHI3 SHOULD BE NEGATIVE
C J=1,2 OR 3
IF(J.EQ.3) GO TO 110
IF(J.EQ.2) GO TO 111
100 DO 16 IJ=1,4
IK=2*IJ-1
IL=2*IJ
```

ORIGINAL PAGE IS
OF POOR QUALITY

```
D(IK)=A
D(IL)=A2
F(IK)=PHI2
16 F(IL)=PHI1
F(9)=PHI0
GO TO 10
111 DO 17 IJ=2,4
D(IJ)=A2
D(IJ+4)=A2
F(IJ)=PHI1
17 F(IJ+4)=PHI1
D(1)=A3
D(5)=A3
F(1)=PHI2
F(5)=PHI2
F(9)=PHI0
GO TO 10
110 DO 18 IJ=1,4
IK=2*IJ-1
D(IK)=A3
18 F(IK)=PHI3
D(2)=A2
D(6)=A2
D(4)=A
D(8)=A
F(2)=PHI1
F(6)=PHI1
F(4)=PHI2
F(8)=PHI2
F(9)=PHI0
10 CONTINUE
EVIB=T*(8.62E-5)
D(9)=0.
RETURN
END
SUBROUTINE INITIAL
COMMON/BLK1/H, EPS(30,30), ITRAC(30,30,20)
COMMON/BLK2/UO, UM, UE, UOS, LMS, UES, DELT
COMMON/BLK3/XLAM, TSNAP, M, T, TMIG, IEVAP, ICREAT
COMMON/BLK4/FAA(9), D(9), FAB(9), FBA(9), DS(9), FBB(9)
COMMON/BLK5/LAYER(30,30)
COMMON/BLK6/N1, N2, LETA, M2, LAST
COMMON/BLK7/PHI1, PHI2, PHI3, PHI0, J, PHS1, PHS2, PHS3, PHS0
COMMON/BLK8/ISWTCH
COMMON/BLK9/A, AS, EVIB, EVIBS, RD
COMMON/BLK10/LL1, LL2, U1, MAXH, TA, TB
C M=ARRAY SIZE
C INITIALIZE SUBSTRATE GEOMETRY AND HEIGHTS H
INTEGER H(30,30)
```

ORIGINAL PAGE 13
OF POOR QUALITY

```

DO 312 IK=1,30
DO 311 IJ=1,30
ITRAC(IK,IJ,1)=0
311 H(IJ,IK)=1
312 CONTINUE
CALL FACE(FAA,DS,AS,J,PHS1,PHS2,PHS3,PHSD,EVIBS,T)
CALL FACE(FBB,D,A,J,PHI1,PHI2,PHI3,PHIO,EVIB,T)
C CHECK SIGNS ON POTENTIALS
DO 20 II=1,9
FBA(II)=FAA(II)
FAB(II)=FBB(II)
20 CONTINUE
FBA(9)=FAA(9)+UD-UDS
FAB(9)=FBB(9)+UDS-UD
DO 41 IK=1,30
DO 40 IJ=1,30
40 EPS(IJ,IK)=UDS
41 CONTINUE
ITYPE=0
C ITYPE=0 SUBSTRATE MATERIAL A-TYPE
C ITYPE=1 GROWING MATERIAL B-TYPE
C FLAT SURFACE FOR NOW
C THIS IS THE PLACE TO PUT IN GEOMETRY CHANGES INITIALIZING SUBSTRATE
C RADIUS OF CURVATURE EXPERIMENT INITIALIZED HERE. EXAMPLE:A LEFT EDGE
C DO 300 JJ=1,28
C 300 CALL ADATDM(FAA,LL1,JJ)
C THIS IS THE PLACE TO PUT IN A TRAP NEAR CENTER EPS(10,10)=UDS-TRAP
C FAA CORRECTED FOR FIRST LAYER ADDITION ONLY AFTER FIRST LAYER BUILD UP
WRITE(6,100)
100 FORMAT(1X,25HINITIAL SUBSTRATE HEIGHTS ,//)
DO 200 IJ=LL1,LL2
WRITE(6,101)(H(IJ,I),I=LL1,LL2)
101 FORMAT(10X,20I2)
200 CONTINUE
DO 201 IJ=LL1,LL2
WRITE(6,202) (EPS(IJ,I),I=LL1,LL2)
202 FORMAT(10X,20F6.2)
201 CONTINUE
RETURN
END
SUBROUTINE DIFF(II,JJ,DMIG,IN,JN)
COMMON/BLK1/H,EPS(30,30),ITRAC(30,30,20)
COMMON/BLK2/UD,UM,UE,UDS,UMS,UES,DELT
COMMON/BLK3/XLAM,TSNAP,M,T,THIG,IEVAP,ICREAT
COMMON/BLK4/FAA(9),D(9),FAB(9),FBA(9),DS(9),FBB(9)
COMMON/BLK5/LAYER(30,30)
COMMON/BLK7/PHI1,PHI2,PHI3,PHIO,J,PHS1,PHS2,PHS3,PHSD
COMMON/BLK8/ISWTC
COMMON/PLK10/LL1,LL2,U1,MAXH,TA,TB

```

ORIGINAL PA 113
OF POOR QUALITY

```

DIMENSION IV(8,2),IS(8,2),WW(8),Q(8)
INTEGER W(8)
INTEGER H(30,30)
IC=0
C   RANDOM WALK FROM SITE I TO NI
    DMIG=0.
C   FIND AVAILABLE SITES (IF ANY)
C   IS(8) IS LIST OF SAVED AVAILABLE SITES, IC IS NUMBER OF SITES
DO 10 IJK=1,8
W(IJK)=0.
10  CONTINUE
C   REMOVE ADATOM
    IJK=H(II,JJ)
    IF(IJK.LE.0)ITYPER=0
    IF(IJK.LE.0)GO TO 20
    ITYPER=ITRAC(II,JJ,IJK)
20  CONTINUE
    CALL SUBATOM(II,JJ,ITYPER)
    CALL XYX
    JJ1=JJ+1
    JJ0=JJ-1
    II1=II+1
    II0=II-1
    IF(JJ1.GT.22)JJ1=3
    IF(JJ0.LT.3)JJ0=22
    IF(II1.GT.22)II1=3
    IF(II0.LT.3)II0=22
C   FIND AVAILABLE MIGRATION SITES
    IQ=H(II,JJ)+1
    Q(1)=IQ-H(II,JJ1)
    IF(Q(1).LE.0)GO TO 400
    IC=IC+1
    IS(IC,1)=II
    IS(IC,2)=JJ1
    CALL PBOND(II,JJ1,W(IC),J)
400  Q(2)=IQ-H(II1,JJ)
    IF(Q(2).LE.0)GO TO 401
    IC=IC+1
    IS(IC,1)=II1
    IS(IC,2)=JJ
    CALL PBOND(II1,JJ,W(IC),J)
401  Q(3)=IQ-H(II,JJ0)
    IF(Q(3).LE.0)GO TO 402
    IC=IC+1
    IS(IC,1)=II
    IS(IC,2)=JJ0
    CALL PBOND(II,JJ0,W(IC),J)
402  Q(4)=IQ-H(II0,JJ)
    IF(Q(4).LE.0)GO TO 40?

```

```

IC=IC+1
CALL PBOND(IIO,JJ,W(IC),J)
IS(IC,1)=IIO
IS(IC,2)=JJ
403 Q(5)=IQ-H(IIO,JJ1)
IF(Q(5).LE.0)GO TO 404
IC=IC+1
IS(IC,1)=IIO
IS(IC,2)=JJ1
CALL PBOND(IIO,JJ1,W(IC),J)
404 Q(6)=IQ-H(II1,JJ1)
IF(Q(6).LE.0)GO TO 405
IC=IC+1
IS(IC,1)=II1
IS(IC,2)=JJ1
CALL PBOND(II1,JJ1,W(IC),J)
405 Q(7)=IQ-H(II1,JJ0)
IF(Q(7).LE.0)GO TO 406
IC=IC+1
IS(IC,1)=II1
IS(IC,2)=JJ0
CALL PBOND(II1,JJ0,W(IC),J)
406 Q(8)=IQ-H(IIO,JJ0)
IF(Q(8).LE.0)GO TO 407
IC=IC+1
IS(IC,1)=IIO
IS(IC,2)=JJ0
CALL PBOND(IIO,JJ0,W(IC),J)
407 CONTINUE
JL=4+2*(J-1)-3*(J-1)*(J-2)
C TEST IC
IF(IC.EQ.0)GO TO 500
C WEIGHTED RANDOM WALK
WT=0
IF(IC.EQ.1)GO TO 100
DD 408 IM=1,IC
WT=WT+W(IM)
408 WW(IM)=WT
DD 409 IM=1,IC
409 WW(IM)=WW(IM)/WT
R=URAN(0)
IM=1
411 IF(R.LE.WW(IM))MS=IM
IF(R.LE.WW(IM))GO TO 412
IM=IM+1
IF(IM.EQ.IC)MS=IC
IF(IM.EQ.IC)GO TO 412
GO TO 411
412 IN=IS(MS,1)

```

ORIGINAL PAGE IS
OF POOR QUALITY

```
JN=IS(MS,2)
GO TO 60
100 IN=IS(1,1)
    JN=IS(1,2)
    GO TO 60
500 CONTINUE
C    JUMP TO HIGHER LEVEL ONLY IF RANDOM ENERGY GREATER THAN
C    NEAREST NEIGHBOR BONDS - RANDOM WALK TO NN SITES
    R=URAN(0)
    MSITE=R*JL+2
    IF(MSITE .LE. JL)GO TO 567
C    NO MIGRATION
    IN=II
    JN=JJ
    DMIG=0
570 CALL ADATOM(IN,JN,ITYPER)
    RETURN
567 CONTINUE
    IV(1,1)=II
    IV(1,2)=JJ1
    IV(2,1)=II
    IV(2,2)=JJ0
    IV(3,1)=II1
    IV(3,2)=JJ
    IV(4,1)=II0
    IV(4,2)=JJ
    IV(5,1)=II1
    IV(5,2)=JJ1
    IV(6,1)=II0
    IV(6,2)=JJ0
    IN=IV(MSITE,1)
    JN=IV(MSITE,2)
    DMIG=D(MSITE)
60  CONTINUE
C    TEST FOR MIGRATION OVER BOUNDARIES
    IF(IN.LT.LL1)GO TO 70
    IF(IN.GT.LL2)GO TO 71
    IF(JN.LT.LL1)GO TO 72
    IF(JN.GT.LL2)GO TO 73
    GO TO 80
70  CONTINUE
    IF(JN.EQ.2)GO TO 74
    IF(JN.EQ.23)GO TO 75
    IN=22
    GO TO 80
74  IN=22
    JN=22
    GO TO 80
75  IN=22
```

```
JN=3
GO TO 80
71 IF(JN.EQ.2)GO TO 76
   IF(JN.EQ.23)GO TO 77
   IN=3
   GO TO 80
76 IN=3
   JN=22
   GO TO 80
77 IN=3
   JN=3
   GO TO 80
72 IF(IN.EQ.2)GO TO 74
   IF(IN.EQ.23)GO TO 76
   JN=22
   GO TO 80
73 IF(IN.EQ.2)GO TO 75
   IF(IN.EQ.23)GO TO 77
   JN=3
80 CONTINUE
   CALL ADATOM(IN,JN,ITYPER)
      DMIG=D(2)
   RETURN
   END
   SUBROUTINE PBOND(II,JJ,NNB,JCODE)
   COMMON/BLK1/H,EPS(30,30),ITRAC(30,30,20)
   COMMON/BLK5/LAYER(30,30)
   INTEGER Q(6)
   INTEGER H(30,30)
   NNB=1
   JJ1=JJ+1
   JJ0=JJ-1
   II1=II+1
   II0=II-1
   IQ=H(II,JJ)+1
   IF(JCODE.EQ.3)GO TO 3
   IF(JCODE.EQ.2)GO TO 2
   Q(1)=IQ-H(II,JJ1)
   Q(2)=IQ-H(II1,JJ)
   Q(3)=IQ-H(II,JJ0)
   Q(4)=IQ-H(II0,JJ)
   DO 10 IK=1,4
   IF(Q(IK).LE.0)NNB=NNB+1
10 CONTINUE
   IF(NNB.EQ.5)NNB=1
   RETURN
2 CONTINUE
   Q(1)=IQ-H(II,JJ1)
   Q(2)=IQ-H(II1,JJ1)
```

ORIGINAL PAGE IS
OF POOR QUALITY

```
Q(3)=IQ-H(II1, JJ)
Q(4)=IQ-H(II, JJ0)
Q(5)=IQ-H(II0, JJ0)
Q(6)=IQ-H(II0, JJ)
DO 20 IK=1,6
IF(Q(IK).LE.0)NNB=NNB+1
20 CONTINUE
IF(NNB.EQ.7)NNB=1
RETURN
3 CONTINUE
Q(1)=IQ-H(II, JJ1)
Q(2)=IQ-H(II, JJ0)
DO 30 IK=1,2
IF(Q(IK).LE.0)NNB=NNB+1
30 CONTINUE
IF(NNB.EQ.3)NNB=1
RETURN
END
SUBROUTINE ADATOM(I, J, ITYPE)
COMMON/BLK1/H, EPS(30,30), ITRAC(30,30,20)
COMMON/BLK4/FAA(9), D(9), FAB(9), FBA(9), DS(9), FBB(9)
COMMON/BLK5/LAYER(30,30)
DIMENSION W(9)
INTEGER H(30,30)
IF(H(I, J).LE.0)ISPOT=0
IF(H(I, J).LE.0)GO TO 80
C GO AHEAD AND ADD NEW ADATOMS THEN CORRECT BOUNDARIES IF NECESSARY
ISPOT=ITRAC(I, J, H(I, J))
80 CONTINUE
IF((ISPOT.EQ.0).AND.(ITYPE.EQ.0))GO TO 10
IF((ISPOT.EQ.0).AND.(ITYPE.EQ.1))GO TO 20
IF((ISPOT.EQ.1).AND.(ITYPE.EQ.0))GO TO 30
DO 40 LM=1,9
40 W(LM)=FBB(LM)
GO TO 100
10 DO 50 LM=1,9
50 W(LM)=FAA(LM)
GO TO 100
20 DO 60 LM=1,9
60 W(LM)=FBA(LM)
GO TO 100
30 DO 70 LM=1,9
70 W(LM)=FAB(LM)
100 CONTINUE
```

EPS(I, J)=EPS(I, J)+W(9)

ORIGINAL FILE IS
OF POOR QUALITY

```

EPS(I-1,J+1)=EPS(I-1,J+1)+W(1)
EPS(I,J+1)=EPS(I,J+1)+W(2)
EPS(I+1,J+1)=EPS(I+1,J+1)+W(3)
EPS(I+1,J)=EPS(I+1,J)+W(4)
EPS(I+1,J-1)=EPS(I+1,J-1)+W(5)
EPS(I,J-1)=EPS(I,J-1)+W(6)
EPS(I-1,J-1)=EPS(I-1,J-1)+W(7)
EPS(I-1,J)=EPS(I-1,J)+W(8)
H(I,J)=H(I,J)+1
LAYER(I,J)=LAYER(I,J)+1
ITRAC(I,J,H(I,J))=ITYPE
C IS ADATOM AT AN EDGE?
TEST1=(I-4)*(21-I)
TEST2=(J-4)*(21-J)
IF((TEST1.LT.0).OR.(TEST2.LT.0))GO TO 2
IF((TEST1.EQ.0).OR.(TEST2.EQ.0))CALL EDD(I,J)
RETURN
2 CONTINUE
CALL EDGE(W,I,J)
RETURN
END
SUBROUTINE SUBATOM(I,J,ITYPE)
COMMON/BLK1/H,EPS(30,30),ITRAC(30,30,20)
COMMON/BLK4/FAA(9),D(9),FAB(9),FBA(9),DS(9),FBB(9)
COMMON/BLK5/LAYER(30,30)
DIMENSION W(9)
INTEGER H(30,30)
C GO AHEAD AND SUBTRACT OLD ADATOMS THEN CORRECT BOUNDARIES
IK=H(I,J)-1
IF(IK.LE.0)ION=0
IF(IK.LE.0)GO TO 80
ION=ITRAC(I,J,IK)
80 CONTINUE
IF((ION.EQ.0).AND.(ITYPE.EQ.1))GO TO 10
IF((ION.EQ.0).AND.(ITYPE.EQ.0))GO TO 20
IF((ION.EQ.1).AND.(ITYPE.EQ.1))GO TO 30
DO 40 LM=1,9
40 W(LM)=FAA(LM)
GO TO 100
10 DO 50 LM=1,9
50 W(LM)=FBA(LM)
GO TO 100
20 DO 60 LM=1,9
60 W(LM)=FAA(LM)
GO TO 100
30 DO 70 LM=1,9
70 W(LM)=FAB(LM)
100 CONTINUE

```

ORIGINAL CASE IS
OF POOR QUALITY.

```
EPS(I,J)=EPS(I,J)-W(9)
EPS(I-1,J+1)=EPS(I-1,J+1)-W(1)
EPS(I,J+1)=EPS(I,J+1)-W(2)
EPS(I+1,J+1)=EPS(I+1,J+1)-W(3)
EPS(I+1,J)=EPS(I+1,J)-W(4)
EPS(I+1,J-1)=EPS(I+1,J-1)-W(5)
EPS(I,J-1)=EPS(I,J-1)-W(6)
EPS(I-1,J-1)=EPS(I-1,J-1)-W(7)
EPS(I-1,J)=EPS(I-1,J)-W(8)
ITRAC(I,J,H(I,J))=-1
H(I,J)=H(I,J)-1
LAYER(I,J)=LAYER(I,J)-1
C IS ADATOM AT AN EDGE?
TEST1=(I-4)*(21-I)
TEST2=(J-4)*(21-J)
IF((TEST1.LT.0).OR.(TEST2.LT.0))GO TO 2
IF((TEST1.FQ.0).OR.(TEST2.EQ.0))CALL EDD(I,J)
RETURN
2 CONTINUE
CALL EDGE(W,I,J)
RETURN
END
SUBROUTINE RANDOM(X0,X1,RN)
C X0 IS SEED SUPPLIED BY USER
INTEGER X0,AA,MP,X1
AA=3125
MP=34359738337
X1=MOD(X0*AA,MP)
RN=FLOAT(X1)/FLOAT(MP)
X0=X1
RETURN
END
SUBROUTINE EDGE(W,I,J)
COMMON/BLK1/H,EPS(30,30),ITRAC(30,30,20)
DIMENSION W(9)
INTEGER H(30,30)
C ADJUST FOR EDGE EFFECTS CASES WHERE I=3,22,J=3,22
IF(I.EQ.3)GO TO 20
IF(I.EQ.22)GO TO 25
IF(J.EQ.3)GO TO 30
IF(J.EQ.22)GO TO 35
RETURN
20 CONTINUE
C TOP EDGE I=3
IF(J.EQ.3)GO TO 21
IF(J.EQ.22)GO TO 22
```

EPS(22,J-1)=EPS(2,J-1)
EPS(22,J)=EPS(2,J)
EPS(22,J+1)=EPS(2,J+1)
EPS(23,J-1)=EPS(3,J-1)
EPS(23,J)=EPS(3,J)
EPS(23,J+1)=EPS(3,J+1)
H(23,J)=H(3,J)

RETURN

21

EPS(22,22)=EPS(2,2)
EPS(2,22)=EPS(2,2)
EPS(22,2)=EPS(2,2)
EPS(2,23)=EPS(2,3)
EPS(22,23)=EPS(2,3)
EPS(22,3)=EPS(2,3)
EPS(22,4)=EPS(2,4)
EPS(23,4)=EPS(3,4)
EPS(3,23)=EPS(3,3)
EPS(23,23)=EPS(3,3)
EPS(23,3)=EPS(3,3)
EPS(4,23)=EPS(4,3)
EPS(4,22)=EPS(4,2)
EPS(3,22)=EPS(3,2)
EPS(23,2)=EPS(3,2)
EPS(23,22)=EPS(3,2)
H(3,23)=H(3,3)
H(23,23)=H(3,3)
H(23,3)=H(3,3)

RETURN

22

CONTINUE

H(23,22)=H(3,22)
H(23,2)=H(3,22)
H(3,2)=H(3,22)
EPS(22,21)=EPS(2,21)
EPS(23,21)=EPS(3,21)
EPS(2,2)=EPS(2,22)
EPS(22,2)=EPS(2,22)
EPS(22,22)=EPS(2,22)
EPS(22,23)=EPS(2,23)
EPS(22,3)=EPS(2,23)
EPS(2,3)=EPS(2,23)
EPS(23,23)=EPS(3,23)
EPS(23,3)=EPS(3,23)
EPS(3,3)=EPS(3,23)
EPS(23,22)=EPS(3,22)
EPS(23,2)=EPS(3,22)
EPS(3,2)=EPS(3,22)
EPS(4,3)=EPS(4,23)
EPS(4,2)=EPS(4,22)

RETURN

ORIGINAL FILE IS
OF POOR QUALITY

```
25 CONTINUE
C BOTTOM EDGE I=22
IF(J.EQ.3)GO TO 26
IF(J.EQ.22)GO TO 27
EPS(2,J-1)=EPS(22,J-1)
EPS(3,J-1)=EPS(23,J-1)
EPS(3,J)=EPS(23,J)
EPS(2,J)=EPS(22,J)
EPS(3,J+1)=EPS(23,J+1)
EPS(2,J+1)=EPS(22,J+1)
H(2,J)=H(22,J)
RETURN
```

```
26 CONTINUE
H(22,23)=H(22,3)
H(2,3)=H(22,3)
H(2,23)=H(22,3)
EPS(21,22)=EPS(21,2)
EPS(21,23)=EPS(21,3)
EPS(2,4)=EPS(22,4)
EPS(3,4)=EPS(23,4)
EPS(3,3)=EPS(23,3)
EPS(3,23)=EPS(23,3)
EPS(23,23)=EPS(23,3)
EPS(3,2)=EPS(23,2)
EPS(3,22)=EPS(23,2)
EPS(23,22)=EPS(23,2)
EPS(2,2)=EPS(22,2)
EPS(2,22)=EPS(22,2)
EPS(22,22)=EPS(22,2)
EPS(2,3)=EPS(22,3)
EPS(2,23)=EPS(22,3)
EPS(22,23)=EPS(22,3)
H(2,22)=H(22,22)
H(2,2)=H(22,22)
H(22,2)=H(22,22)
RETURN
```

```
27 CONTINUE
EPS(21,2)=EPS(21,22)
EPS(21,3)=EPS(21,23)
EPS(22,3)=EPS(22,23)
EPS(2,3)=EPS(22,23)
EPS(2,23)=EPS(22,23)
EPS(23,3)=EPS(23,23)
EPS(3,3)=EPS(23,23)
EPS(3,23)=EPS(23,23)
EPS(23,2)=EPS(23,22)
EPS(3,2)=EPS(23,22)
EPS(3,22)=EPS(23,22)
EPS(3,21)=EPS(23,21)
```

ORIGINAL PAGE IS
OF POOR QUALITY

```
EPS(2,21)=EPS(22,21)
EPS(22,2)=EPS(22,22)
EPS(2,2)=EPS(22,22)
EPS(2,22)=EPS(22,22)
RETURN
30 CONTINUE
IF(I.EQ.3)GO TO 21
IF(I.EQ.22)GO TO 26
H(I,23)=H(I,3)
EPS(I-1,23)=EPS(I-1,3)
EPS(I,23)=EPS(I,3)
EPS(I+1,23)=EPS(I+1,3)
EPS(I-1,22)=EPS(I-1,2)
EPS(I,22)=EPS(I,2)
EPS(I+1,22)=EPS(I+1,2)
RETURN
35 CONTINUE
IF(I.EQ.3)GO TO 22
IF(I.EQ.22)GO TO 27
H(I,2)=H(I,22)
EPS(I-1,3)=EPS(I-1,23)
EPS(I,3)=EPS(I,23)
EPS(I+1,3)=EPS(I+1,23)
EPS(I-1,2)=EPS(I-1,22)
EPS(I,2)=EPS(I,22)
EPS(I+1,2)=EPS(I+1,22)
RETURN
END
SUBROUTINE EDD(I,J)
COMMON/BLK1/H,EPS(30,30),ITRAC(30,30,20)
INTEGER H(30,30)
IF(I.EQ.4)GO TO 20
IF(I.EQ.21)GO TO 25
IF(J.EQ.4)GO TO 30
IF(J.EQ.21)GO TO 35
20 CONTINUE
IF(J.EQ.4) GO TO 21
IF(J.EQ.21)GO TO 22
EPS(23,J+1)=EPS(3,J+1)
EPS(23,J)=EPS(3,J)
EPS(23,J-1)=EPS(3,J-1)
RETURN
21 EPS(3,23)=EPS(3,3)
EPS(4,23)=EPS(4,3)
EPS(5,23)=EPS(5,3)
EPS(23,23)=EPS(3,3)
EPS(23,3)=EPS(3,3)
EPS(23,4)=EPS(3,4)
EPS(23,5)=EPS(3,5)
```

ORIGINAL PAGE IS
OF POOR QUALITY

```
RETURN
22  EPS(3,2)=EPS(3,22)
    EPS(4,2)=EPS(4,22)
    EPS(5,2)=EPS(5,22)
    EPS(23,2)=EPS(3,22)
    EPS(23,20)=EPS(3,20)
    EPS(23,21)=EPS(3,21)
    EPS(23,22)=EPS(3,22)
    RETURN
25  CONTINUE
    IF(J.EQ.4)GO TO 26
    IF(J.EQ.21)GO TO 27
    EPS(2,J-1)=EPS(22,J-1)
    EPS(2,J)=EPS(22,J)
    EPS(2,J+1)=EPS(22,J+1)
    RETURN
26  EPS(2,3)=EPS(22,3)
    EPS(2,4)=EPS(22,4)
    EPS(2,5)=EPS(22,5)
    EPS(2,23)=EPS(22,3)
    EPS(20,23)=EPS(20,3)
    EPS(21,23)=EPS(21,3)
    EPS(22,23)=EPS(22,3)
    RETURN
27  EPS(22,2)=EPS(22,22)
    EPS(21,2)=EPS(21,22)
    EPS(20,2)=EPS(20,22)
    EPS(2,2)=EPS(22,22)
    EPS(2,20)=EPS(22,20)
    EPS(2,21)=EPS(22,21)
    EPS(2,22)=EPS(22,22)
    RETURN
30  IF(I.EQ.4)GO TO 21
    IF(I.EQ.21)GO TO 26
    EPS(I-1,23)=EPS(I-1,3)
    EPS(I,23)=EPS(I,3)
    EPS(I+1,23)=EPS(I+1,3)
    RETURN
35  IF(I.EQ.4)GO TO 22
    IF(I.EQ.21)GO TO 27
    EPS(I-1,2)=EPS(I-1,22)
    EPS(I,2)=EPS(I,22)
    EPS(I+1,2)=EPS(I+1,22)
    RETURN
END
SUBROUTINE STOFIN(TSTART,TSTOP)
COMMON/BLK1/H,EPS(30,30),ITRAC(30,30,20)
COMMON/BLK2/UO,UM,UE,UOS,UMS,UES,DELT
COMMON/BLK3/XLAM,TSNAP,M,T,TMIG,IEVAP,ICREAT
```

ORIGINAL PAGE IS
OF POOR QUALITY

COMMON/BLK4/FAA(9),D(9),FAB(9),FBA(9),DS(9),FBB(9)
COMMON/BLK5/LAYER(30,30)
COMMON/BLK6/N1,N2,LETA,M2,LAST
COMMON/BLK7/PHI1,PHI2,PHI3,PHIO,J,PHS1,PHS2,PHS3,PHSO
COMMON/BLK8/ISWTCH
COMMON/BLK9/A,AS,EVIB,EVIBS,RD
COMMON/BLK10/LL1,LL2,U1,MAXH,TA,TB

C VALUES OF PARAMETERS COME VIA COMMON STATEMENTS

INTEGER H(30,30)
DIMENSION IYMIG(400,3)
DIMENSION IRSIT(300,3)
DIMENSION IKC(20,2), IV(401)
DIMENSION DC(400),HTS(10)
ITIME=1.0
ITHREE=1
IF(ISWTCH.EQ.0)GO TO 6
CALL GROW(ITHREE)

6 CONTINUE
ITHREE=ITHREE+1
IRPLUS=0
IMIGK=0
DO 504 JJ=1,3
DO 503 II=1,400
IYMIG(II,JJ)=0

503 CONTINUE

504 CONTINUE
TTIME=TSTART
UEVAP=UE
UMIGR=UM
ICOUNT=0
IOUT=0
PROBC=0.
PROBE=0.
PROBM=0.

C IBULK IS BULK DIFFUSION COUNTER-REMOVE ADATOMS FROM SURFACE

IBULK=0
WT1=2.

C WT1 IS WEIGHT FOR BULK DIFFUSION

C QB IS BULK DIFFUSION ENERGY BARRIER

XKT=T*(8.62E-5)
TOUT=TSNAP
QD=UM-UO-PHIO
TAUD=(1.0E-12)*EXP(QD/XKT)

C TAUD IS THE MEAN TIME BETWEEN HOPS

C NHOP IS THE NO. OF HOPS IN DELT SECONFAA

2 XNHOP=DELT/TAUD
XNSAMP=(1.0E12)*TAUD
XNOFP=(1.0E12)*DELT
XNSCAN=TOUT/DELT

ORIGINAL PAGE IS
OF POOR QUALITY

```
QB=WT1*QD
UBULK=UO+PHIO+QB
IF(UBULK.GE.UE)UBULK=UE-.001
TT1=1./(1.+WT1)
XNTOUT=TOUT-DELT/2.
C INITIALIZE TIME COUNTER FOR CASE WHERE IJK=0
TINIT=DELT/2.
XXLAM=XLAM/DELT
C XXLAM IS REALLY RD=DEPOSITION RATE
I XIJK=XLAM
IJK=XIJK
C IJK IS NUMBER OF RANDOM DEPOSITIONS DURING DELT
C IF DELT IS VERY SMALL XIJK IS ALWAYS LESS THAN ONE AND HENCE IJK=0
C IN CASE IJK=0 GO TO 700 SCAN SURFACE AND PERFORM MIGRATIONS/EVAPORATIONS
C DURING THE DELT INTERVAL AND THEN RETURN TO 1
C UPDATE TINIT IF IJK =0
IF(IJK .EQ. 0) TINIT=TINIT+DELT
C HAS ENOUGH TIME ELAPSED FOR THE ADDITION OF ONE ADATOM?
XXIJK=XXLAM*TINIT
IXIJK=XXIJK
IF(IXIJK .GT.0)IJK=IXIJK
IF(IJK.GT.0)TINIT=DELT/2.
C IF DEPOSITION RATE IS ZERO GO TO 700 SCAN SURFACE
IF(XLAM .LE. 0.)GO TO 700
IF(IJK .EQ. 0) GO TO 700
IRPLUS=IRPLUS+IJK
CALL URNS(IJK,IRSIT,M)
DO 500 IL=1,IJK
C ADD THERMALLY ACCOMODATED ADATOMS
IRS=IRSIT(IL,1)
JCS=IRSIT(IL,2)
ITYPE=IRSIT(IL,3)
CALL ADATOM(IRS,JCS,ITYPE)
500 CONTINUE
700 CONTINUE
IX=0
IY=0
IZ=0
IB=0
C IF LAYER IS 1 THEN UDS,UMS,UES DOMINATES
C CREATION, MIGRATION, EVAPORATION
C NOW DO ALL MIGRATIONS FOR SITES WITH FLAGS
NSCAN=0
DO 502 JJ1=LL1,LL2
DO 501 II1=LL1,LL2
IF(EPS(II1,JJ1).GT.UMIGR)GO TO 25
IF(LAYER(II1,JJ1).LE.0)GO TO 501
RAN=URAN(0)
ABC=-ALOG(RAN)/XNOFP
```

ORIGINAL PAGE IS
OF POOR QUALITY

```
ENGY=-XKT*ALOG(ABC)
U=EPS(II1,JJ1)+ENGY
IF(U.LT.UMIGR)GO TO 30
IF(U.LT.UBULK)GO TO 25
IF(U.LT.UE)GO TO 16
GO TO 20
16 IF(RAN.GT.TT1)GO TO 25
   IB=IB+1
   GO TO 20
C   MIGRATION OCCURS
25 IY=IY+1
   NSCAN=NSCAN+1
   IYMIG(NSCAN,1)=II1
   IYMIG(NSCAN,2)=JJ1
   IYMIG(NSCAN,3)=1
   GO TO 501
C   EVAPORATION
20 IZ=IZ+1
   NSCAN=NSCAN+1
   IYMIG(NSCAN,1)=II1
   IYMIG(NSCAN,2)=JJ1
   IYMIG(NSCAN,3)=0
   GO TO 501
30 IX=IX+1
501 CONTINUE
502 CONTINUE
   ICDUNT=ICDUNT+1
   TOTAL=IX+IY+IZ
   ICREAT=ICREAT+IX
   IEVAP=IEVAP+IZ-IB
   IMIGR=IMIGR+IY
   IBULK=IBULK+IB
   IF(NSCAN.EQ.0)GO TO 506
   CALL MIXUP(IV,NSCAN)
   DO 505 IK=1,NSCAN
   IJ=IV(IK)
   II1=IYMIG(IJ,1)
   JJ1=IYMIG(IJ,2)
   ITYPE=IYMIG(IJ,3)
   IF(ITYPE.EQ.0)GO TO 508
   CALL DIFF(II1,JJ1,DMIG,NI1,NJ1)
   TMIG=TMIG+DMIG
   GO TO 505
508 CONTINUE
   ITYR=0
   IF(H(II1,JJ1).LE.0)GO TO 70
   ITYR=ITRAC(II1,JJ1,H(II1,JJ1))
70 CONTINUE
   CALL SUBATOM(II1,JJ1,ITYR)
```

ORIGINAL PAGE IS
OF POOR QUALITY

```
505 CONTINUE
506 CONTINUE
TTIME=TTIME+DELT
C OUTPUT EVERY TOUT SECONDS
IF(TTIME .GE. XNTOUT) GO TO 652
GO TO 1
652 CONTINUE
XNTOUT=TTIME+TOUT-DELT/2.
C BEFORE STOPPING DO AVERAGES FOR THIS DELT RUN
C RE IN UNITS OF ADATOMS/SEC TO CONVERT TO NM/SEC MULTIPLY BY(.1*A)/400
C RE=EVAPORATION RATE
RE=FLOAT(IEVAP)/TTIME
C RG=AVG GROWTH RATE IN NM/SEC
RG=A*(FLOAT(IRPLUS-IEVAP-IBULK))/FLOAT(M2)
RG=.1*RG/TTIME
C RG IN UNITS OF NM/SEC
C RF=ROUGHNESS FACTOR ; EBAR=AVG POTENTIAL WELL
EBAR=0
DO 100 II=LL1,LL2
DO 101 JJ=LL1,LL2
EBAR=EBAR+EPS(II,JJ)
101 CONTINUE
100 CONTINUE
EBAR=EBAR/FLOAT(M2)
PF=ABS((UD-EBAR)/UD)*100
C PF IS ROUGHNESS FACTOR BY WAY OF POTENTIAL DEVIATION FROM NORM
XN=ICOUNT
CALL UPDATE(RF,THETA,TH2,DC,HTS,J)
IF(ISWTCH.EQ.0)GO TO 5
CALL GROW(ITHREE)
5 CONTINUE
ITHREE=ITHREE+1
N=XN
ICC=0
DO 50 II=1,400
IF(DC(II).EQ.0)GO TO 50
IF(ICC.GT.20)GO TO 50
ICC=ICC+1
IKC(ICC,1)=II
IKC(ICC,2)=DC(II)
50 CONTINUE
WRITE(6,298)TTIME,((IKC(II,JJ),JJ=1,2),II=1,ICC)
298 FORMAT(1X,6HTIME=,F8.3,5X,37HDENSITY OF CLUSTERS (SIZE,FREQUENCY)
1 ,/,T20,(10(1H(,I3,1H,,I3,1H),2X)),/,T20,(10(1H(,I3,1H,,I3,1H),2X
2)))
WRITE(6,299) (LAYER(3,JJ),JJ=3,22),(LAYER(3,JJ),JJ=3,22),N,J,XNHOP
299 FORMAT(10X,40I1,T60,6H N=,I9 ,T80,5H J=,I2,T100,5HNDOP=,
1E14.7)
WRITE(6,300)(LAYER(4,JJ),JJ=3,22),(LAYER(4,JJ),JJ=3,22),IMIGR,
```

ORIGINAL PAGE IS
OF POOR QUALITY

```

1ICREAT,IEVAP,IBULK
300  FORMAT(10X,40I1,T60,6HIMIGR=,I9,T80,7HICREAT=,I9,T100,6HIEVAP=,I9,
      1T120,6HIBULK=,I6)
      WRITE(6,301)(LAYER(5,JJ),JJ=3,22),(LAYER(5,JJ),JJ=3,22),THETA,TH2,
      1TAUD,TA
301  FORMAT(10X,40I1,T60,9HTHETA(1)=,F8.4,T80,9HTHEA(2)=,F8.3,T100,
      15HTAUD=,E14.5,T122,3HTA=,F5.0)
      WRITE(6,302)(LAYER(6,JJ),JJ=3,22),(LAYER(6,JJ),JJ=3,22),IRPLUS,
      1XNHOP,TMIG,TB
302  FORMAT(10X,40I1,T60,7HIRPLUS=,I9,T80,5HNNHOP=,E14.7,T100,5HTMIG=,
      1E14.7,T122,3HTB=,F5.0)
      WRITE(6,303)(LAYER(7,JJ),JJ=3,22),(LAYER(7,JJ),JJ=3,22),RE,RG,RF
303  FORMAT(10X,40I1,T60,3HRE=,F9.4,T80,3HRG=,F9.4,T100,3HRF=,F9.4)
      WRITE(6,304)(LAYER(8,JJ),JJ=3,22),(LAYER(8,JJ),JJ=3,22),XNOFP,
      1EBAR,XNSAMP
304  FORMAT(10X,40I1,T60,5HNOFP=,E14.7,T80,5HEBAR=,F8.3,2X,
      110HNSAMPPHOP=,E14.7)
      WRITE(6,310)(LAYER(9,JJ),JJ=3,22),(LAYER(9,JJ),JJ=3,22),HTS
310  FORMAT(10X,40I1,T60,4HHTS=,10F4.0 )
      DO 201 II=10,22
      WRITE(6,305)(LAYER(II,JJ),JJ=3,22),(LAYER(II,JJ),JJ=3,22)
305  FORMAT(10X,40I1)
201  CONTINUE
      IOUT=IOUT+1
      ITEST1=MOD(IOUT,2)
      IF(ITEST1.EQ.0)GO TO 60
      WRITE(6,306)
306  FORMAT( /)
      GO TO 61
60   CONTINUE
      WRITE(6,311)
311  FORMAT(1H1)
61   CONTINUE
      IF(TTIME.GE.TSTOP)GO TO 876
      IF((TTIME+DELT/2.).LT. TSTOP) GO TO 1
876  CONTINUE
      IF(ISWTCH.EQ.1) CALL NFRAME
      RETURN
      END
      SUBROUTINE XYX
      COMMON/BLK1/H,EPS(30,30),ITRAC(30,30,20)
      COMMON/BLK5/LAYER(30,30)
C    UPDATE FRINGES OF PERIODIC PATTERN
      INTEGER H(30,30)
      DO 6 I=3,22
      LAYER( 1, I)=LAYER(21, I)
      H(1,I)=H(21,I)
      LAYER( 2, I)=LAYER(22, I)
      H(2,I)=H(22,I)

```

```
LAYER(23,I )=LAYER( 3, I)  
H(23,I)=H(3,I)  
LAYER(24, I)=LAYER( 4, I)  
H(24,I)=H(4,I)  
LAYER( I, 1)=LAYER( I,21)  
H(I,1)=H(I,21)  
LAYER( I, 2)=LAYER( I,22)  
H(I,2)=H(I,22)  
LAYER( I,23)=LAYER( I, 3 )  
H(I,23)=H(I, 3)  
LAYER( I,24)=LAYER( I, 4)  
H(I,24)=H(I,4)
```

6 CONTINUE

C CORNERS UPDATED

```
LAYER( 1, 1)=LAYER(21,21)  
H(1,1)=H(21,21)  
LAYER( 1, 2)=LAYER(21,22)  
H(1,2)=H(21,22)  
LAYER( 2, 1)=LAYER(22,21)  
H(2,1)=H(22,21)  
LAYER( 2, 2)=LAYER(22,22)  
H(2,2)=H(22,22)  
LAYER(23, 1)=LAYER( 3,21)  
H(23,1)=H(3,21)  
LAYER(23, 2)=LAYER( 3,22)  
H(23,2)=H(3,22)  
LAYER(24, 1)=LAYER( 4,21)  
H(24,1)=H(4,21)  
LAYER(24, 2)=LAYER( 4,22)  
H(24,2)=H(4,22)  
LAYER( 1,23)=LAYER(21, 3)  
H(1,23)=H(21,3)  
LAYER( 1,24)=LAYER(21,4 )  
H(1,24)=H(21,4)  
LAYER( 2,23)=LAYER(22, 3)  
H(2,23)=H(22,3)  
LAYER( 2,24)=LAYER(22, 4)  
H(2,24)=H(22,4)  
LAYER(23,23)=LAYER( 3, 3)  
H(23,23)=H(3,3)  
LAYER(23,24)=LAYER( 3, 4)  
H(23,24)=H(3,4)  
LAYER(24,23)=LAYER( 4, 3)  
H(24,23)=H(4,3)  
LAYER(24,24)=LAYER( 4, 4)  
H(24,24)=H(4,4)  
DO 7 I=3,22  
EPS(1,I)=EPS(21,I)  
EPS(2,I)=EPS(22,I)
```

ORIGINAL PAGE IS
OF POOR QUALITY

```
EPS(23,I)=EPS(3,I)
EPS(24,I)=EPS(4,I)
EPS(I,1)=EPS(I,21)
EPS(I,2)=EPS(I,22)
EPS(I,23)=EPS(I,3)
EPS(I,24)=EPS(I,4)
```

7 CONTINUE

C CORNERS UPDATED

```
EPS(1,1)=EPS(21,21)
EPS(1,2)=EPS(21,22)
EPS(2,1)=EPS(22,21)
EPS(2,2)=EPS(22,22)
EPS(23,1)=EPS(3,21)
EPS(23,2)=EPS(3,22)
EPS(24,1)=EPS(4,21)
EPS(24,2)=EPS(4,22)
EPS(1,23)=EPS(21,3)
EPS(1,24)=EPS(21,4)
EPS(2,23)=EPS(22,3)
EPS(2,24)=EPS(22,4)
EPS(23,23)=EPS(3,3)
EPS(23,24)=EPS(3,4)
EPS(24,23)=EPS(4,3)
EPS(24,24)=EPS(4,4)
```

RETURN

END

SUBROUTINE URNS(L,IRSIT,M)

COMMON/BLK10/LL1,LL2,U1,MAXH,TA,TB

DIMENSION IRSIT(300,3)

C ALPHA DEPENDENT UPON THICKNESS OF B ON A OR HEIGHT

A0=.1

B0=.2

ALPHA=A0*EXP(-B0*MAXH)

C SCALE Y TO SITE INTERVAL

DO 10 I=1,L

Y1=URAN(0)

Y2=URAN(0)

IRSIT(I,1)=LL1+Y1*M

IRSIT(I,2)=LL1+Y2*M

IRSIT(I,3)=1

IF(Y1.LT.ALPHA)IRSIT(I,3)=0

10 CONTINUE

RETURN

END

SUBROUTINE UPDATE(RF,THETA,TH2,DC,HTS,JCODE)

COMMON/BLK1/H,EPS(30,30),ITRAC(30,30,20)

COMMON/BLK5/LAYER(30,30)

COMMON/BLK10/LL1,LL2,U1,MAXH,TA,TB

COMMON/BLK12/C

ORIGINAL PRINTING
OF POOR QUALITY

```
INTEGER B(30,30),C(30,30)
INTEGER H(30,30)
DIMENSION DC(400),HTS(10)
DIMENSION NEXT(400,2)
C RF=ROUGHNESS FACTOR , RF=1 FOR FLAT SURFACE
C THETA=COVERAGE, DC=DENSITY OF CLUSTERS(1,2,3,...,10)
TB=0
TA=0
DO 80 II=3,22
DO 81 JJ=3,22
IJ=H(II,JJ)
IF(ITRAC(II,JJ,IJ).EQ.0)TA=TA+1
IF(ITRAC(II,JJ,IJ).EQ.1)TB=TB+1
81 CONTINUE
80 CONTINUE
DO 5 I=1,400
5 DC(I)=0.
CALL XYX
C THETA =COVERAGE
DO 10 II=1,10
10 HTS(II)=0.
DO 50 I=3,22
DO 50 J=3,22
DO 51 IK=1,10
IF(LAYER(I,J).GE.IK)HTS(IK)=HTS(IK)+1
51 CONTINUE
50 CONTINUE
THETA=HTS(1)/400
TH2=HTS(2)/400
MAX=1
DO 100 II=1,10
IF(HTS(II).GE.20.)MAX=II
100 CONTINUE
MAXH=MAX
DO 8 I=1,24
DO 8 J=1,24
C(I,J)=1
B(I,J)=0.
8 CONTINUE
DO 9 I=1,24
DO 9 J=1,24
IF(LAYER(I,J).GE.MAX)B(I,J)=1.
9 CONTINUE
SUM=0.
DO 60 I=3,22
DO 60 J=3,22
60 SUM=SUM+IABS(H(I,J)-H(I,J+1))
RF=1+SUM/400.
ILST=0
```

```
INXT=0
ICT=0
DO 20 I=3,22
DO 20 J=3,22
IF(B(I,J).EQ.0)GO TO 20
LI=I
LJ=J
CALL CORRECT(LI,LJ)
25 ICT=ICT+1
ILJ=LJ+1
IF(B(LI,ILJ).EQ.0)GO TO 21
IF(C(LI,ILJ).EQ.0)GO TO 21
ILST=ILST+1
NEXT(ILST,1)=LI
NEXT(ILST,2)=ILJ
CALL CORRECT(LI,ILJ)
21 ILJ=LJ-1
IF(B(LI,ILJ).EQ.0)GO TO 22
IF(C(LI,ILJ).EQ.0)GO TO 22
ILST=ILST+1
NEXT(ILST,1)=LI
NEXT(ILST,2)=ILJ
CALL CORRECT(LI,ILJ)
22 IF(JCODE.EQ.3)GO TO 24
ILI=LI+1
IF(B(ILI,LJ).EQ.0)GO TO 23
IF(C(ILI,LJ).EQ.0)GO TO 23
ILST=ILST+1
NEXT(ILST,1)=ILI
NEXT(ILST,2)=LJ
CALL CORRECT(ILI,LJ )
23 ILI=LI-1
IF(B(ILI,LJ).EQ.0)GO TO 74
IF(C(ILI,LJ).EQ.0)GO TO 74
ILST=ILST+1
NEXT(ILST,1)=ILI
NEXT(ILST,2)=LJ
CALL CORRECT(ILI,LJ)
74 IF(JCODE.EQ.1)GO TO 24
ILI=LI-1
ILJ=LJ-1
IF(B(ILI,ILJ).EQ.0)GO TO 76
IF(C(ILI,ILJ).EQ.0)GO TO 76
ILST=ILST+1
NEXT(ILST,1)=ILI
NEXT(ILST,2)=ILJ
CALL CORRECT(ILI,ILJ)
76 ILI=LI+1
ILJ=LJ+1
```

```

IF(B(ILI,ILJ).EQ.0)GO TO 24
IF(C(ILI,ILJ).EQ.0)GO TO 24
ILST=ILST+1
NEXT(ILST,1)=ILI
NEXT(ILST,2)=ILJ
CALL CORRECT(ILI,ILJ)
24  B(LI,LJ)=0
    C(LI,LJ)=0
    IF(LI.GT.3)GO TO 30
    B(23,LJ)=0
    C(23,LJ)=0
30  IF(LI.LT.22)GO TO 31
    B(2,LJ)=0
    C(2,LJ)=0
31  IF(LJ.GT.3)GO TO 32
    B(LI,23)=0
    C(LI,23)=0
32  IF(LJ.LT.22)GO TO 33
    B(LI,2)=0
    C(LI,2)=0
33  CONTINUE
    IF(INXT.EQ.ILST)GO TO 26
    INXT=INXT+1
    LI=NEXT(INXT,1)
    LJ=NEXT(INXT,2)
    IF(LI.LT.3)LI=22
    IF(LI.GT.22)LI=3
    IF(LJ.LT.3)LJ=22
    IF(LJ.GT.22)LJ=3
    GO TO 25
26  ILST=0
    INXT=0
    DC(ICT)=DC(ICT)+1
    ICT=0
20  CONTINUE
    RETURN
    END
SUBROUTINE CORRECT(II,JJ)
COMMON/BLK5/LAYER(30,30)
COMMON/BLK12/C
INTEGER C(30,30)
C(II,JJ)=0
IF(JJ.EQ.2)GO TO 2
IF(JJ.EQ.3)GO TO 3
IF(JJ.EQ.22)GO TO 22
IF(JJ.EQ.23)GO TO 23
IF(II.EQ.2)GO TO 32
IF(II.EQ.3)GO TO 33
IF(II.EQ.22)GO TO 34

```

```

IF(II.EQ.23)GO TO 35
RETURN
2 C(II,22)=0
17 IF(II.EQ.2)C(22,JJ)=0
IF(II.EQ.3)C(23,JJ)=0
IF(II.EQ.22)C(2,JJ)=0
IF(II.EQ.23)C(3,JJ)=0
GO TO 24
3 C(II,23)=0
GO TO 17
22 C(II,2)=0
GO TO 17
23 C(II,3)=0
GO TO 17
32 C(22,JJ)=0
18 IF(JJ.EQ.2)C(II,22)=0
IF(JJ.EQ.3)C(II,23)=0
IF(JJ.EQ.22)C(II,2)=0
IF(JJ.EQ.23)C(II,3)=0
GO TO 24
33 C(23,JJ)=0
GO TO 18
34 C(2,JJ)=0
GO TO 18
35 C(3,JJ)=0
GO TO 18
24 CONTINUE
IF((II.EQ.3).AND.(JJ.EQ.3))C(23,23)=0
IF((II.EQ.3).AND.(JJ.EQ.22))C(23,2)=0
IF((II.EQ.22).AND.(JJ.EQ.3))C(2,23)=0
IF((II.EQ.22).AND.(JJ.EQ.22))C(2,2)=0
RETURN
END
SUBROUTINE MIXUP(IS,NS)
DIMENSION L(401),IS(401)
IC=1
IF(NS.EQ.1)GO TO 100
DO 50 KS=1,NS
50 L(KS)=KS
M=NS
500 IF(M.EQ.2)GO TO 102
R=RANF(0)
I=1+R*M
IF( I.EQ.1)GO TO 51
IF(I.EQ.M)GO TO 52
IS(IC)=L(I)
L(I)=L(M)
M=M-1
IC=IC+1

```

```
GO TO 500
51  IS(IC)=L(1)
    L(1)=L(M)
    M=M-1
    IC=IC+1
    GO TO 500
52  IS(IC)=L(M)
    M=M-1
    IC=IC+1
    GO TO 500
100 IS(1)=1
    RETURN
102 R=RANF(0)
    I=1+R*M
    IF(I.EQ.1)GO TO 101
    IS(IC)=L(2)
    IS(IC+1)=L(1)
    RETURN
101 IS(IC)=L(1)
    IS(IC+1)=L(2)
    RETURN
END
```

ORIGINAL PAGE IS
OF POOR QUALITY

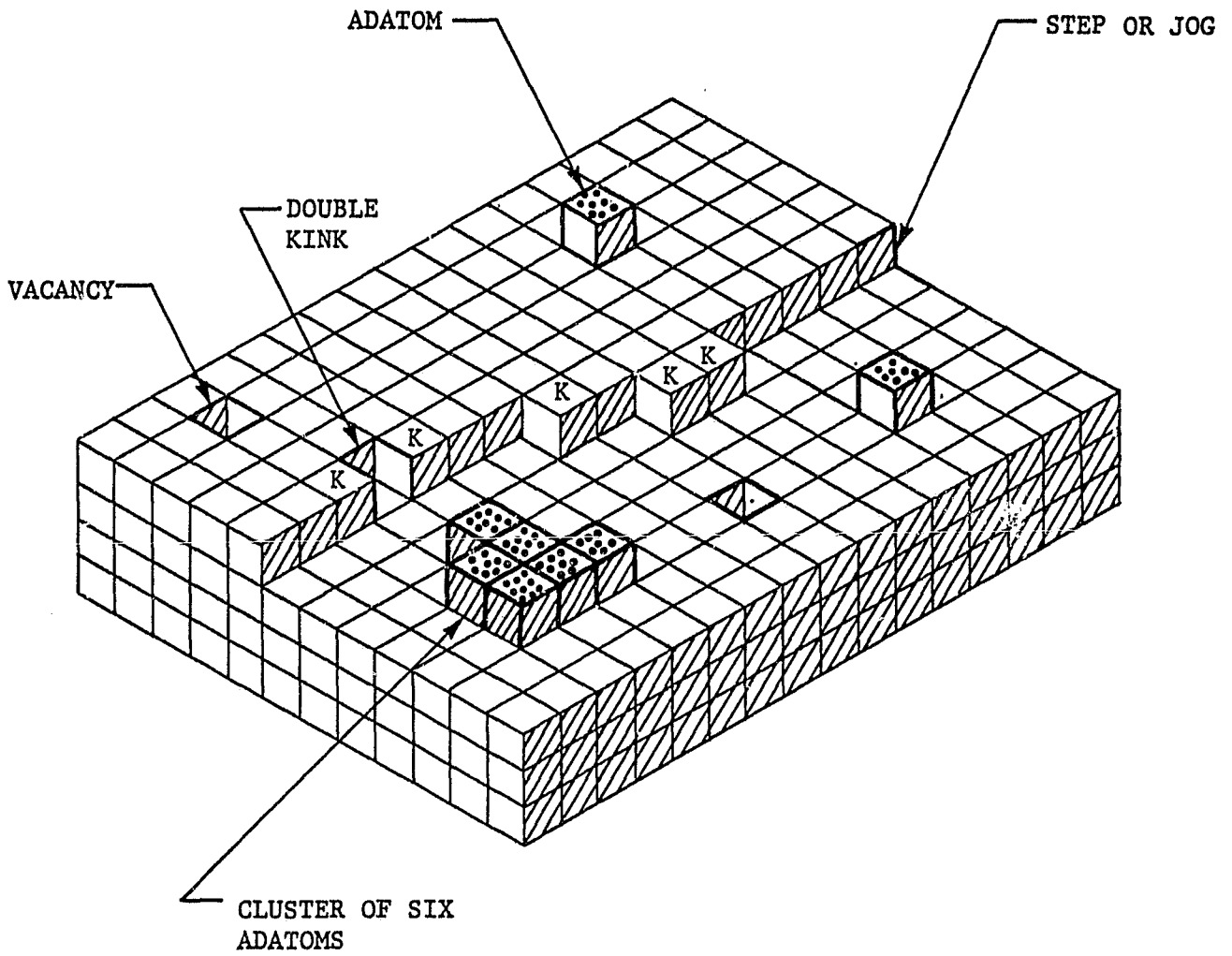


Figure 1. SCS model for crystal growth.

ORIGINAL PAGE IS
OF POOR QUALITY

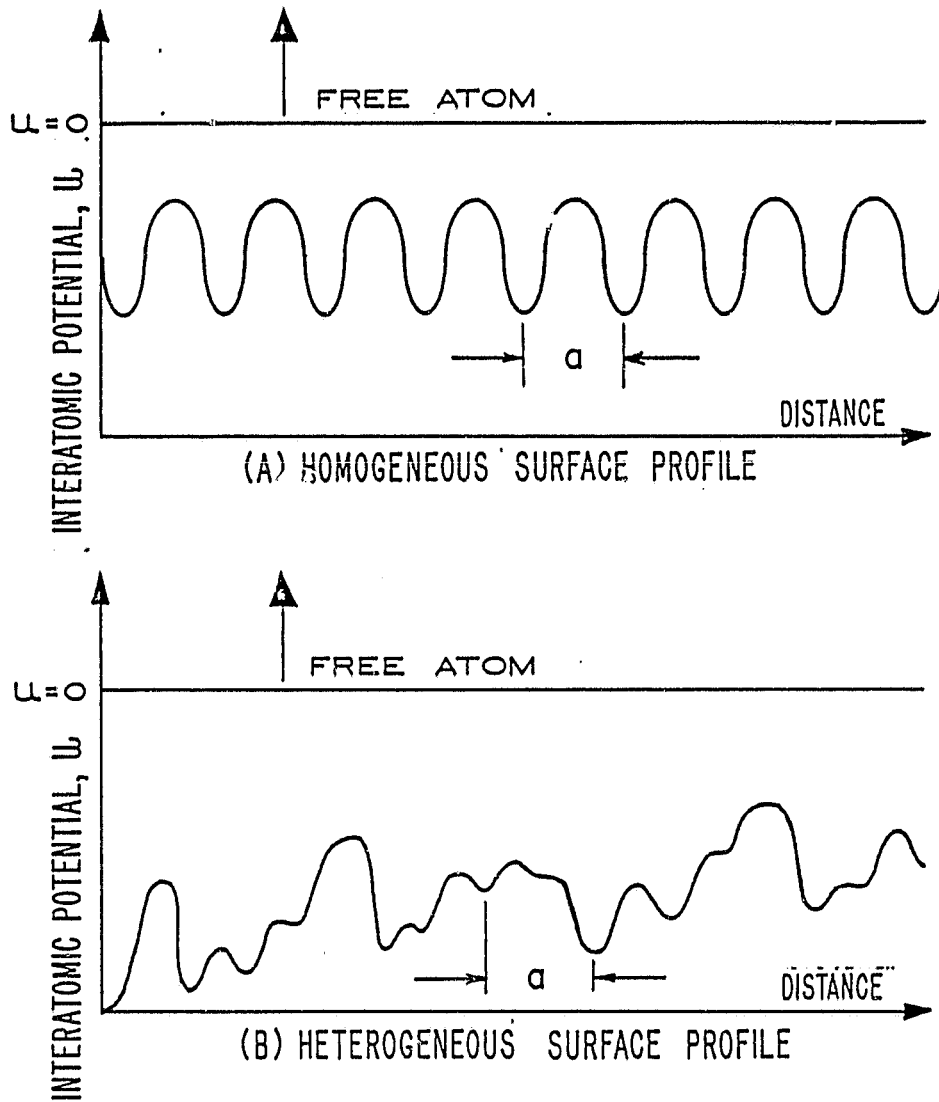
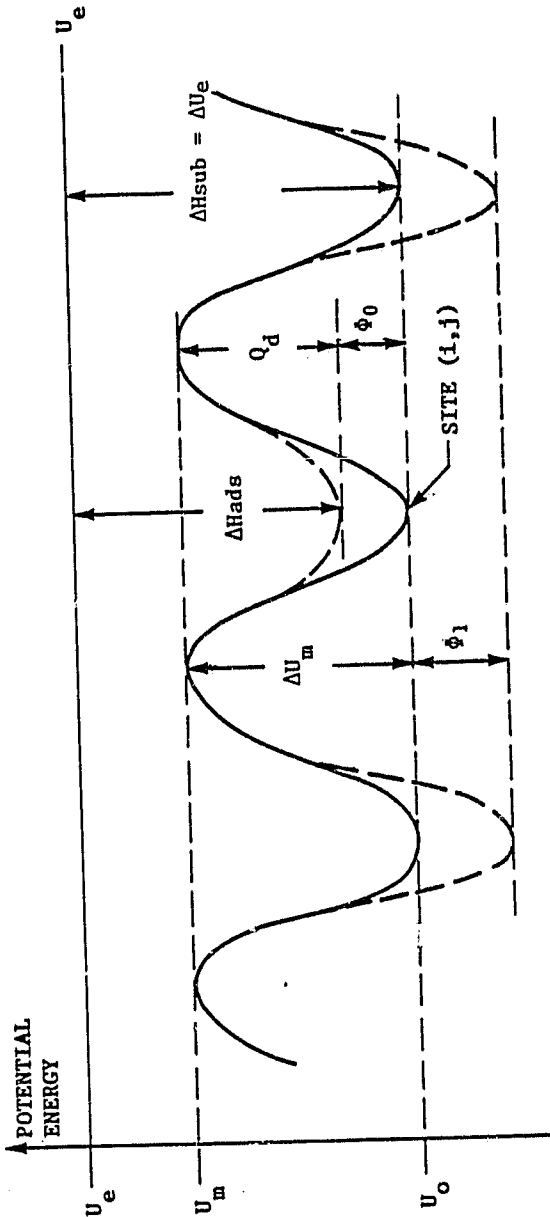


Figure 2. Profile of surface potentials (a) uniform homogeneous surface (b) vacancies, dislocations, kinks, jogs and impurities disturb the surface potential.



ΔH_{ads} = HEAT OF ADSORPTION FOR SINGLE ADATOM

ΔH_{sub} = HEAT OF SUBLIMATION

U_e = EVAPORATION BARRIER

U_m = MIGRATION BARRIER

U_0 = $-\Delta H_{evap}$ = NOMINAL VALUE FOR POTENTIAL UNIFORM SURFACE

ϕ_0 = $\Delta H_{evap} - \Delta H_{ads}$ = POTENTIAL CHANGE DUE TO ADDITION OF ADATOM AT SITE (i,j)

ϕ_1 = NEAREST NEIGHBOR POTENTIAL CHANGE

ϕ_2 = SECOND NEAREST NEIGHBOR POTENTIAL CHANGE

Q_d = DIFFUSION ACTIVATION ENERGY

Figure 3. Potentials for a uniform flat surface (solid line) and potential after an adatom has been added to site (i,j) (dashed line).

ORIGINAL PAGE IS
OF POOR QUALITY

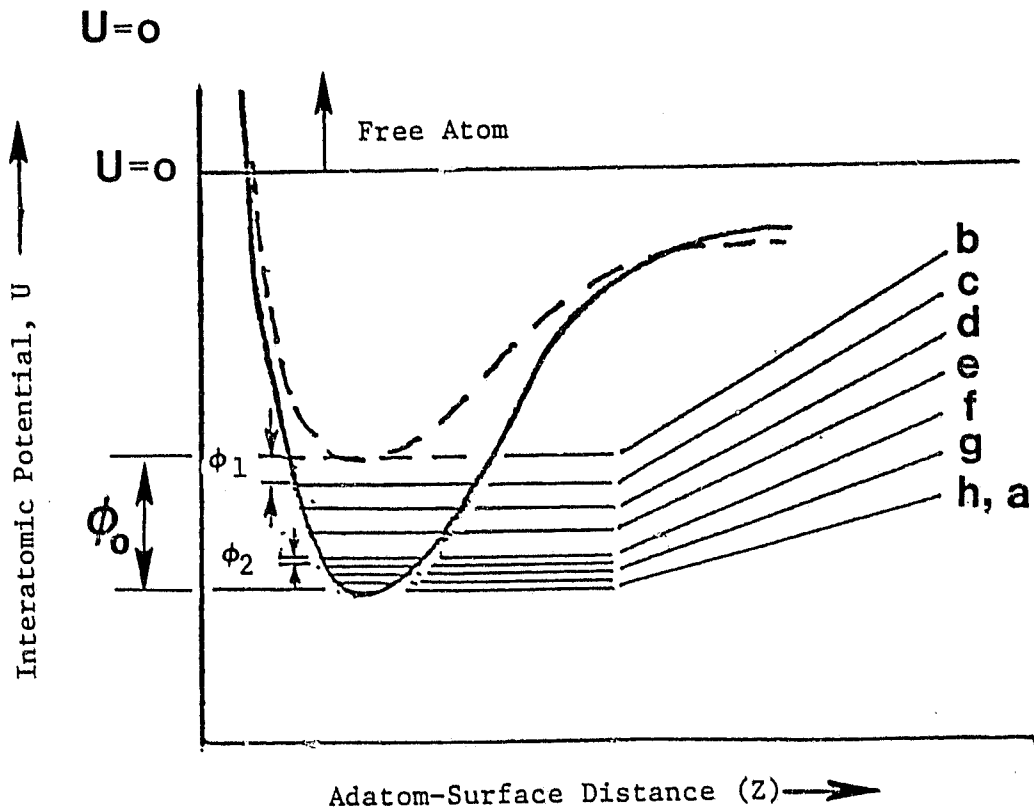
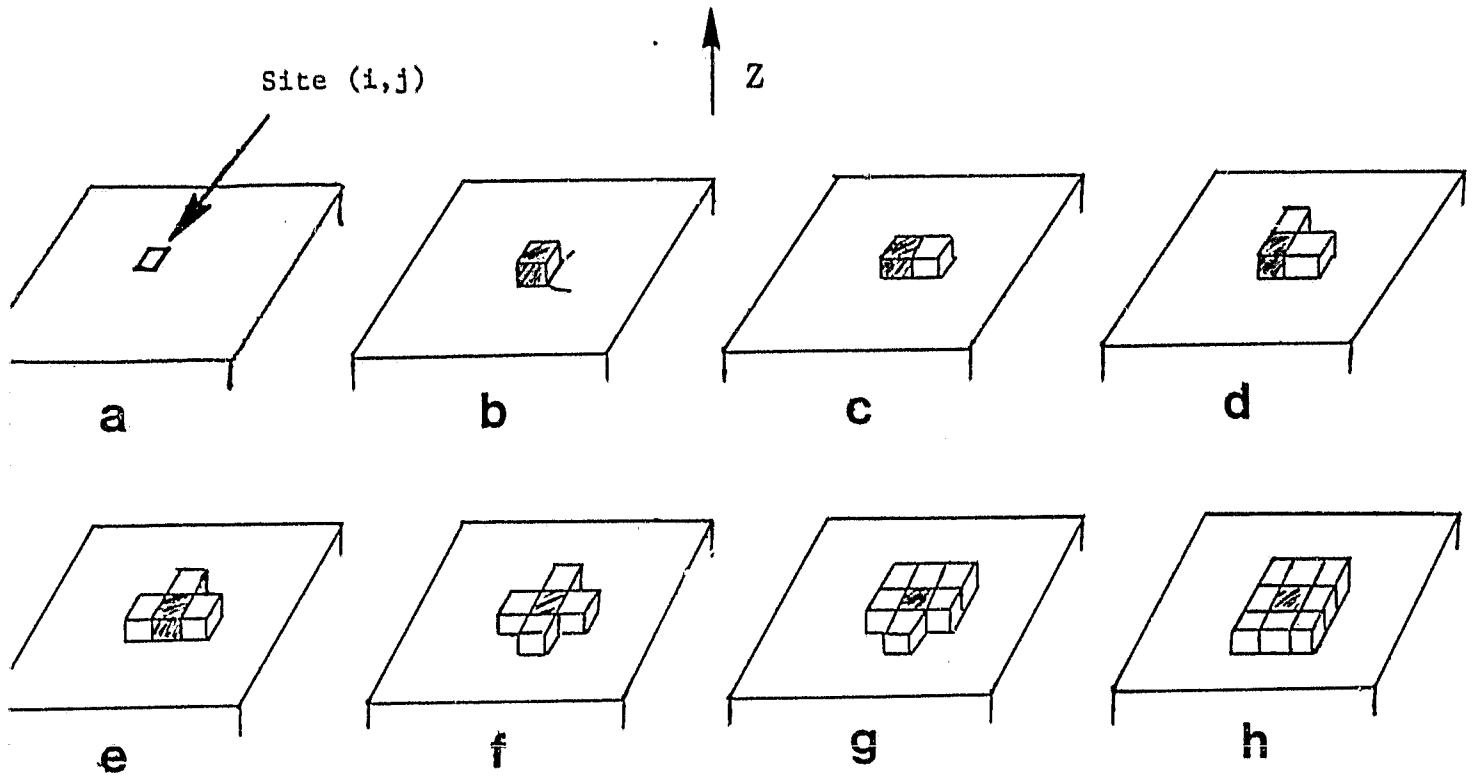
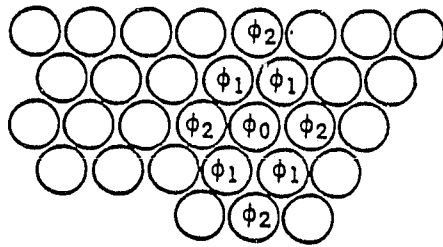
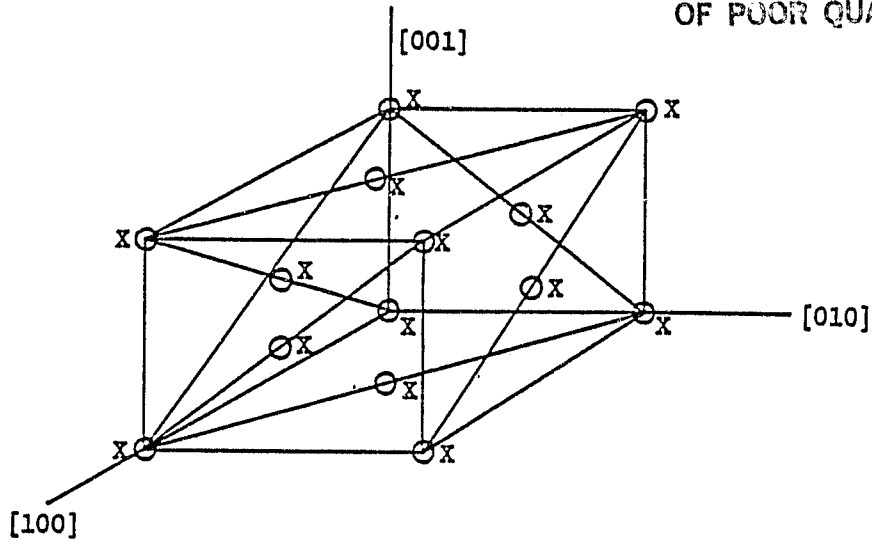


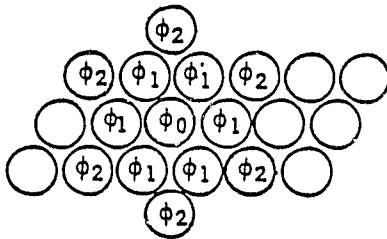
Figure 4. Potential variation at an arbitrary site (i,j).

ORIGINAL PAGE IS
OF POOR QUALITY



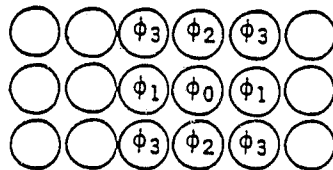
MNEMONIC MASK

$-\phi_2$	$-\phi_1$	$-\phi_2$
$-\phi_1$	ϕ_0	$-\phi_1$
$-\phi_2$	$-\phi_1$	$-\phi_2$



MNEMONIC MASK

	$-\phi_2$		
$-\phi_2$	$-\phi_1$	$-\phi_1$	$-\phi_2$
	$-\phi_1$	ϕ_0	$-\phi_1$
	$-\phi_2$	$-\phi_1$	$-\phi_1$
			$-\phi_2$



MNEMONIC MASK

$-\phi_3$	$-\phi_2$	$-\phi_3$
$-\phi_1$	ϕ_0	$-\phi_1$
$-\phi_3$	$-\phi_2$	$-\phi_3$

Figure 5. FCC model and potential changes associated with different crystal orientations.

ORIGINAL PAGE IS
OF POOR QUALITY

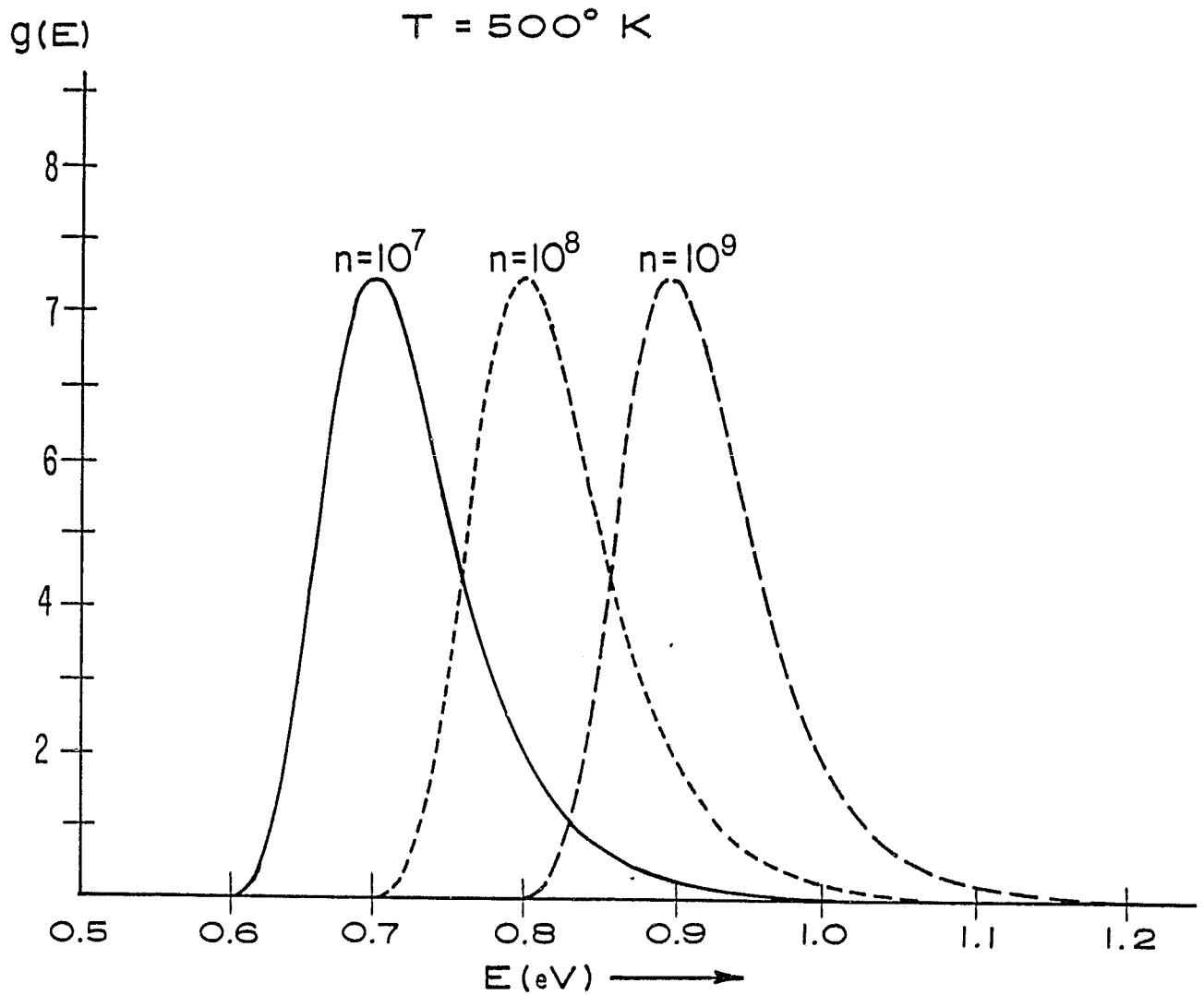


Figure 6. Probability density for the Boltzmann ordered statistic $E_{(n)}$ with $n = 10^7, 10^8, 10^9$ and $T = 500 \text{ K}$.

ORIGINAL PAGE IS
OF POOR QUALITY

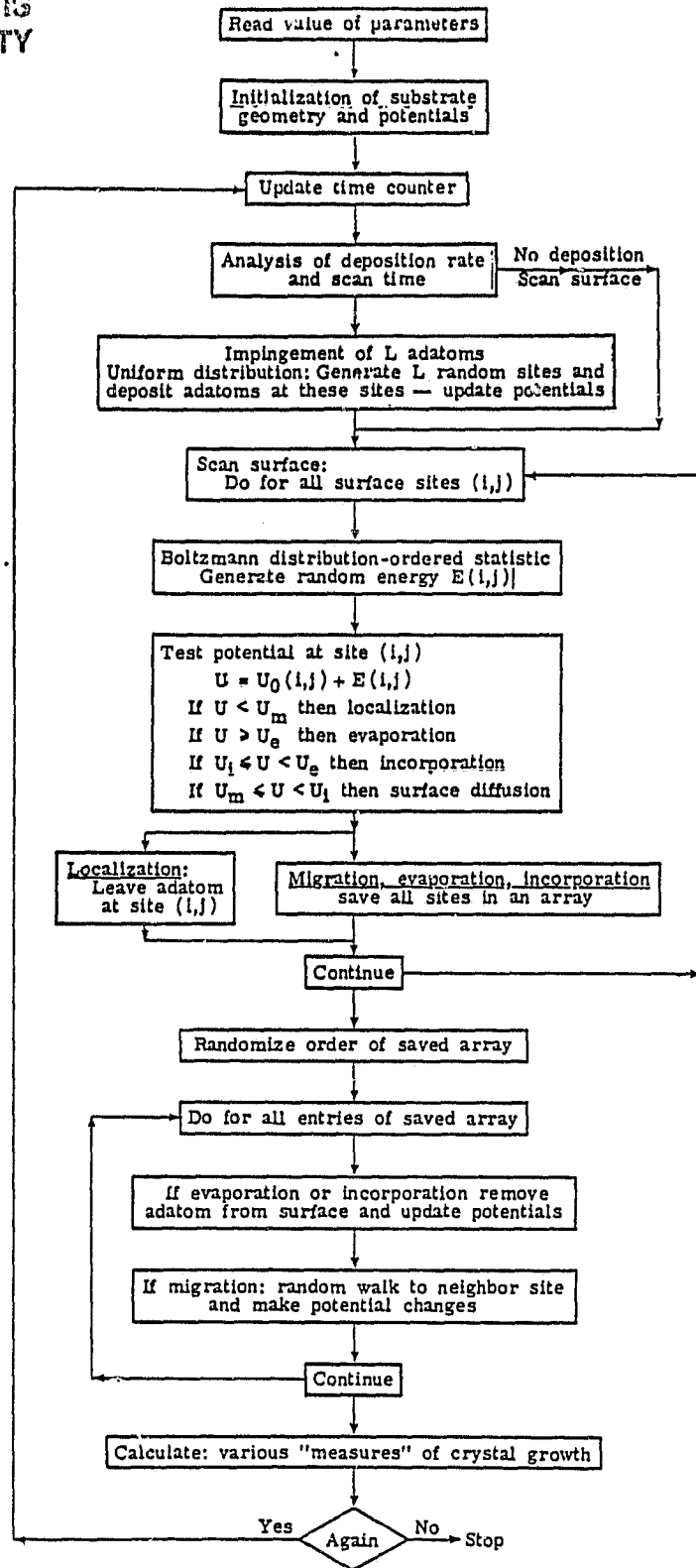


Figure 7. Flowchart for the Monte Carlo SOS computer simulation of thin film growth.

ORIGINAL PAGE IS
OF POOR QUALITY

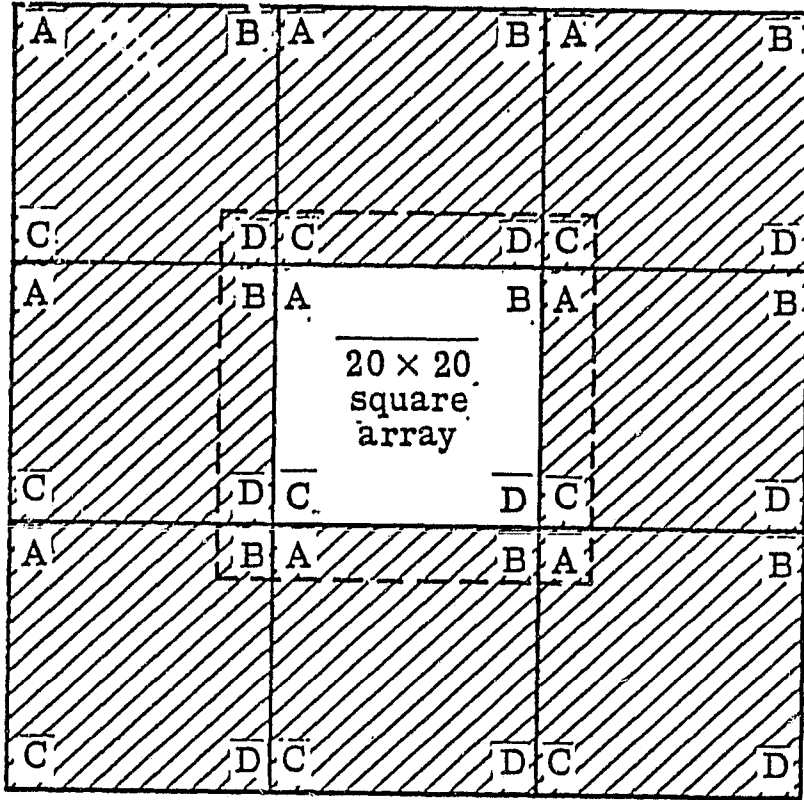


Figure 8. A 20×20 square array with periodic extension.

ORIGINAL PAGE IS
OF POOR QUALITY

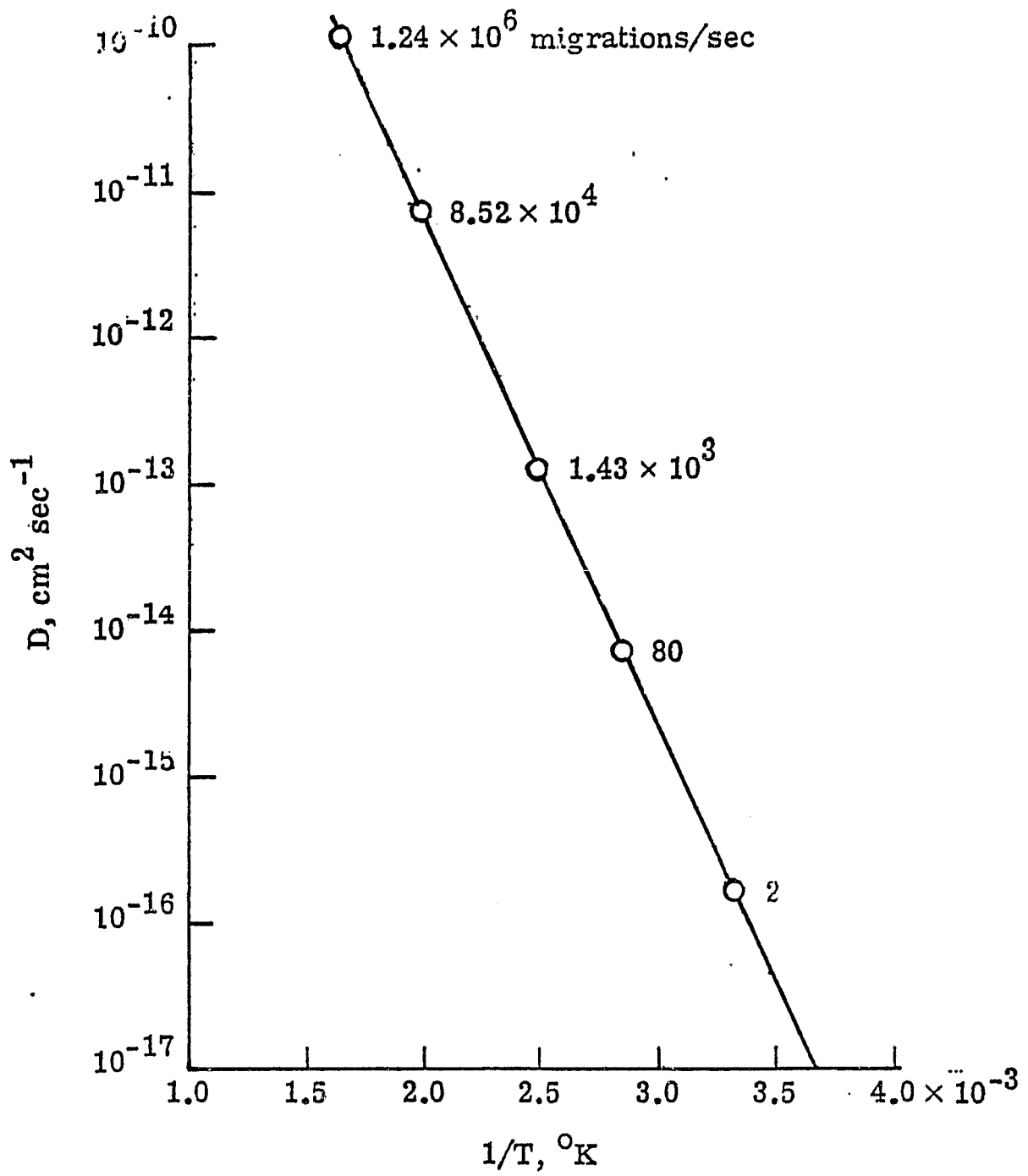


Figure 9. Diffusion coefficient vs. inverse temperature.

ORIGINAL PAGE IS
OF POOR QUALITY

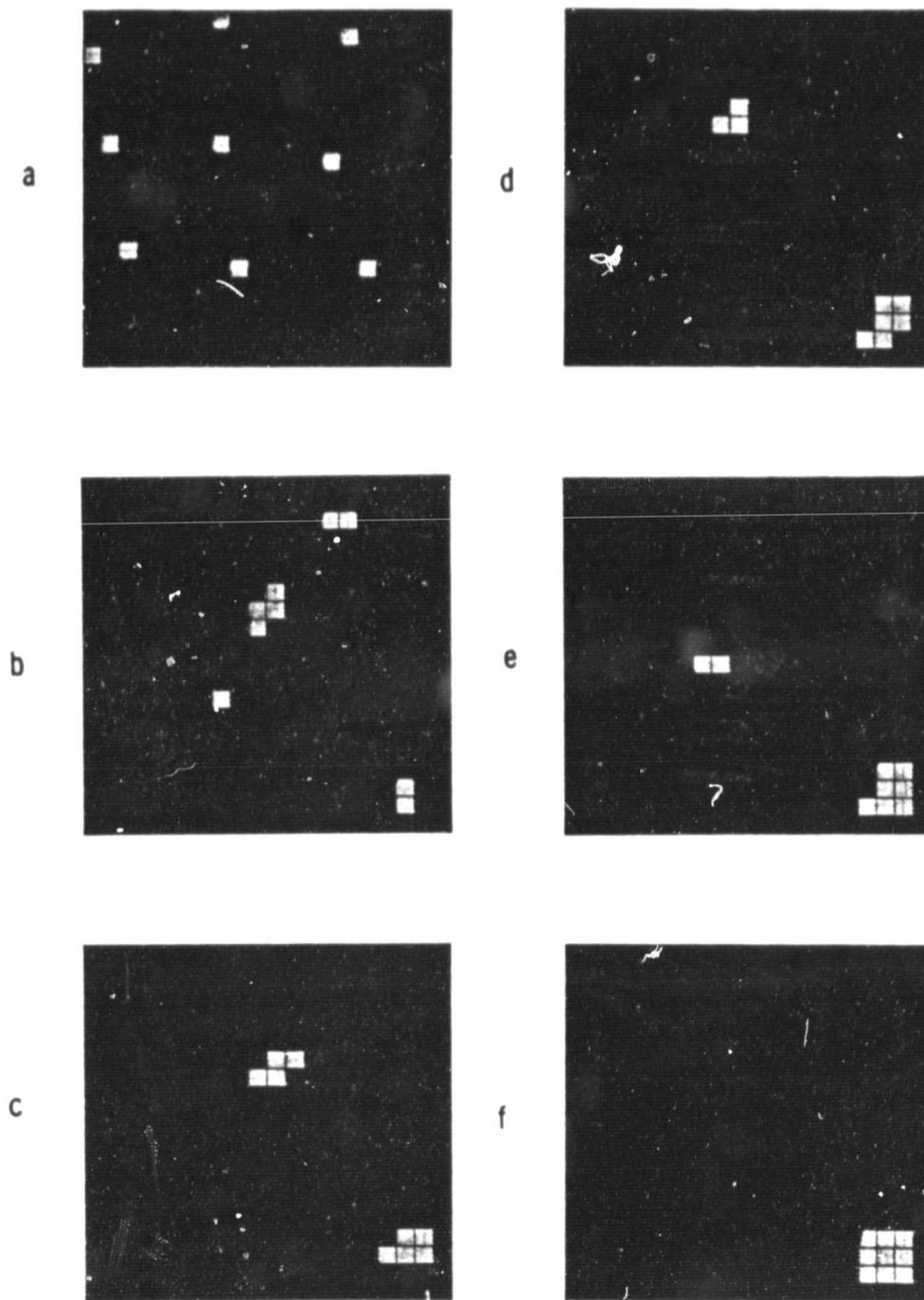


Figure 10. Clustering of dispersed adatoms on a uniform surface:
 $T = 600$ K, (a) $t = 0$, (b) $t = 0.1$ s, (c) $t = 0.3$ s,
(d) $t = 0.5$ s, (e) $t = 0.7$ s, (f) $t = 1.0$ s.

ORIGINAL PAGE IS
OF POOR QUALITY

1st layer

-3.87	-5	-3.87
-5	-6	-5
-3.87	-5	-3.87

2nd layer

-3.87	-3.87	-3.87
-3.87	-5	-3.87
-3.87	-3.87	-3.87

Figure 11. Trap potential variation for first and second layer.

ORIGINAL PAGE IS
OF POOR QUALITY

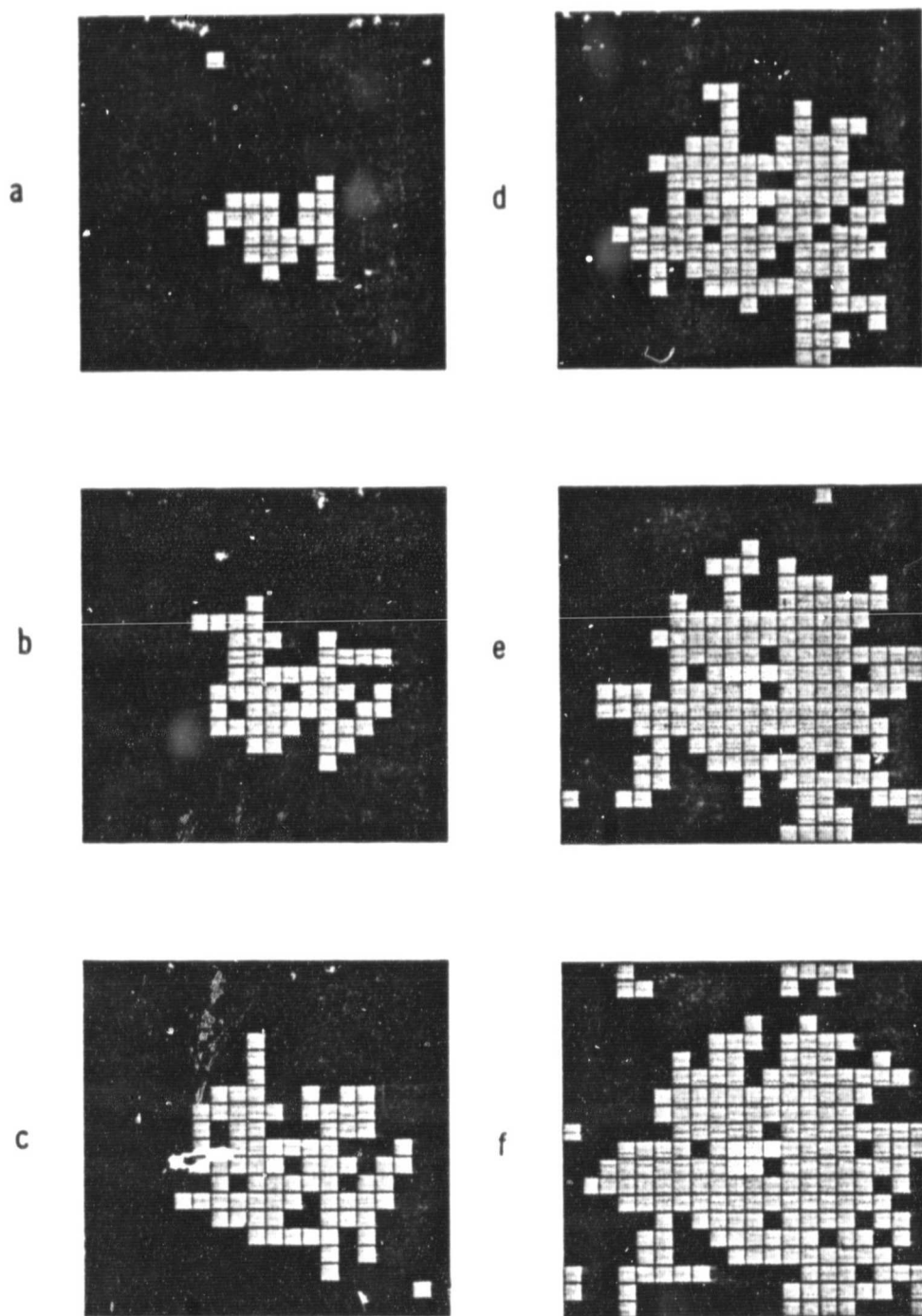


Figure 12 Growth around a trap: $T = 550$ K, (a) $t = 0.5$ s, (b) $t = 0.8$ s, (c) $t = 1.1$ s, (d) $t = 1.4$ s (e) $t = 1.7$ s, (f) $t = 2.0$ s, $R_d = 0.2778$ nm/sec.

ORIGINAL PAGE IS
OF POOR QUALITY

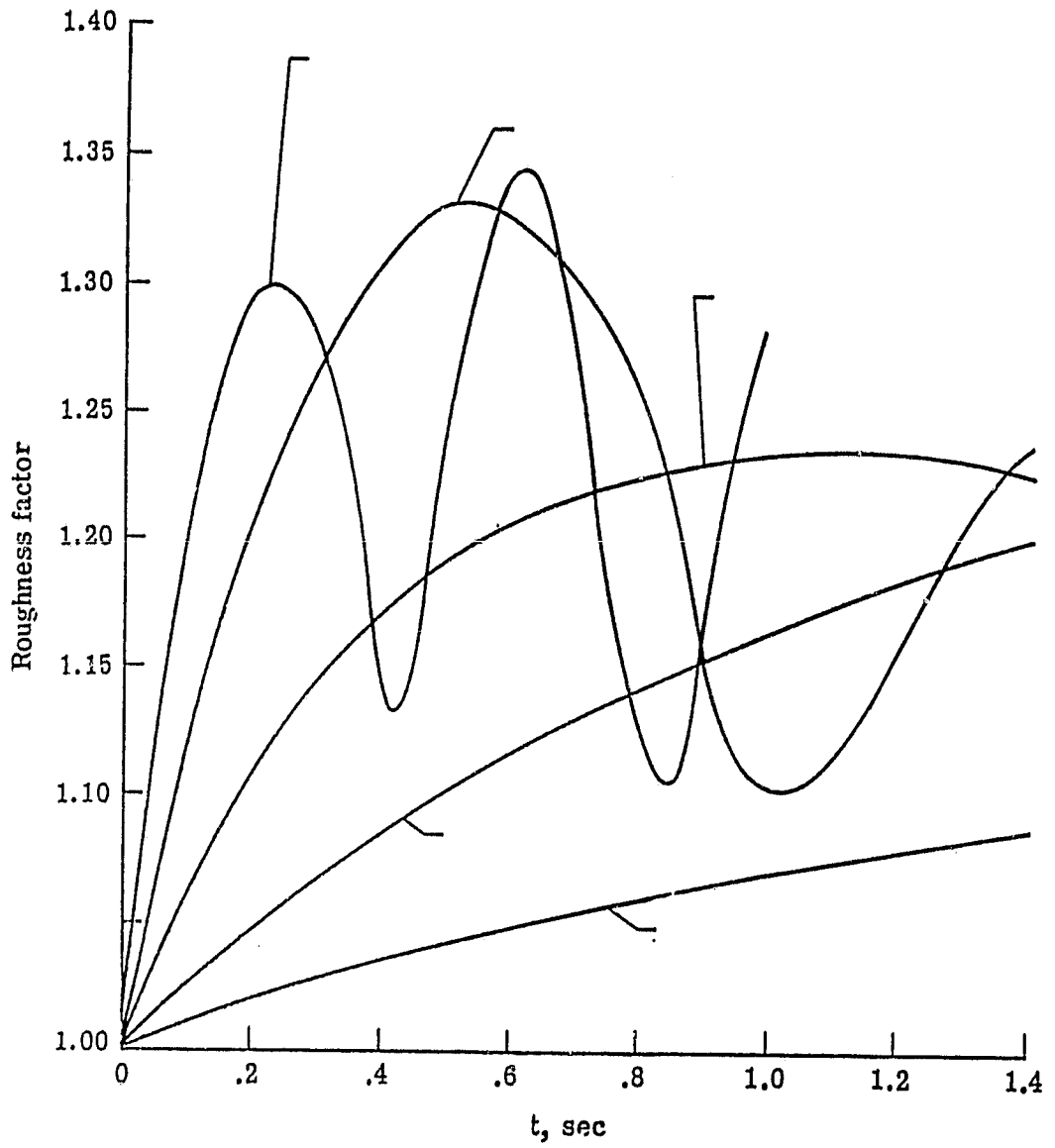


Figure 13. Surface roughness factor for $T = 500$ K and several deposition rates.

CHARACTERISTICS
OF POOR QUALITY

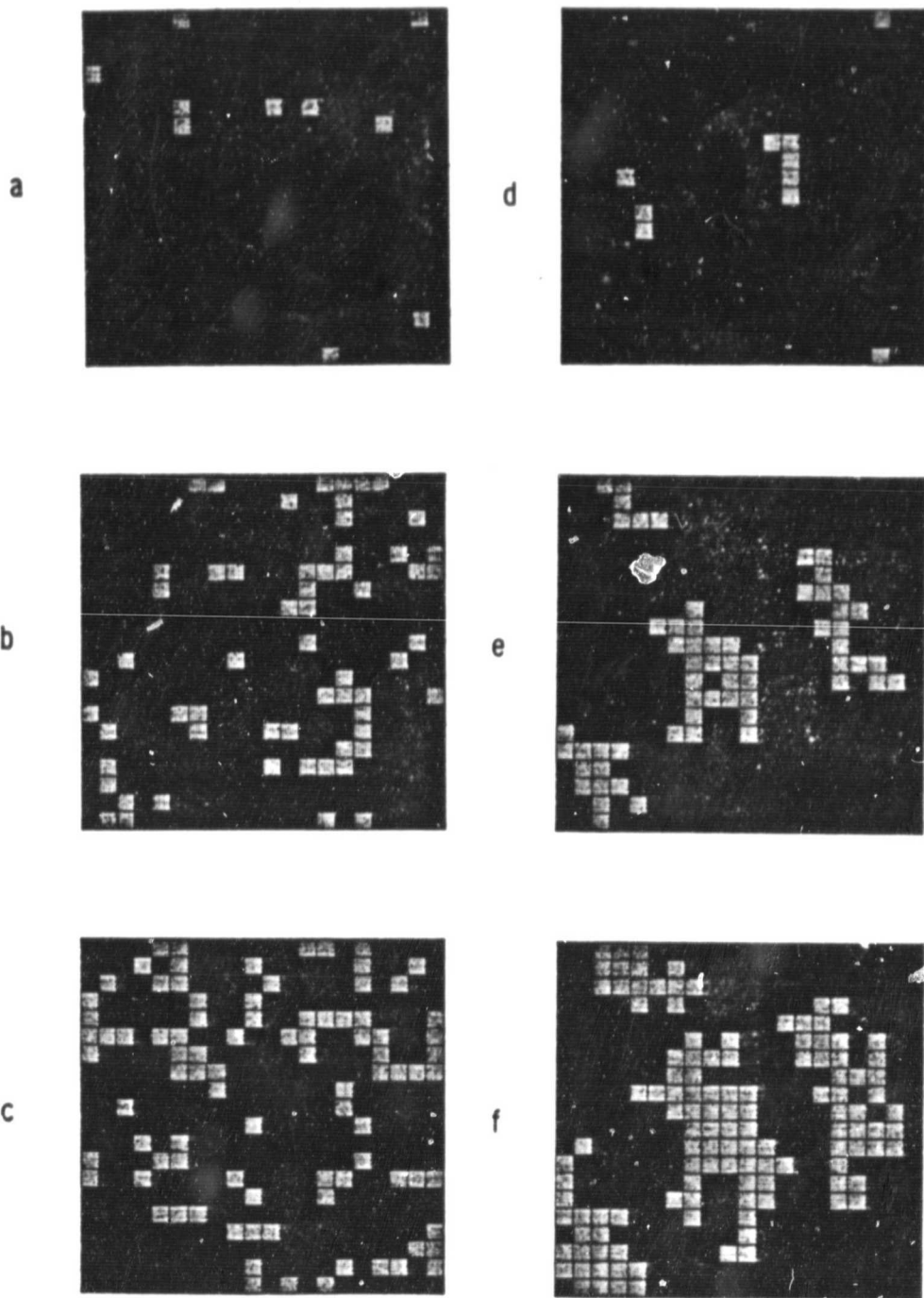


Figure 14. Thin film growth for $R_d = 0.2778$ nm/sec for two different temperatures, $T = 300$ K, (a) $t = 0.5$ s, (b) $t = 3.0$ s, (c) $t = 6.0$ s, $T = 400$ K, (d) $t = 0.5$ s, (e) $t = 3.0$ s (f) $t = 6.0$ s.

ORIGINAL PAGE IS
OF POOR QUALITY

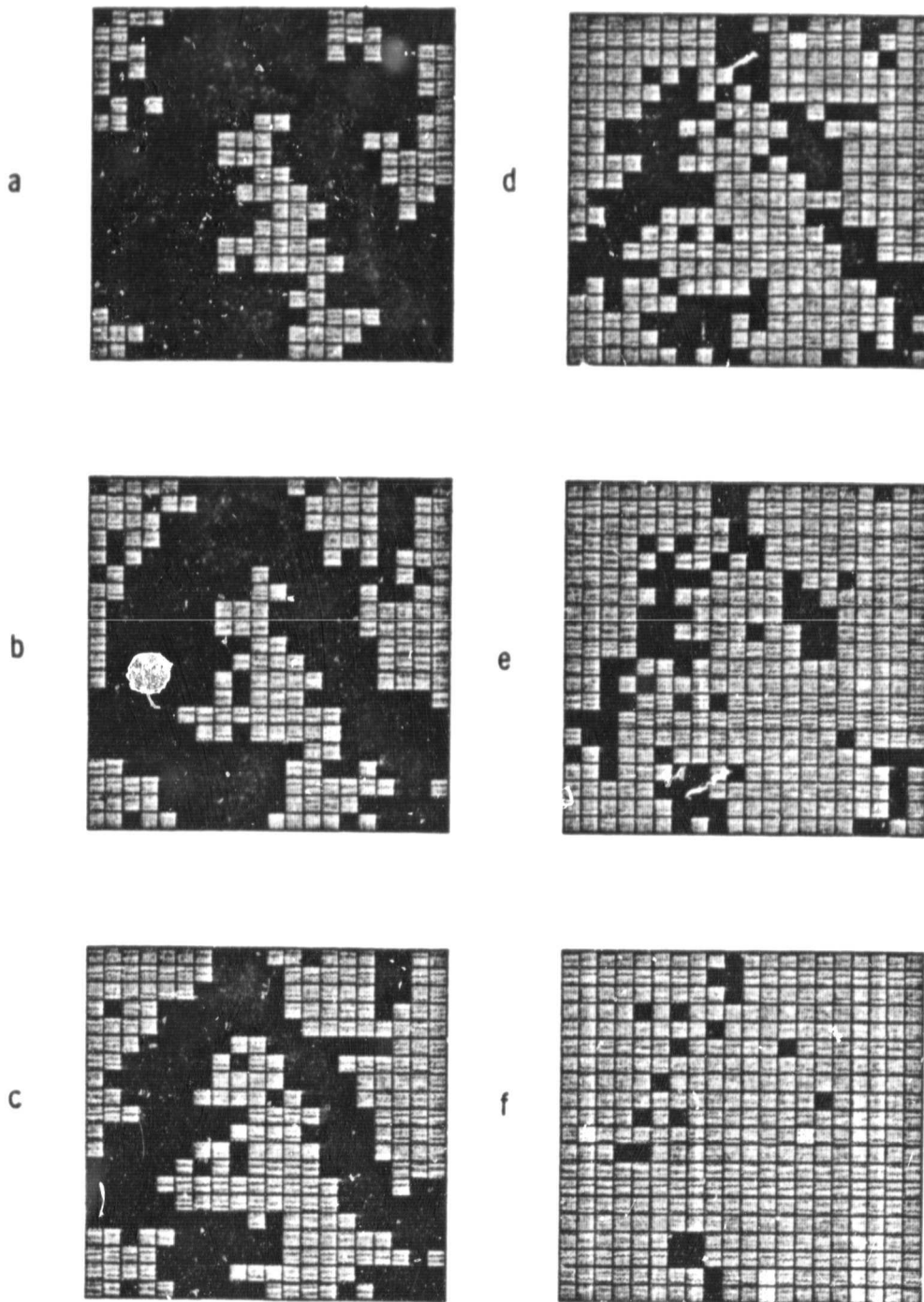


Figure 15. Thin film growth for $R_d = 0.2778$ nm/sec, $T = 500$ K, (a) $t = 0.5$ s, (b) $t = 0.8$ s, (c) $t = 1.1$ s, (d) $t = 1.4$ s, (e) $t = 1.7$ s, (f) $t = 2.0$ s.

ORIGINAL PAGE IS
OF POOR QUALITY

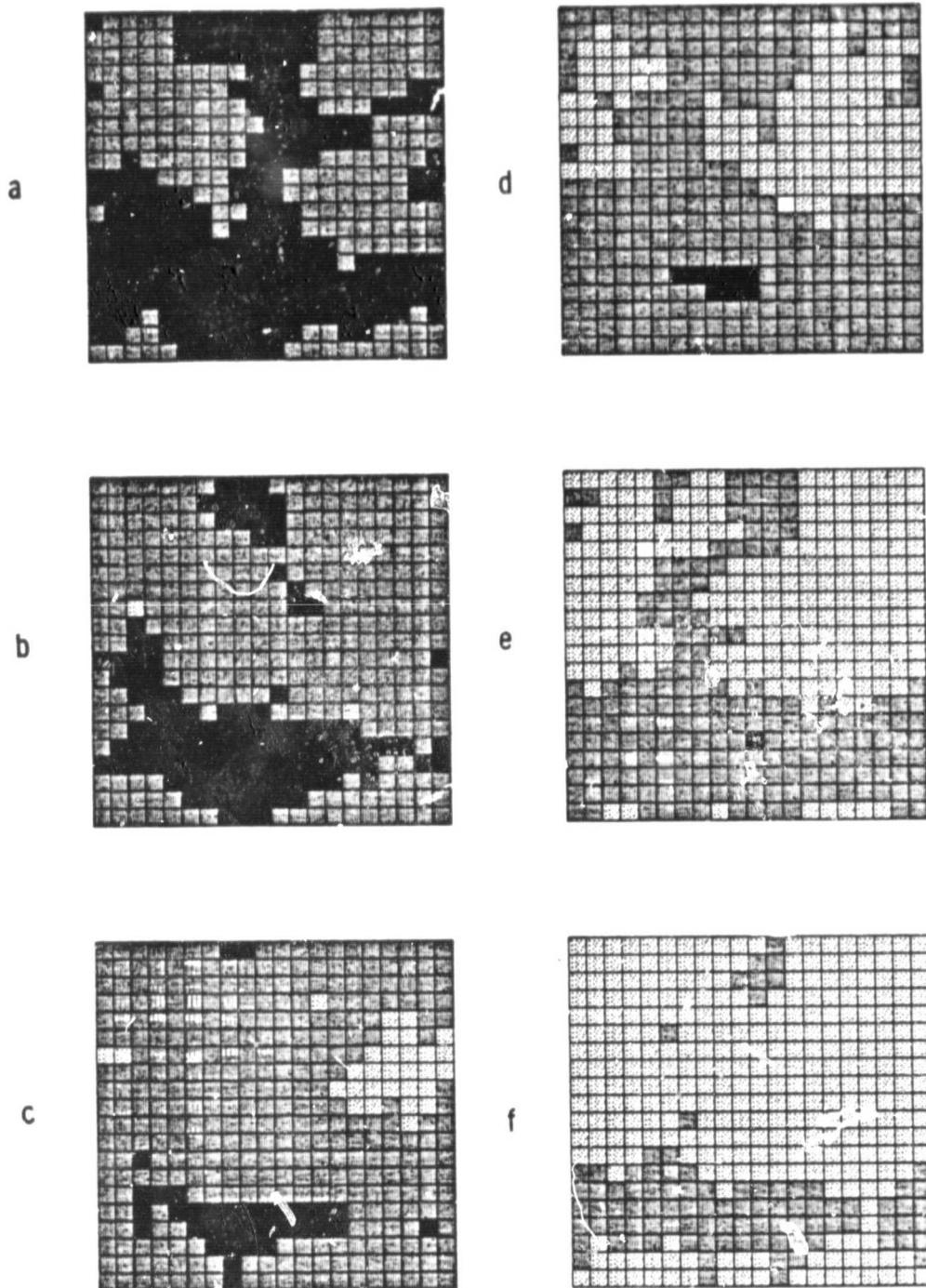


Figure 16. Thin film growth for $R_d = 0.5556$ nm/sec, $T = 600$ K,
(a) $t = 0.5$ s, (b) $t = 0.8$ s, (c) $t = 1.1$ s, (d) $t = 1.4$ s,
(e) $t = 1.7$ s, (f) $t = 2.0$ s.

ORIGINAL PAGE IS
OF POOR QUALITY

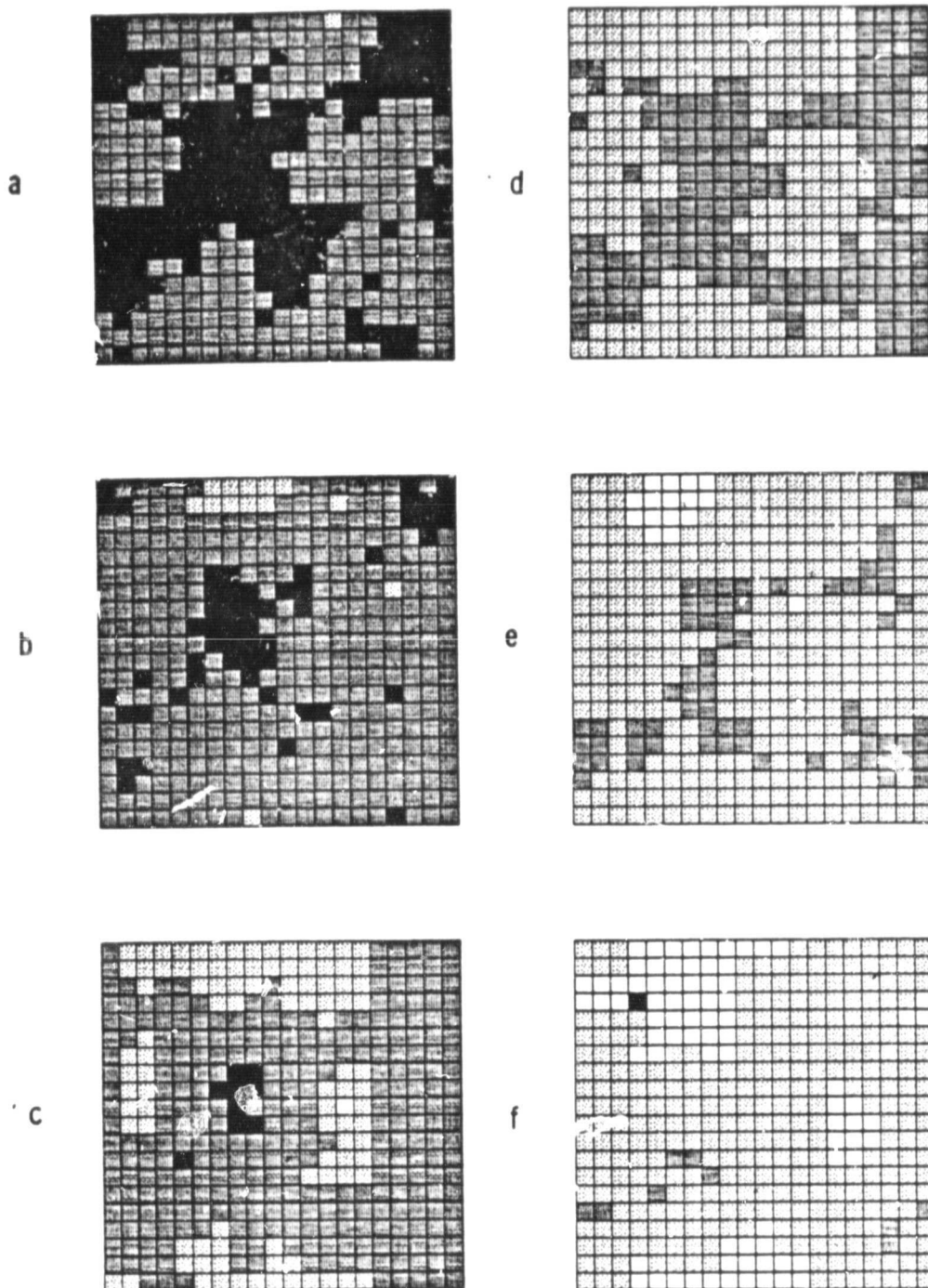


Figure 17. Thin film growth for $R_1 = 1.389$ nm/sec, $T = 600$ K,
(a) $t = 0.25$ s, (b) $t = 0.4$ s, (c) $t = 0.55$ s, (d) $t =$
 0.7 s, (e) $t = 0.85$ s (f) $t = 1.0$ s.

ORIGINAL PAGE IS
OF POOR QUALITY

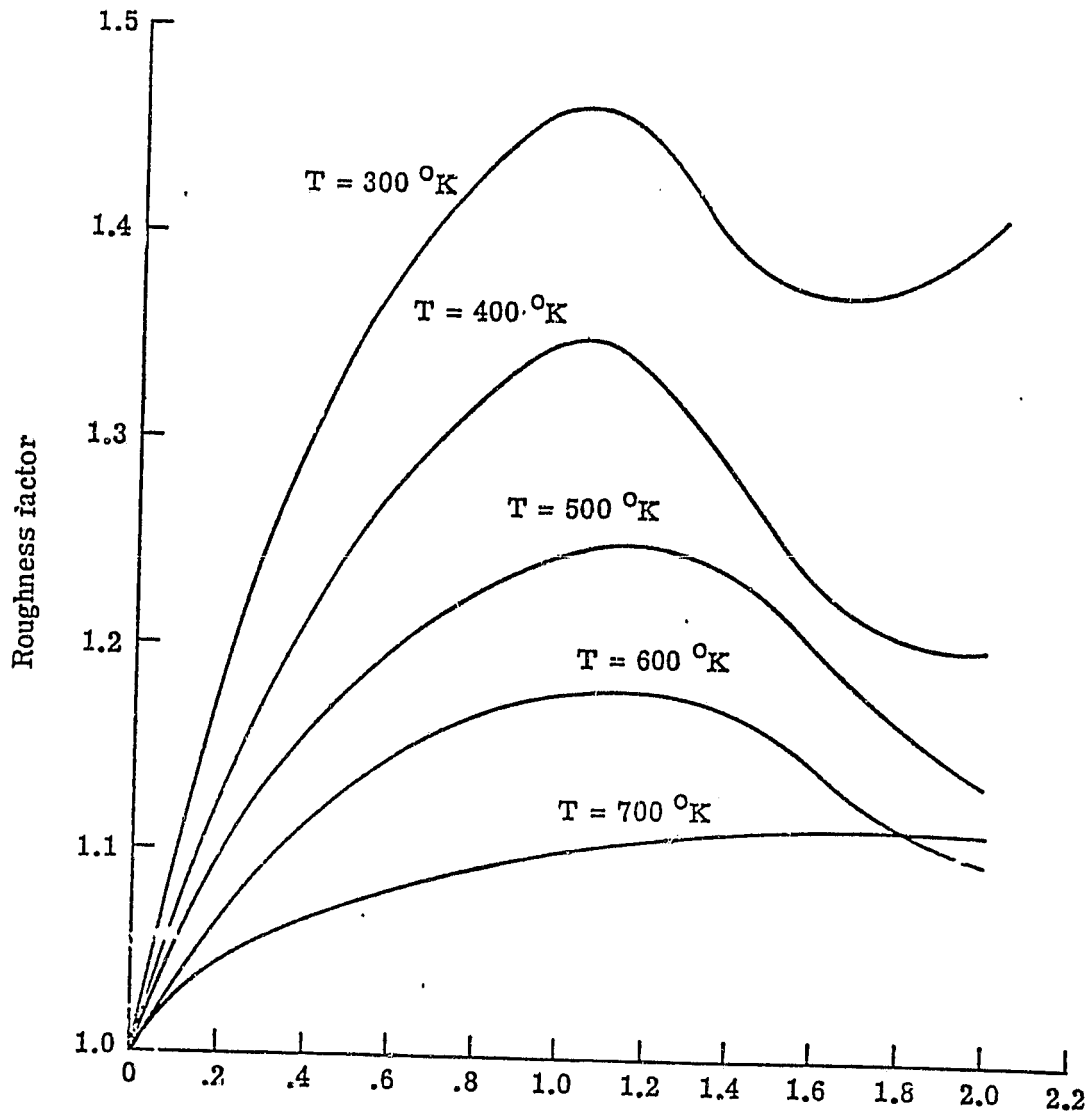


Figure 18. Surface roughness factor for $R_d = 0.2778$ nm/sec and various temperatures.

ORIGINAL PAGE IS
OF POOR QUALITY

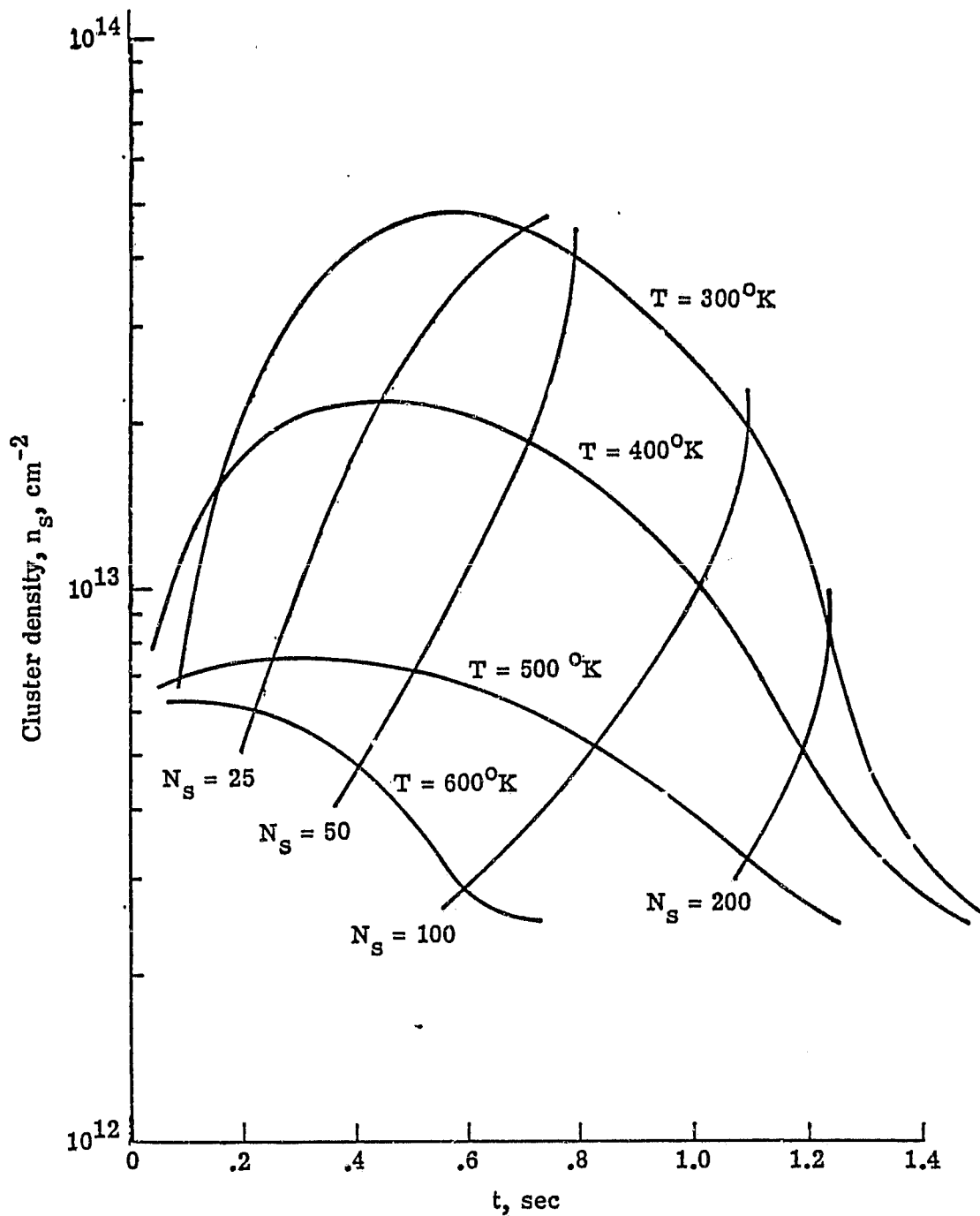


Figure 19. Nucleation density n_s as a function of time with constant cluster curves for 25, 50, 100 and 200 atoms. The decrease in n_s corresponds to growth coalescence.

ORIGINAL PAGE IS
OF POOR QUALITY

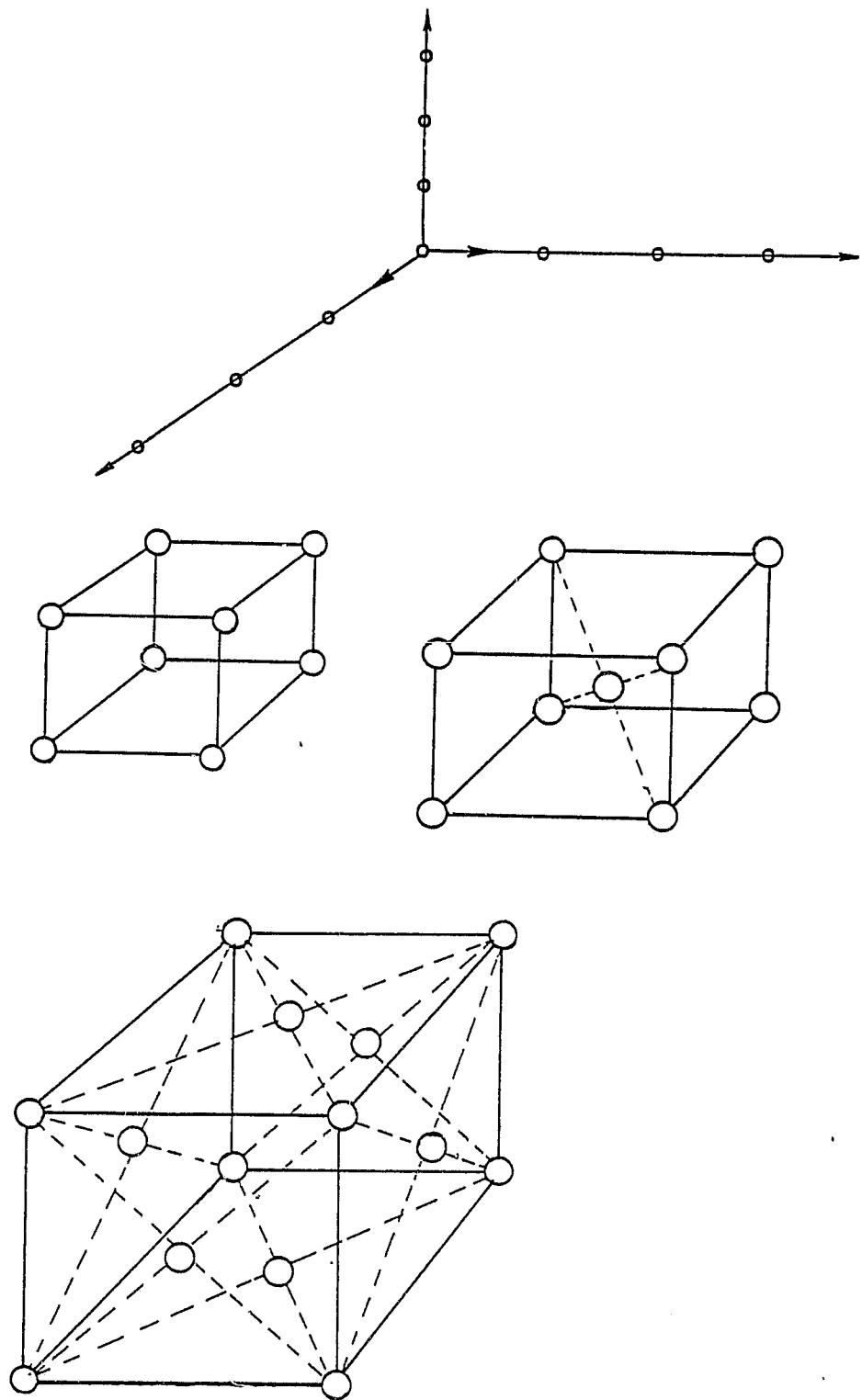


Figure 21. Basis vectors for P,I,F lattice structures.

ORIGINAL PAGE IS
OF POOR QUALITY

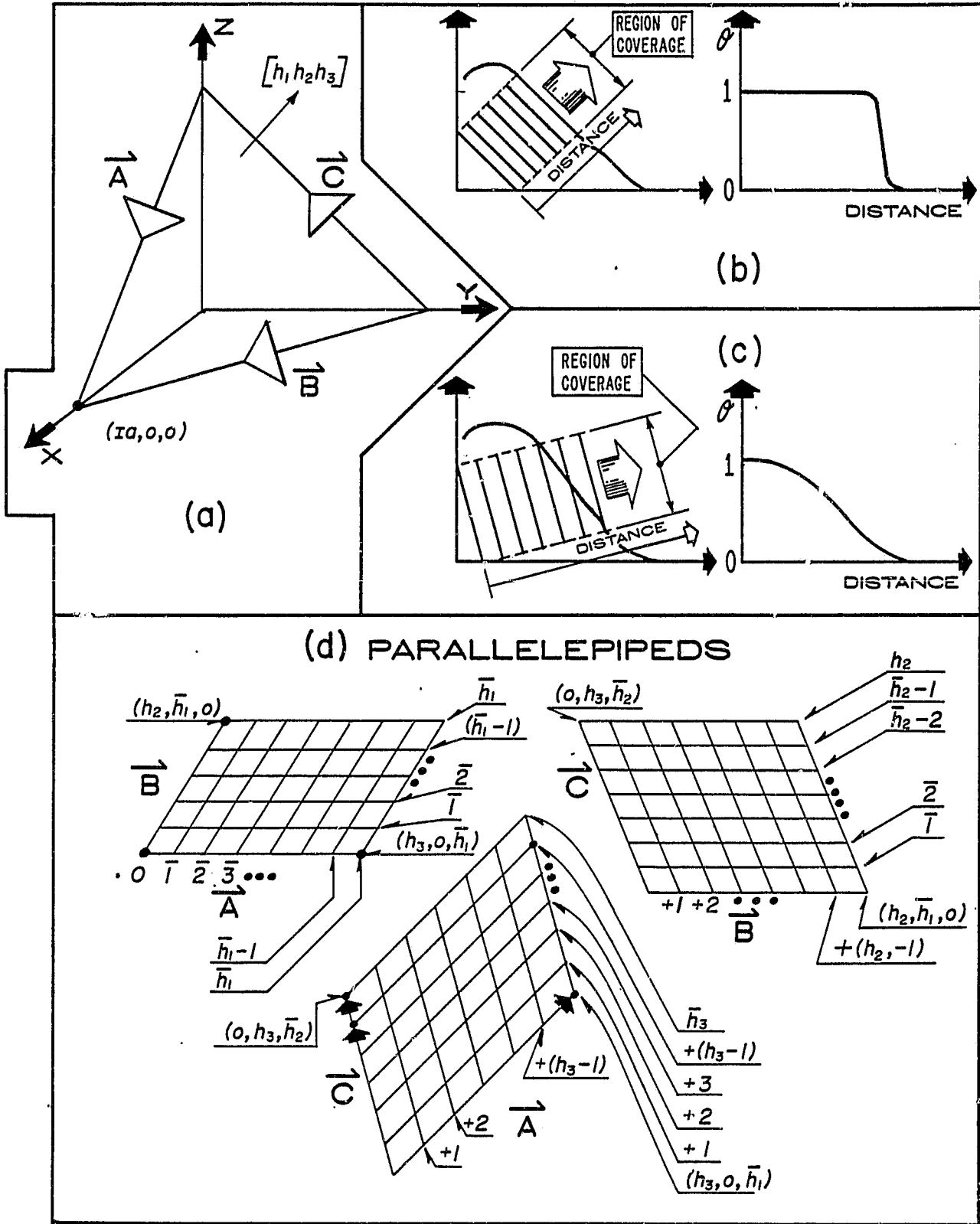


Figure 22. Crystal planes (a) their orientation and coverage with distance (b) and (c), and (d) $\vec{A}, \vec{B}, \vec{C}, \vec{A}$ and \vec{B}, \vec{C} primitive cells.

ORIGINAL PAGE IS
OF POOR QUALITY

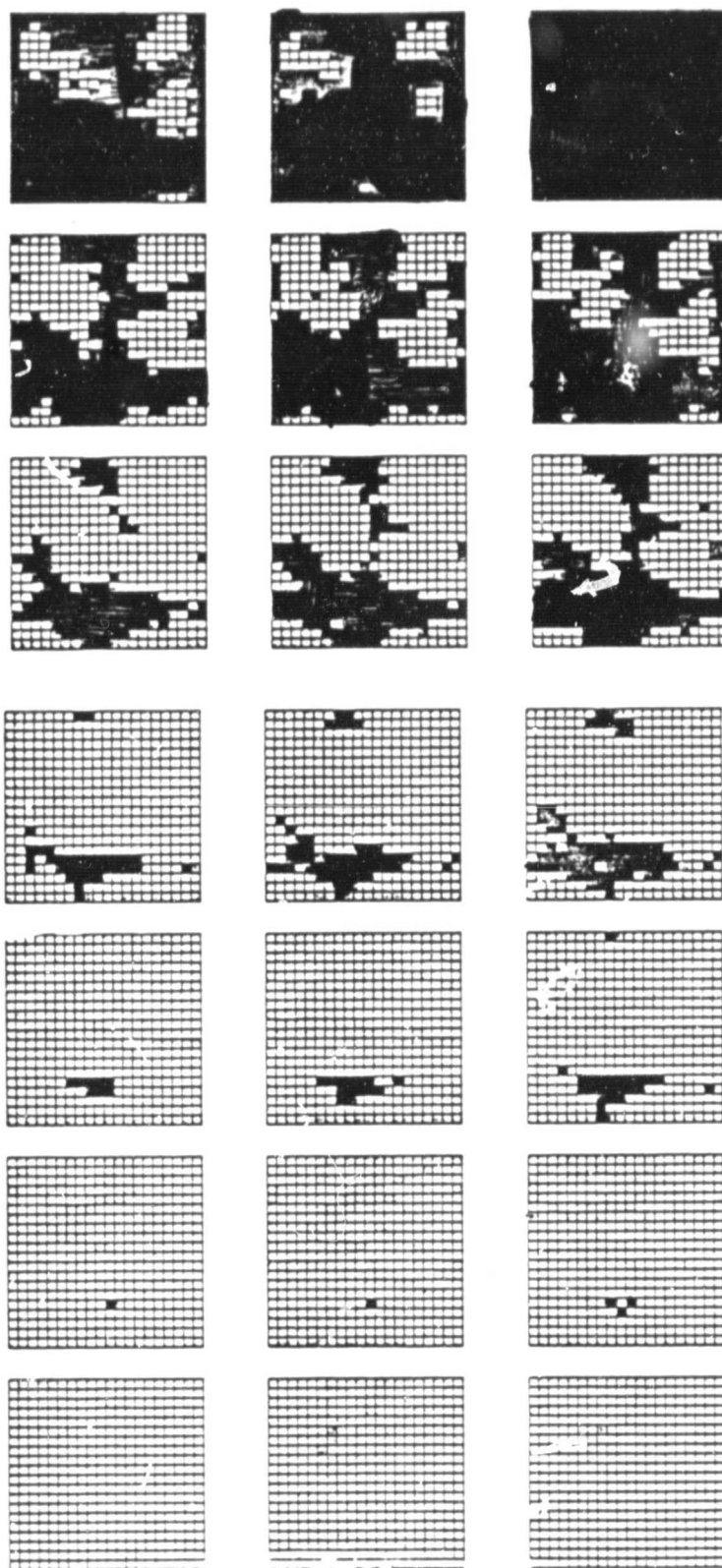


Figure 23. Graphic output from computer program. Snapshots are read from top to bottom and right to left. Each snapshot represents 0.1 sec., $R_d = 0.556$ nm/sec., $\Delta t = 10^{-4}$ sec. (1,000 samples of each surface adatom during each snapshot interval), $T = 600$ K, (100) surface, $U_o = -3.87$ eV, $\Delta H_{ads} = 1.7$ eV, $Q_d = 0.7$ eV, $U_m = -1.0$ eV, $n = 10^8$ (Boltzmann ordered statistic parameter).